Roy Knoechel
Ph.D.
Biology

Phytoplankton species productivity and dynamics

Roy Knoechel
Ph.D.
Biology

Phytoplankton species productivity and dynamics

A STUDY OF THE SEASONAL PHYTOPLANKTON SPECIES DYNAMICS IN A

NORTH - TEMPERATE ZONE LAKE, UTILIZING ^{14}C TRACK AUTORADIOGRAPHY.

by

Roy Knoechel

A thesis submitted to the Faculty of Graduate

Studies and Research in partial fulfilment of

the requirement for the degree of Doctor of

Philosophy.

Department of Biology   November, 1975
McGill University
Montreal, Canada

Ph.D.   Biology

Roy Knoechel

A study of the seasonal phytoplankton species dynamics in a
north - temperate zone lake, utilizing ^{14}C track autoradiography.

ABSTRACT

Track autoradiography was used to quantitatively determine the
individual carbon fixation rates of five planktonic diatom and one
blue-green algal species in a small, naturally eutrophic lake. Track
autoradiography was chosen over the grain density technique because
the quantitative application of the latter was shown to involve very
complex control procedures. The results indicate strong photoinhibition
on bright days, an absence of marked temperature effects on in situ
photosynthesis and, for one species at least, the dependence of the
maximum photosynthetic rate on nutrient inputs. While diatom cell growth
determines the maximum possible rate of population increase, the
population realized is largely a function of the sinking losses. Sinking
in turn is principally a function of the death rate. Succession in
all six species was largely the result of differential sinking rates
rather than differential growth rates.

D. Ph.   Biologie

Roy Knoechel

Etude de la dynamique saisonnière de quelques
espèces du phytoplancton d'un lac tempéré, au ^{14}C.
moyen de la technique de l'autoradiographie au

ABSTRAIT

Une technique d'autoradiographie fut utilisée afin de mesurer

quantitativement le taux individuel de fixation du carbone de cinq

espèces de diatomées planctoniques ainsi que d'une algue bleue-verte

dans un petit lac, naturellement eutrophe. L'autoradiographie fut

préférée à la technique de la densité du grain parce qu'il fut montré

que l'application quantitative de cette dernière nécessitait l'utilisation

de méthodes de contrôle fort complexes. Les résultats montrent une

photo-inibition prononcée pour les journées ensoleillées, une absence

d'effets marqués de la température sur le taux de photosynthèse in situ

et, dans le cas d'une espèce au moins, que le taux maximum de photo-

synthèse dépend des apports en sels nutritifs. Tandis que la croissance

cellulaire des diatomées détermine le taux d'accroissement maximum de

la population, la population effective est en grande partie fonction

des pertes par sédimentation. A son tour, la sédimentation se révèle

être principalement une foncion du taux de mortalité. La succession

observée des six espèces fut en majeure partie le résultat des taux

différentiels de sédimentation plutôtque des taux différentiels de

croissance.

The thesis is presented as a series of four inter-connected papers in publication format as permitted under the regulations of the Graduate Faculty of McGill University. These regulations also require the following statement as to the elements of the thesis that are considered to be "contributions to original knowledge".

The technique presented in this thesis for applying track auto-radiography to the study of phytoplankton communities is a contribution to original knowledge. It has never before been possible to quantitatively measure carbon incorporation at the cellular level in mixed phytoplankton assemblages. Thus the data presented here for six algal species are original contributions to knowledge. The mathematical formulations for calculation of the growth constant differential necessary to account for changes in species composition (Part 3) and for simultaneous calculation of death and sinking rates (Part 4) are similarly original.

ACKNOWLEDGEMENTS

TABLE OF CONTENTS

LIST OF FIGURES AND PLATES

LIST OF TABLES

GENERAL INTRODUCTION

The objective of this study was to develop and utilize a technique for measuring _in situ_ production at the species level in order to elucidate the factors affecting algal production and population dynamics in nature.

The initial approach was to utilize grain density autoradiography because at the outset of the study several papers were published which suggested the utility of this technique. However, a consideration of the assumptions involved in its quantitative application led to the rejection of this approach. The basis for judging the technique unsuitable as well as suggested remedial procedures are presented as Part 1 which has been accepted for publication in Limnology and Oceanography (1976).

From a theoretical viewpoint the seldom used technique of track autoradiography appeared better suited to quantitative studies. The procedures developed to apply this technique to the study of phytoplankton and laboratory validation of its quantitative capability are presented in Part 2 which has also been accepted for publication in the above journal (1976).

A diatom -- blue-green succession was the first ecological problem investigated. The literature offered a host of plausible hypotheses as to why such a succession would occur. Through monitoring the productivity of the two main species involved, _Tabellaria fenestrata_ and _Anabaena planctonica_, it was possible to evaluate the various alternatives to determine that the primary driving force behind this succession was

differential sinking rates (Part 3). The results are being published in the Verhandlungen of the International Association of Theoretical and Applied Limnology (1975).

The last manuscript presented here explores the productivity and population dynamics of the 5 major species in a naturally eutrophic lake (Part 4).

The appendices contain data not suitable for inclusion in the preceding manuscripts but relevant to the thesis.

Part 1

The applicability of grain density autoradiography to the

quantitative determination of algal species production:

a critique.

ABSTRACT

Grain density autoradiography can be utilized to quantitatively determine the productivity of individual species in mixed phytoplankton assemblages but only after grain counts have been corrected for the effects of source geometry on efficiency as well as for the effects of spurious grain formation and erasure. The common simplifying assumption made by all workers to date, that the grain count over a cell is directly proportional to the cell's radioactivity, is never realized with mixed species assemblages and those attempts at quantification are invalid. The procedure of apportioning total filterable radioactivity to the cells counted in autoradiographic preparations is also suspect. A method of data correction is presented which makes quantification feasible.

INTRODUCTION

Autoradiography is a potentially powerful tool for measuring individual species productivity in mixed phytoplankton assemblages. There are two basic techniques. Track autoradiography uses thick emulsion layers to record the paths of particles in their entirety as a string of silver grains while grain-density autoradiography uses a thin layer of emulsion to record only the initial portions of tracks and then relates the density of grains produced to the amount of radioactivity present. The first method is inherently quantitative (see Part 2, this thesis) while the second is not. In molecular biology grain-density autoradiography has been widely used as a rapid and easy means of demonstrating qualitatively the simple presence or absence of a tracer-labeled substance while track autoradiography has been avoided as being unnecessarily precise and a more difficult technique to master. Thus it is natural that the widely used grain-density method was the one first applied to the field of algal ecology. Initially it was used to gain qualitative information about the distribution of label in monospecific communities (e.g. Brock and Brock 1969) a purpose for which it is eminently suitable. The warning that the technique was not directly useable for obtaining quantitative information in mixed species assemblages (Brock and Brock. 1968, p.25) has been disregarded in all such subsequent studies (Watt 1971, Maguire and Neill 1971, Gutel'makher 1973, Stull et al. 1973, Stross and Pemrick 1974) with resultant internal errors of several hundred percent (see efficiency ranges estimated in Table 1). Invalidating errors arise from three principle sources. Firstly through inadequate cell preparation and lack of controls during the autoradiographic processing.

Table 1. A summary of the techniques used in various studies,

including controls used and efficiency and filtration

corrections employed. The estimated range of efficiency

reported for each study is based only on the size and

shape of the specimens and presumes that cell preparation

and control procedures have been adequate.

---

indicates that information was not given or not explicit.

These values are the diameters of species with spherical shape estimated from the
stated volumes or carbon contents, excepting those of Stross and Pemrick for
which all species are band-shaped and size data were not given.

The upper limit for the band-shaped source width depends on the size of the
Fragilaria colonies (which was not stated).

All values are from the appropriate efficiency curve (Fig. 4 and 5) using the
estimated cell sizes shown above. In the studies not using Kodak AR-10 stripping
film the preparation thickness and consequently the half-distance depend entirely
on the particular dipping and drying techniques employed and this will affect
the minimum efficiency estimates.

II personal communication.

	Watt	Maguire and Neill	Gutel'makher	Stull et al.	Stross and Pemrick
Emulsion	Kodak NTB2 1:1 dilution	Kodak AR-10	NIIKhimfoto type "M" 1:2	Kodak AR-10	Kodak NTB2 1:1 dilution
Developer	Kodak D-19 5 min., 20°	Kodak D-19	? *	Kodak D-19	Kodak D-11 2 min.
Cell preparation	filtered, freeze dried, exposed to HCl and acetone fumes	centrifuged, .002 N HCl rinse, distilled water rinse, sonification	repeatedly dried on slide over alcohol flame to concentrate, 40° oven, 5 min. in 96% alcohol	filtered, air dried, cleared with acetone vapor	filtered, tapwater rins resuspended, mounted on slides 45-60° oven
Fixative	none	ethanol-formaldehyde or ethanol	Formalin	none	none or Formalin (controls onl
Chemography control?	yes - dark bottle	?	no	no	no
Latent image erasure control?	no	?	no	no	no
Size and shape correction?	no	no	no	no	no
Self-absorption correction?	no	yes, but incorrect factors	no	no	no
Filtration correction?	no	no	no	no	grain counts not converted to carbon uptake rate
Estimated [†] cell sizes (μm)	5 to 60+	2.5 to 30	< 4 to 8	3 to 15+	2 wide to [‡] 60+
Area counted	over cell?	cell plus 5 μm	over cell?	over cell [‖] plus one cell width	over cell?
Estimated [§] range of efficiency (%)	20 to 70	55 to 80	15 to 30	20 to 50+	15 to 80

Secondly through the failure to consider the effect of cell size and shape on the distribution of silver grains produced. Thirdly through the erroneous assumption that filterable radioactivity measures only the radioactivity in the cells. A summary of the techniques used in previous studies is provided (Table 1).

It is the purpose of this paper to outline both the principal steps that must be taken if grain density results are to be quantified and to describe a method whereby recent advances in the field of autoradiography can be adapted to algal research.

CELL PREPARATION AND AUTORADIOGRAPHIC PROCESSING

There are two requirements that must be met in preparing the cells. First the procedure must not extract the cell contents or destroy the delicate species, and secondly any fixatives used either must not interfere with the subsequent autoradiography or else their effects must be rigidly controlled.

Several researchers have followed a procedure in which the cells are filtered live and the filter subsequently cleared with acetone fumes prior to autoradiographic processing (Watt 1971, Stull et al. 1973). Acetone is an organic solvent commonly employed to extract cell pigments and will thus cause translocation of label and may cause the destruction of delicate cells. Stross and Pemrick (1974), who used filtration followed by resuspension and mounting on slides, noted that this treatment allowed them to identify only the diatoms in their preparations while many other species had initially been present. They were thus unable to equate total filter activity with that of the specimens they observed. This limitation was, however, not recognized in the two former studies.

A not very desirable alternative, if acetone clearing
is necessary for optical resolution, is the procedure devised by Fuhs
and Canelli (1970) in which the filters are not treated with acetone
until after they are processed and developed. While this may still des-
troy delicate organisms it will at least not translocate material until
after the autoradiography is completed.

Other studies have chosen not to use the filtration method but to
instead fix and mount the cells on slides by a variety of means (Maguire
and Neill 1971, Gutel'makher 1973). The repeated drying of cell suspensions
over an alcohol flame by the latter author is an unnecessarily harsh
procedure certain to cause cell damage and loss of activity. Both studies
employed formalin as the fixative, although it is well known for its in-
ability to adequately preserve delicate flagellates (acid lugol has been
suggested as a preferred alternative (e.g. Vollenweider 1974)). We have
described elsewhere a mounting procedure which does preserve these delicate
cells (see Part 2, this thesis).

The choice of fixative has an additional importance in that it may
affect the photographic emulsion. In autoradiography the energy loss
from a beta particle is recorded chemically as a latent image in a special
emulsion. This latent image is subsequently developed to produce a silver
grain. Although not generally appreciated, latent images are not uniquely
the result of this energy loss but are also produced by heat, pressure,
and chemical reduction (Rogers 1969). Once formed these latent images
are subject to erasure by chemical agents or by the small amount of water
that always remains in the emulsion. The cause of a particular silver
grain must remain ambiguous, therefore strict control and standardization pro-
cedures must be applied if grain counts are to have even qualitative meaning.
For example, to minimize errors resulting from chemical reduction or

artifacts caused by stresses during drying, the background count must be made over non-radioactive specimens on the same slide rather than over empty areas which can be relatively free of such effects. An even better method is to apply an impermeable film over the slide prior to applying the emulsion thereby eliminating chemical interaction (Rogers, 1969). We have observed spurious grains (chemography) occasionally when using acid lugols as a preservative (Fig. 1C). They were recognized as artifacts becaus the slides had been prepared for track autoradiography (see Part 2, this thesis) making it obvious that the grain production was not associated with radioactivity. Chemography is so highly variable that cells showing massive grain production may lie adjacent to others that are relatively free of the artifact (Fig. 1A). Similarly, we have observed that glutaraldehyde can cause chemography while Rogers (1969) observed it to cause grain erasure with the differences probably due to the impurities in commercial glutaraldehyde solutions. Formalin, used in several studies, (see above) has been cited by Rogers (1969) as causing drastic latent image erasure and thus should be strictly avoided. It is therefore not surprising that Stross and Pemrick (1974), who used formalin only on their "control" specimens, observed that the latter always yielded grain counts lower than background! To check for latent image erasure it is necessary to vary the exposure period so that it can be demonstrated that grain production is a linear function of time.

THE EFFECT OF SPECIMEN GEOMETRY ON GRAIN COUNT

After obtaining grain counts due to radioactivity the data must be corrected for efficiency differences resulting from geometric considerations before they can be interpreted quantitatively. The effect of cell size

Figure 1. A. Anabaena filament showing massive but localized

chemography.

B. A nanoplankter with one disintegration but no

resultant overlying silver grains (beta particle

track not in focus at 7 o'clock position).

C. A similar nanoplankter which appears to be

highly labeled but which is actually non-radioactive

(no tracks present; both B and C are on the same

autoradiography slide).
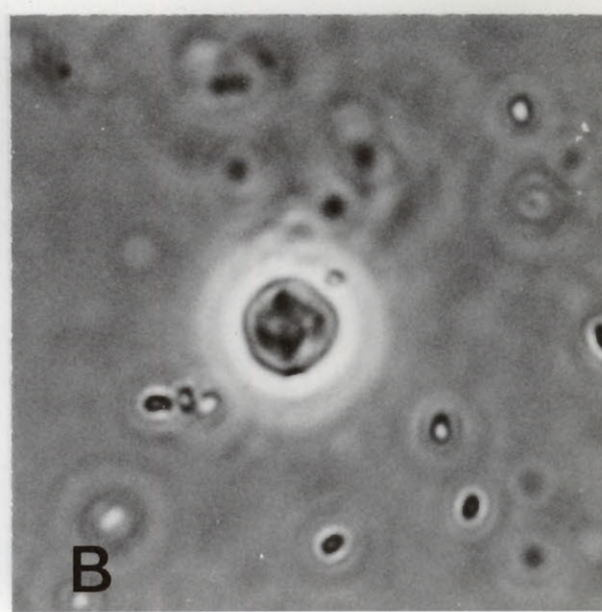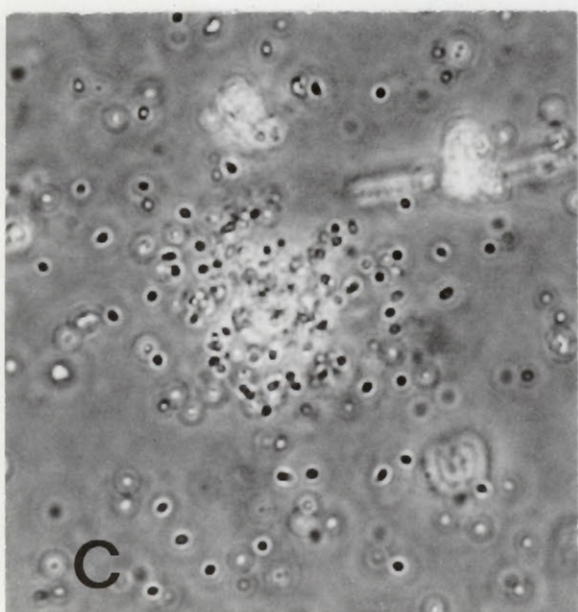
and shape becomes evident when considering that although a beta particle originates from a point source it releases energy continuously after leaving the source. The distance traveled is a function of the density of the medium and the energy of the particle (0-155 keV for ^{14}C). In nuclear emulsion the pathlengths of ^{14}C particles vary from 0-100 μm and they may contain anywhere from 0 to 80 silver grains depending upon the initial energy level (Levi and Rogers 1963). The importance of this effect is most readily demonstrated graphically (Fig. 2). In this drawn to scale illustration the emulsion layer represents Kodak AR-10 stripping film with a thickness during exposure of approximately 3.6 μm (Rogers 1969). Particles from a point source would be expected to yield a fairly even grain production over an area 12 μm in diameter (Fig. 3). Using a grain spacing of 1 μm for ^{14}C beta tracks (Levi and Rogers 1963) yields the grain distirubtion of an "average" disintegration (Fig. 2). With three hypothetical disc-shaped algal specimens of 2, 4 and 12 μm diameter it is evident that the resultant grain counts would be 1, 2, and 7 grains respectively. Thus the larger specimen would be construed as having 3.5 to 7 times the activity of the smaller cells despite the fact that the absolute radioactivity is identical. Every study to date has made the erroneous assumption (Table 1) that this geometry effect is negligible and that the number of grains over any cell is directly proportional to the cell's radioactivity. The result is a severe underestimation of the activity of small cells, compounded by an overestimation of the activity of large cells by the subsequent apportionment of the total ^{14}C filter activity to the cells observed.

In the above example we have considered several disc-shaped specimens of differing diameter. It is, however, intuitively obvious that the shape

Figure 2. Grain production (•) from a point source (o) showing

that the grain count over cells increases with

specimen size (A,B,C) even when the radioactivity is

the same.

emulsion

specimen

A B C

slide

2 μm

4 μm

12 μm
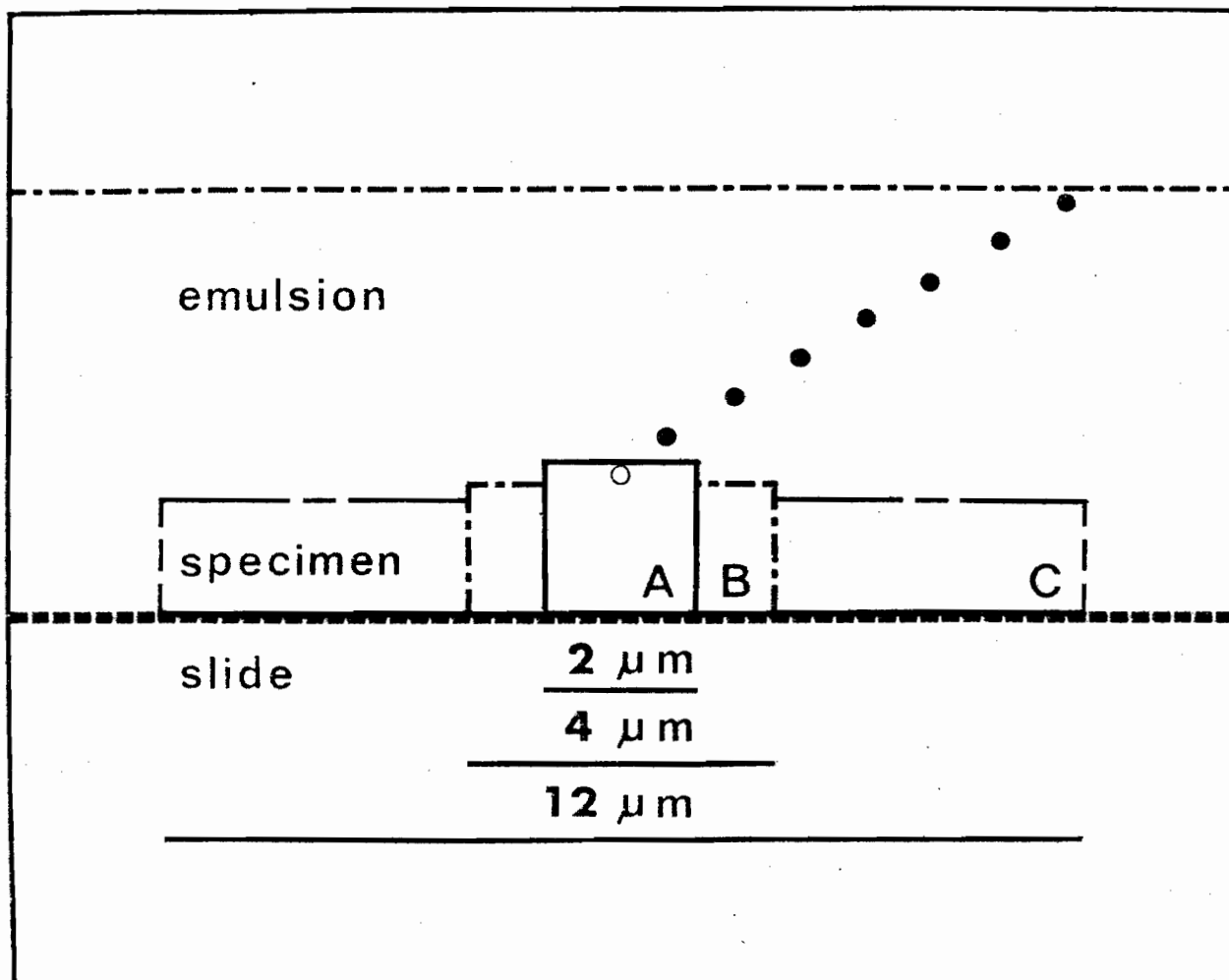
Figure 3. Predicted mean distance traveled horizontally (B) by ^{14}C beta particles arising from a point source in Kodak AR-10 stripping film.

emulsion

A

a

° point source
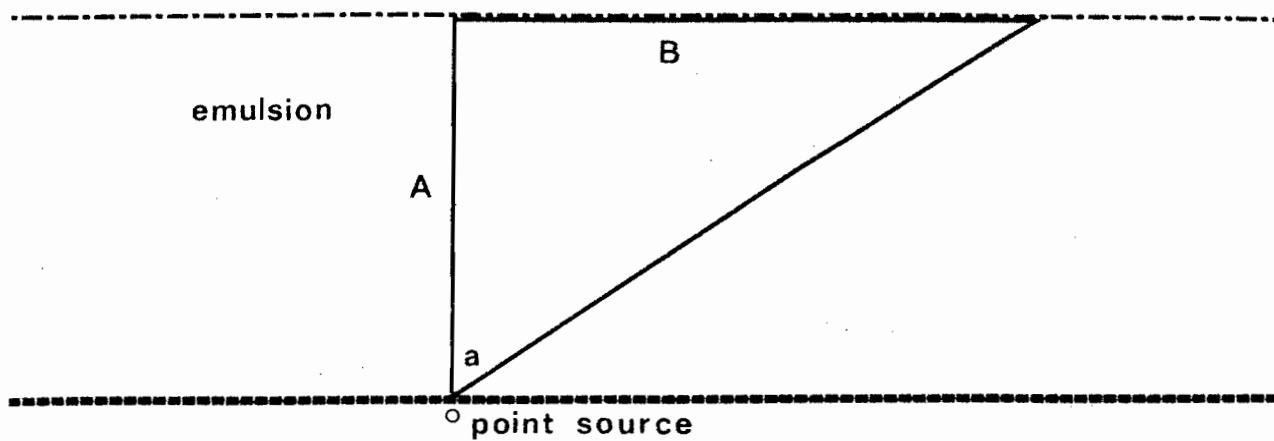
A = 3.6 um

∠ a°	B = A tan a
10	0.63
20	1.31
30	2.08
40	3.02
50	4.29
60	6.24
70	9.89
80	20.42

$\bar{x} = 5.99$

of the specimen also plays a role so that a narrow rectangular source
will have a lower grain count than a disc source of equal surface area
because the grain distribution around the point source is in all cases
circular.

Since the number of grains produced and their spatial relationship
to the specimen depend on both the size and shape of the source and the
thickness of the emulsion as well as the energy of the isotope in question,
a common denominator is required so as not to have to empirically determine
a correction factor for the particular combination of these parameters
found in each study. Salpeter, Bachmann and Salpeter (1969) succeeded
in this by utilizing the concept of half-distance (HD), the distance from
a point source within which half of the produced silver grains are located,
and produced empirical grain distribution curves for disc and band-shaped
sources. These curves can be applied to any emulsion and any beta-emitting
isotope requiring only that the HD for the particular experimental conditions
is first determined.

We have constructed estimated efficiency curves for disc and band-
shaped algal sources (Fig. 4 and 5) by combining the empirical curves of
Salpeter et al. (1969) with an HD estimate of 3.1 μm reported by Bleecken
(1961) for ^{35}Sulfur using Kodak AR-10 stripping-film. As ^{35}S
has an energy similar to ^{14}C (167 vs 155 keV) the curves
provide a reasonable estimate of the geometry effect for reported algal
studies. Referring again to the hypothetical disc-shaped algal sources
with diameters of 12, 4, and 2 μm the curve (Fig.4) provides efficiency
estimates of 42%, 16%, and 8% respectively. Thus the grain counts observ-
able under conditions of equal radioactivities would be proportionately
5.3:2:1, in close agreement with what we predicted from the graphic

Figure 4. Estimated efficiency (%) of grain counts over disc-
shaped sources in Kodak AR-10 as a function of
specimen diameter (μm). Grain counts made over
the cell only (a), plus outside to 5 μm (b) and
plus outside to 10 μm (c).
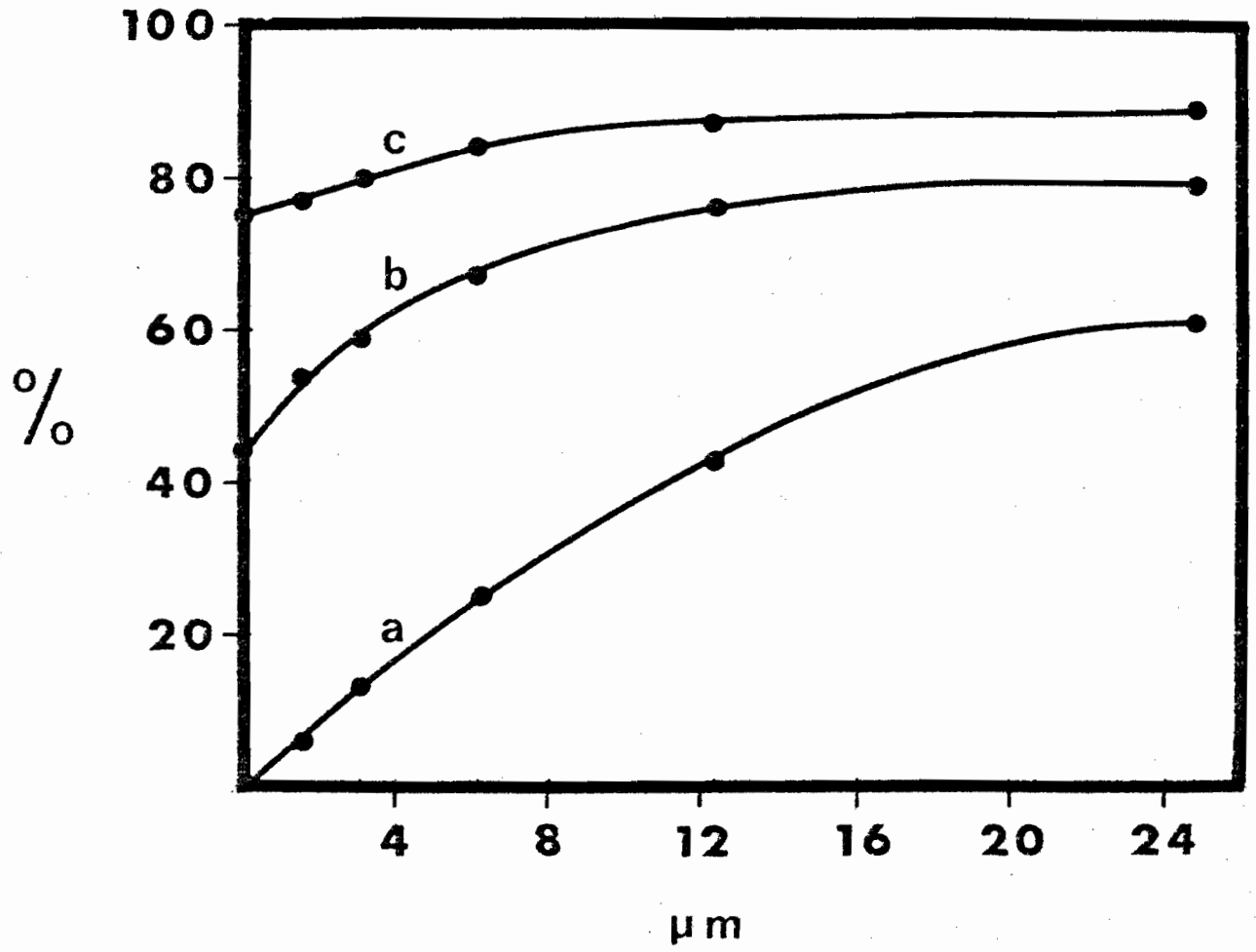
Figure 5. Estimated efficiency (%) of grain counts over band-
shaped sources in Kodak AR-10 as a function of specimen
width. Grain counts made over the cell only (a),
plus outside to 5 μm (b) and plus outside to 10 μm
(c), the dimensions given are cell lengths.
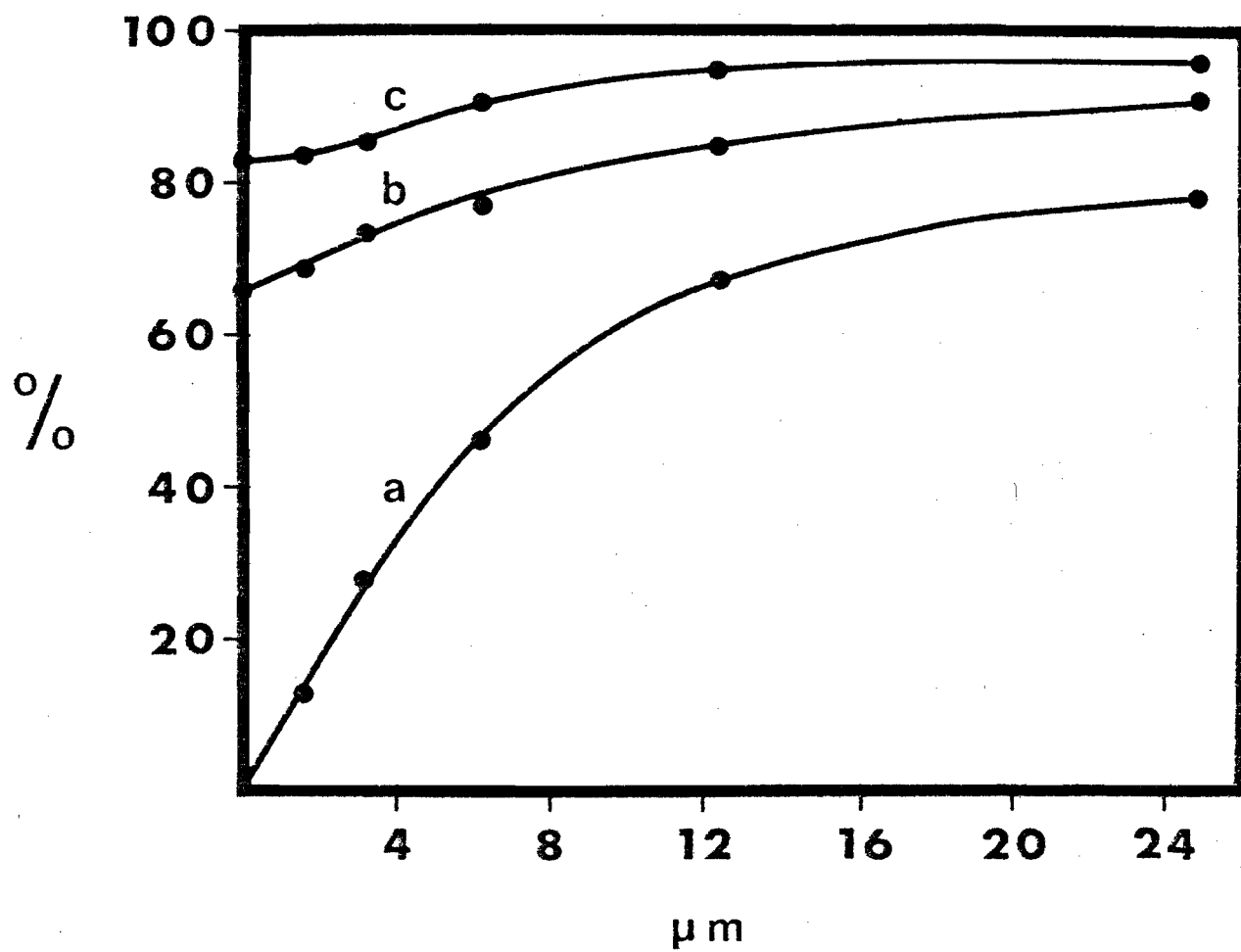
analysis (Fig. 2).

Geometry also affects efficiency through self-absorption of beta particles by the cells. The magnitude of this effect, which depends on the thickness and density of the cells as well as the energy level of the particles, has been measured for ^{14}C using Geiger-Müller systems (Hendler 1959; Jitts and Scott 1961). The predicted relationship between cell thickness and self-absorption as derived from the data of Hendler (1959, Table 1) and assuming a dried algal specimen density of 1.10 is presented (Fig. 6). Rogers (1969) greatly overestimated self-absorption, probably due to a misinterpretation of Hendler's data. The latter presented "thickness" only in terms of mg $BaCO_3$ cm^{-2} and the change to biological material requires the following conversion:

At unit density 1 g cm^{-3} equals a 1 g cm^{-2} layer of 1 cm thickness

Converting to mg: 1 mg cm^{-2} = 10 μm   since 1 cm = 10,000 μm

$BaCO_3$ specific gravity = 4.43 g cm^{-3}

Therefore 1 mg $BaCO_3$ cm^{-2} = $\frac{10 \text{ μm}}{4.43}$ = 2.26 μm

If dried algal material is 1.10 g cm^{-3} then $BaCO_3$ is 4.03 times as dense.

Thus: 1 mg $BaCO_3$ cm^{-2} = 2.26 μm x 4.03 = 9.10 μm algal material.

Rogers seems to have considered 1 mg cm^{-2} to equal only a 1 μm layer at unit density. Since his estimates were cited by Maguire and Neill (1971) their data require re-evaluation as do the remaining studies (Table 1) as they lack correction factors altogether.

We propose two approaches to data correction. The first is to count all grains within a distance from the cell that is large in relation to the HD thereby greatly increasing the efficiency of small cells. This equalization of efficiency was partly realized by Maguire and Neill (1971) when they counted to a distance of 5 μm from the cell. A larger distance

Figure 6. Effect of self-absorption expressed as efficiency

(%) versus cell thickness (μm) assuming an algal

specimen density of 1.10. Linear regression

equation: $y = 100.0 - 0.98\ x$
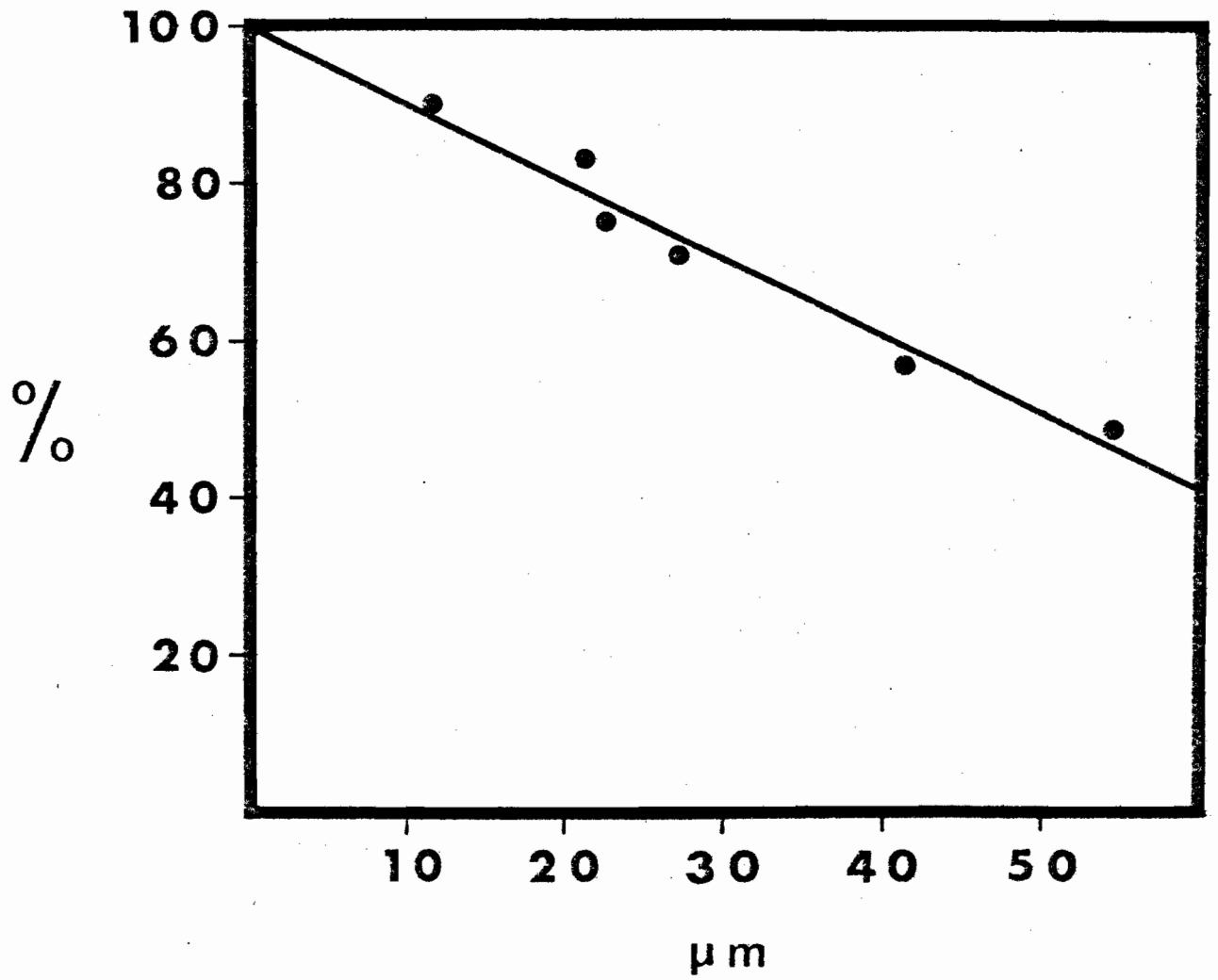
(e.g. 10 μm) is recommended as it will give a more stable efficiency (curve c vs. b in Figs. 4 and 5). This effect can be further enhanced by employing a thinner emulsion layer, thereby reducing the HD. Thinner layers can be obtained by dilution of the liquid emulsions already in use, however, it is difficult to produce layers of uniform thickness and thin layers are more likely to have stress artifacts occur during drying. The alternative approach is to count only those grains overlying the cell and then to apply a correction factor determined from the efficiency curves. Both methods require subsequent correction for self-absorption. The latter method has the advantage of simplified grain counting but is very dependent on an accurate HD determination while the former is less dependent on HD but suffers the difficulty of delineating the area around the cell to be counted and thus requires greater care in slide preparation to ensure adequate spacing of the specimens.

CONVERSION OF GRAIN COUNTS TO ABSOLUTE RADIOACTIVITY

Corrected grain counts must still be converted into a measure of absolute radioactivity. The common practise of apportioning total filterable radioactivity has several potential sources of serious error. This procedure has assumed that all of the filterable radioactivity was associated only with the organisms counted microscopically. Neglect of the smaller species during counting as well as the destruction of delicate cells during processing will lead to an overestimation of activity of the remaining organisms, the magnitude depending upon the species composition. Additionally there is the filtration effect (Arthur and Rigler 1967) in which disintegrations per ml retained on the filter increases with decreasing filtration volumes. This effect has been attributed to the presence of filterable extracellular colloidal and organic materials (Schindler et al.

1972, Nalewajko and Lean 1972). If these materials are indeed extra-cellular under natural conditions then they are of no consequence in determining cell growth rates and should not enter into their calculation. Schindler and Nighswander (1970) have found that this material may constitute as much as 70% of total carbon fixed and thus the growth rate may be greatly overestimated.

The above sources of error probably explain the extremely high in situ growth rates estimated by Stull et al. (1973) and by Jassby and Goldman (1974), both using filterable ^{14}C as an estimate of particulate carbon formation compared to those reported in this Thesis (Parts 3 & 4) utilizing track autoradiography and Peterson et al. (1974) employing lakewater chemostats.

It is important that future autoradiography studies empirically determine a corrected grain yield per disintegration factor, through the addition of specimens of known activity to the samples, as this will allow a direct conversion of grain count to radioactivity thereby eliminating both the problems associated with neglecting species and with apportioning filterable activity. Such reference sources would also provide a control for the effects of latent image erasure and chemography and will allow the correction curves (Figs. 4 and 5) to be evaluated.

Only when chemography and latent image erasure have been carefully controlled, when grain counts have been corrected for the relationships between geometry and efficiency, and when the grain counts have been converted into disintegration rates through an internal standardization procedure, can the results of grain density autoradiography be justifiably termed quantitative and aid in elucidating the roles of individual species in community productivity.

REFERENCES

Arthur, C.R. and F.H. Rigler. 1967. A possible source of error in the ^{14}C method of measuring primary productivity. Limnol. Oceanogr. 12: 121-124.

Bleecken, Von S. 1961. Untersuchung des autoradiographischen Auflösungsver-mögens mit Strahlungsquellen verschiedenes Betaenergien. Atompraxis 7: 321-324.

Brock, L.M. and T.D. Brock. 1968. The application of micro-autoradiographic techniques to ecological studies. Mitt. Internat. Verein. Limnol. 15. 29 p.

Brock, T.D. and M.L. Brock. 1969. The fate in nature of photosynthetically assimilated ^{14}C in a blue-green alga. Limnol. Oceanogr. 14: 604-607.

Fuhs, G.W. and E. Canelli. 1970. Phosphorus-33 autoradiography to measure phosphate uptake by individual algae. Limnol. Oceanogr. 15: 962-967.

Gutel'makher, B.L. 1973. Autoradiography as a method of determining the relative contribution of individual algal species to the primary production of plankton. Hydrobiological J. 9: 61-64.

Hendler, R.W. 1959. Self-absorption correction for carbon-14. Science 130: 772-777.

Jassby, A.D. and C.R. Goldman. 1974. Loss rates from a lake phytoplankton community. Limnol. Oceanogr. 19: 618-627.

Jitts, H.R. and B.D. Scott. 1961. The determination of zero thickness activity in geiger counting of C^{14} solutions used in marine productivity studies. Limnol. Oceanogr. 6: 116-123.

Knoechel, R. and J. Kalff. 1975. Algal sedimentation: the cause of a diatom - blue-green succession. Verh. Internat. Verein. Limnol. 19: in press (Part 3 , this thesis).

Knoechel, R. and J. Kalff. 1976. Track autoradiography, a method for the determination of phytoplankton species productivity. Limnol. Oceanogr. in press (Part 2, this thesis).

Levi, H. and A.W. Rodgers. 1963. On the quantitative evaluation of autoradiograms. Mat. Fys. Medd. Dan. Vid. Selsk. 33(11), 51 p.

Maguire, B., Jr. and W.E. Neill. 1971. Species and individual productivity in phytoplankton communities. Ecology 52: 903-907.

Nalewajko, C. and D.R.S. Lean. 1972. Retention of dissolved compounds by membrane filters as an error in the ^{14}C method of primary production measurement. J. Phycol. 8: 37-43.

Peterson, B.J., J.P. Barlow and A. Savage. 1974. The physiological state with respect to phosphorus of Cayaga Lake phytoplankton. Limnol. Oceanogr. 19: 396-408.

Rogers, A.W. 1969. Techniques of Autoradiography (revised ed.) Elsevier, Amsterdam, London, New York 338 p.

Salpeter, M.M., L. Bachmann and E.E. Salpeter. 1969. Resolution in electron microscope radioautography. J. Cell Biol. 41: 1-20.

Schindler, D.W., and J.E. Nighswander. 1970. Nutrient supply and primary production in Clear Lake, Ontario. J. Fish. Res. Bd. Canada 27: 2009-2036.

Schindler, D.W., R.V. Schmidt, and R.A. Reid. 1972. Acidification and bubbling as an alternative to filtration in determining phytoplankton production by the ^{14}C method. J. Fish. Res. Bd. Canada 29: 1627-1631.

Stross, R.G. and S.M. Pemrick. 1974. Nutrient uptake kinetics in phytoplankton: a basis for niche separation. J. Phycol. 10: 164-169.

Stull, E.A., E. de Amezaga, and C.R. Goldman. 1973. The contribution of individual species of algae to primary productivity of Castle Lake, California. Verh. Internat. Verein. Limnol. 18: 1776-1783.

Vollenweider, R.A. (ed.) 1974. A manual on methods for measuring primary production in aquatic environments. I.B.P. Handbook No. 23 (2nd ed.) Blackwell Scientific Publications, Oxford. 225 p.

Watt, W.D. 1971. Measuring the primary production rates of individual phytoplankton species in natural mixed populations. Deep Sea Res. 18: 329-339.

Part 2

Track autoradiography, a method for the determination

of phytoplankton species productivity

ABSTRACT

Track autoradiography permits the quantitative determination of ^{14}C fixation rates of individual phytoplankton species within natural communities following in situ incubations. Rates measured are comparable with those obtained by liquid scintillation counting. Procedures are described and an example of field results is presented. The new method permits elucidation of the role of different algal components in energy flow and also provides a powerful tool for investigating the causes of algal succession in nature .

INTRODUCTION

Although many studies have investigated the production of phyto-plankton communities the role of individual species and the causes for species succession remain obscure. Grain-density autoradiography, a potentially useful tool in understanding phytoplankton dynamics, can be used quantitatively (see Part 1, this thesis) but requires very elaborate control procedures plus the subsequent application of correction factors for the complex effects of size and shape of the specimen on the efficiency of grain production. It is the purpose of this paper to describe an alternative technique, track autoradiography, which we utilize under both laboratory and field conditions to provide absolute quantification of in-dividual species productivity. This technique is relatively free of the many difficulties encountered in grain density studies and the determination of efficiency is greatly simplified.

In grain-density autoradiography a thin emulsion is applied to the specimen and a count of silver grains is made after exposure and development. In track autoradiography a thick emulsion layer is applied so that the passage of a beta particle is recorded as a string of silver grains termed a track. This track is a unique response of the emulsion to the particle and thus there is no confusion with background grains and chemical effects.

Experimental procedure

The ^{14}C dosage is adjusted according to the alkalinity and incubation conditions encountered. The optimum level of labelling for highest pre-cision is 0.1 - 1.0 disintegrations $cell^{-1} day^{-1}$ while the usable range is between 0.01 and 10 disintegrations $cell^{-1} day^{-1}$.

After incubation samples are preserved with 5 - 6 drops of acid
lugols fixative per 100 ml. (Vollenweider, 1974).

Slides to be used for autoradiography are vigorously washed in strong
detergent to make them hydrophilic and are then rinsed and immediately
dipped in a filtered gelatin subbing solution (5g gelatin plus 0.5g chrome
alum liter^{-1}, Rogers 1969) following which they are oven dried.

The preserved samples are concentrated and then rinsed with distilled
water using a plexiglas sliding chamber apparatus (fig.7) modified after
Coulon and Alexander (1972). The use of an O-ring between the upper and
lower plates obviates the need for a grease seal while a coverslip on top of
the sedimentation tube (see Utermöhl, 1958) further prevents leakage by
producing a vacuum. The sedimentation tube we use is 1.6 cm in diameter
while the tube height is a function of the degree of concentration required.
Any inorganic ^{14}C remaining in the solution is driven off during the
succeeding evaporation stage since the lugol preserved samples have a pH of
about 4.0. Rinsing is desirable, however, because non-rinsed slides tend to
have a higher number of background grains due to chemography (see Part
1, this thesis) which can make track recognition difficult. In practice
we routinely rinse slides five times with distilled water allowing at least
2 or 3 hours between rinses and usually including one or two turbulent
rinses in which the material is resuspended followed by overnight resettling
(fig.7). The final (6th) rinse is turbulent and consists of a 100 mg/l
gelatin solution which, when evaporated, provides a suitable base for the
nuclear emulsion. Upon completion of rinsing the sedimentation tube is
removed and the remaining water gradually replaced with ethanol by a vapor

Figure 7. Settling chambers positioned from left to right for

settling, draining, refilling for convection rinse,

and refilling for turbulent rinse.
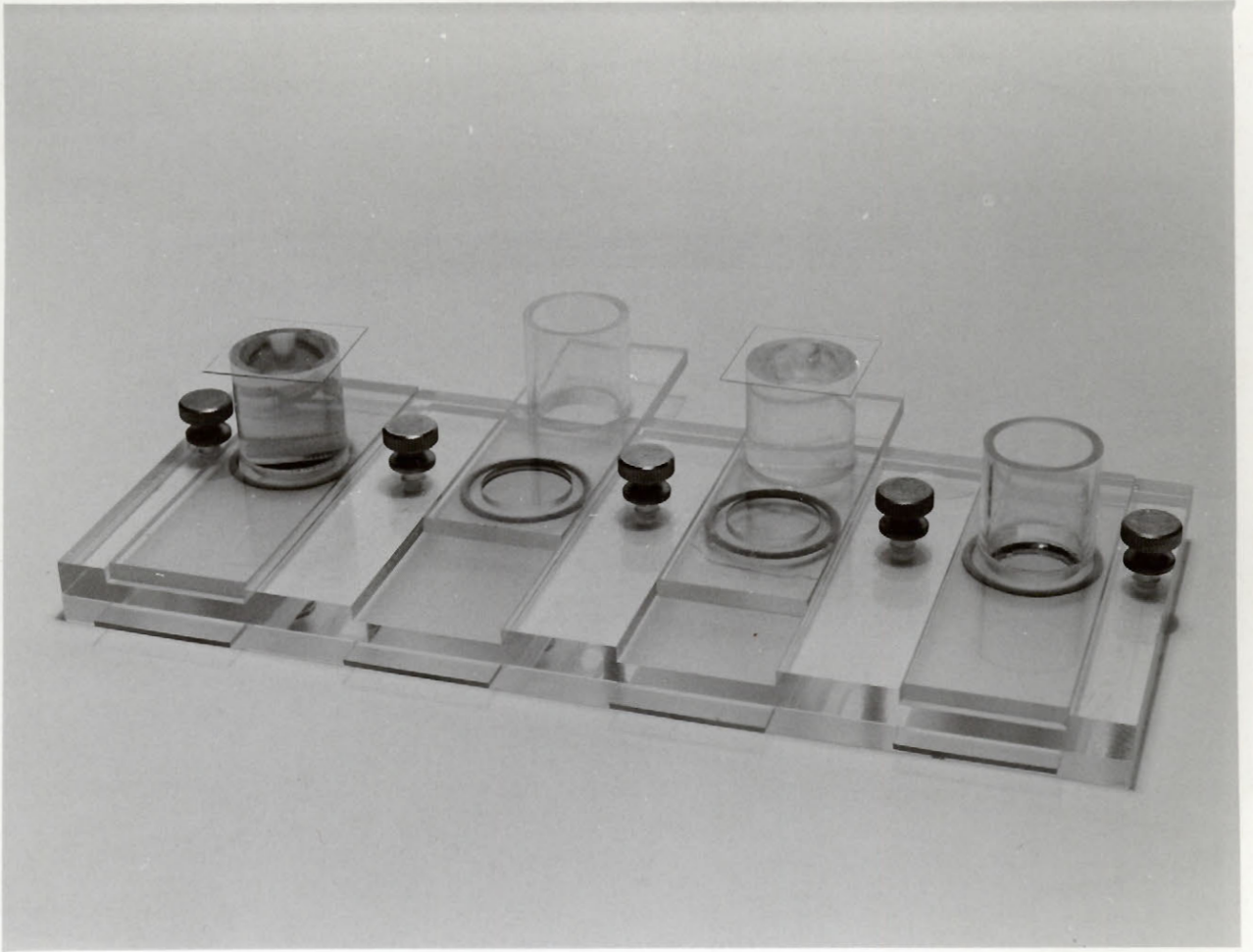
substitution process (Sanford et al. 1969). The subsequent drying
is facilitated with silica gel. Air circulation and frequent changes
of the gel are needed when large numbers of slides are processed.

Autoradiography

We use Kodak NTB3 Nuclear Emulsion, with Kodak NTB2 a second choice
because it has a smaller grain size and lower sensitivity. Where avail-
able Ilford L-5 appears suitable (Rogers, 1969). The emulsion is melted
in a waterbath to approximately 30°C and then poured into a Coplin jar or
other suitably small container for slide dipping. Each slide is dipped
for a few seconds and then withdrawn and immediately turned horizontal
with the preparation side up. The bottom of the slide is wiped clean and
it is placed on an enamel tray, previously inverted in an ice bath, allow-
ing it to gel in seconds. The gelled slides are placed on a clean sur-
face and further dried for at least two hours aided by a small fan.

In order to reduce background grains the safelight (Wratten #2)
should be off both during the drying period and when the emulsion is
initially melted. Further details regarding darkroom procedure can be
found in Rogers (1969). When drying is completed the slides are placed
in black plastic slide boxes, containing freshly dried silica gel
(special low humidity indication type 938), and are then wrapped in foil
and stored in a refrigerator during exposure. A 2-14 day exposure
produces the best results. Longer exposures can result in latent image
erasure (fig.8) while the precision of very short exposures is a function
of the accuracy of correction for the lag period between the time the slide
is dipped and when the emulsion is sufficiently dry to start recording
tracks (fig.9). Slides are developed at room temperature (20-22°) in

Figure 8. Relation between developable latent images (tracks $\text{cell}^{-1}\text{day}^{-1} \times 10^{-2} \pm 95\%$ confidence limits) and length of exposure (days) indicating significant latent image erasure following long exposure.
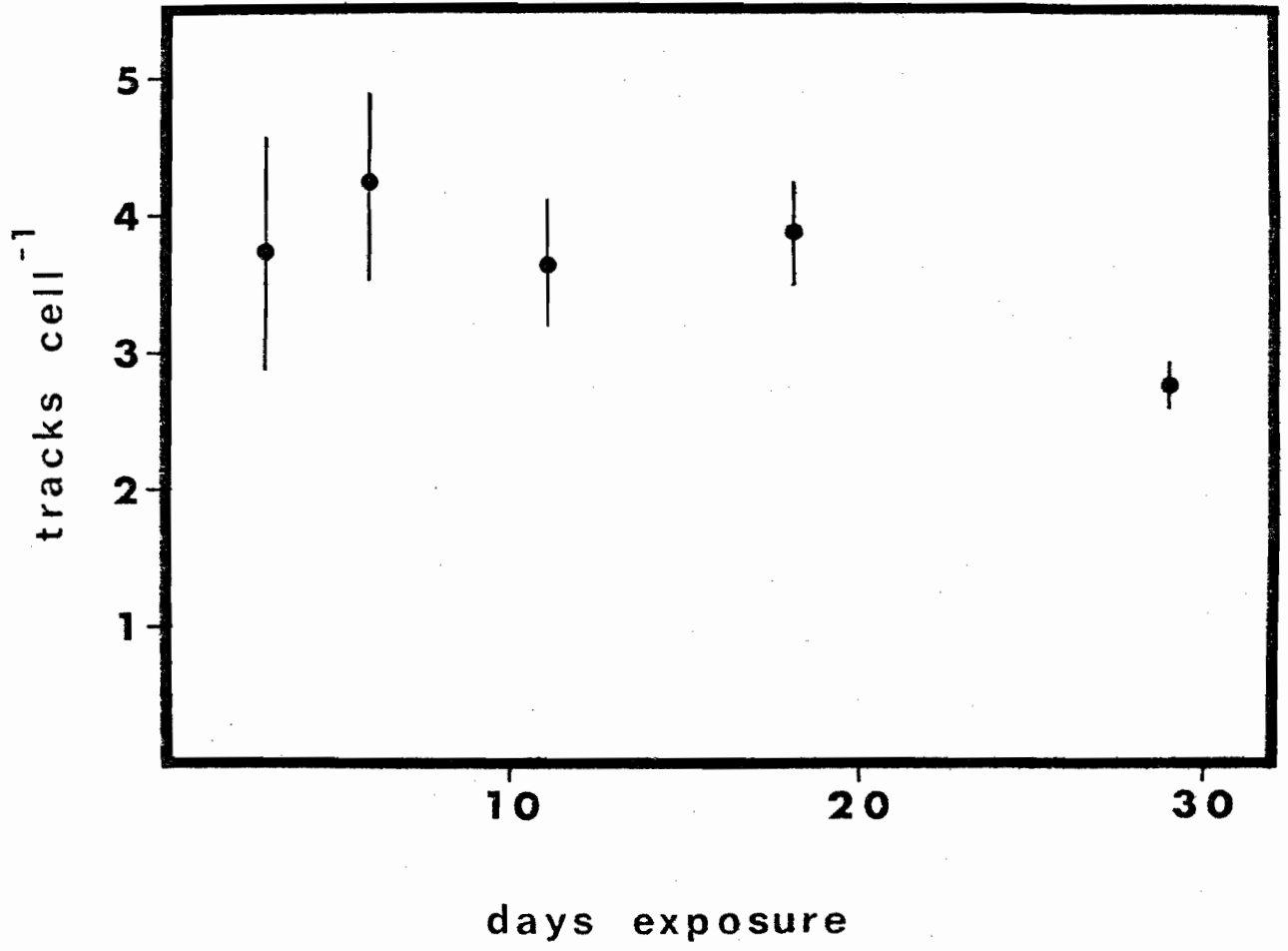
Figure 9. Relation between tracks per cell and exposure period

(hours). The intercept (2.4 hours) shows that the

emulsion is insensitive to beta particles until

completely dry (y = 0.0268 x -0.0649; r = 0.97,

p < 0.01). Data from Table 2.
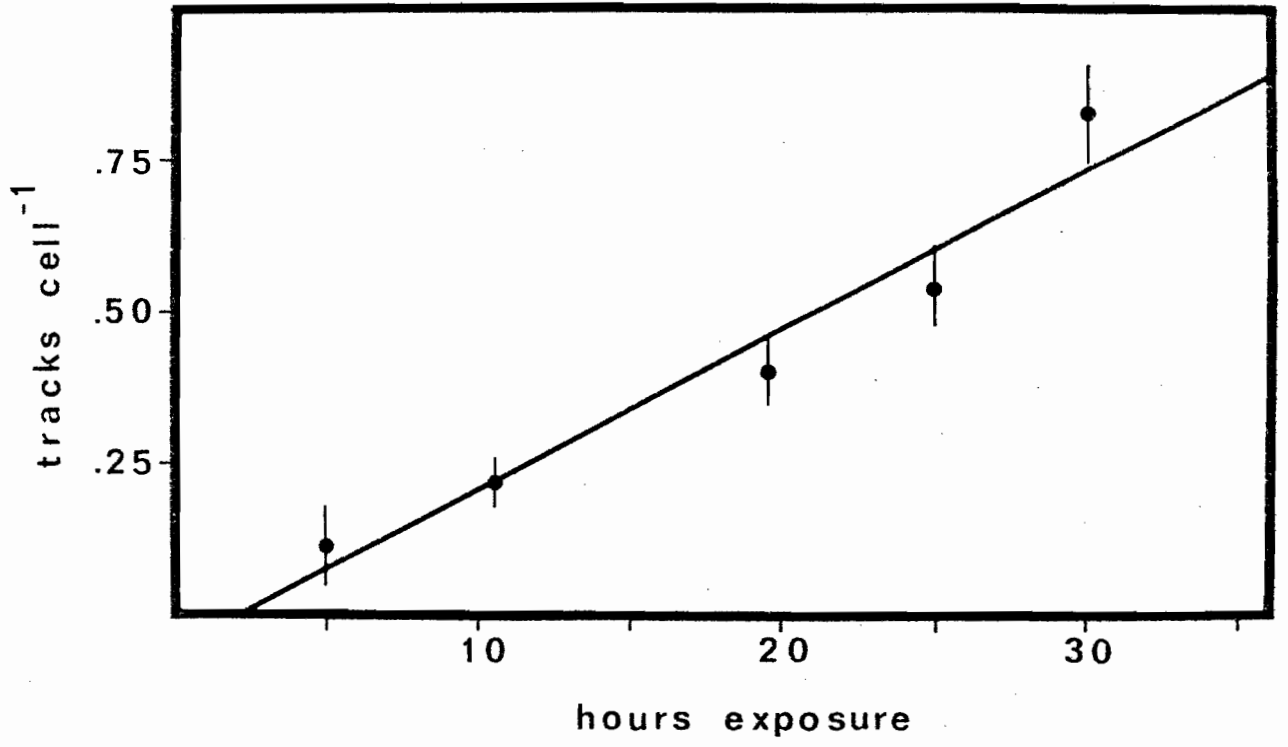
staining dishes with plexiglas holders   that permit horizontal developing with minimum stress on the emulsion.   It is crucial that all the solutions are at exactly the same temperature otherwise the emulsion tends to separate from the slide.   Development time is 8-10 minutes (see below) with magnetic stirring in Kodak D-19 developer followed by 5 minutes in a 1% acetic acid stop bath and finally 30 minutes each in 30% and 10% sodium thiosulfate fixer.   The slides are given two water rinses of at least 15 and 30 minutes following which the excess emulsion is removed and the bottom of the slide is wiped clean.

After complete drying the slide is rewetted with 2 drops of 30% glycerine and a coverslip is mounted.   Evaporation of the excess liquid yields a firm and durable permanent mount in a few hours.   After a day or two the gelatin layer should be at least $35 - 50$ μm thick and the slide is ready for counting.   Slides with layers thinner than 25 μm should be discarded.   These normally result when the emulsion was too hot, or was allowed to drip off of the slide or if there was too long a delay between dipping and gelling.

Ideally, development time should be long enough that all tracks are complete but not so long as to produce an unnecessarily high background (fig.10).   The exact time depends on the rate of stirring and number of slides in the tray as well as the temperature and strength of the developer and thus should be established for the particular procedures used in each laboratory.   We observe that high stirring rates are necessary to circulate the solutions when using horizontal slide holders.   Much slower rates are required when using the standard vertical holders as too

Figure 10. Relation between tracks per cell $\pm$ 95% confidence

limits (————) and development time (minutes). An

exposure of about 8 minutes provides an adequate

safety margin without production of high background

(- - -, visible grains per 1000 um^2).
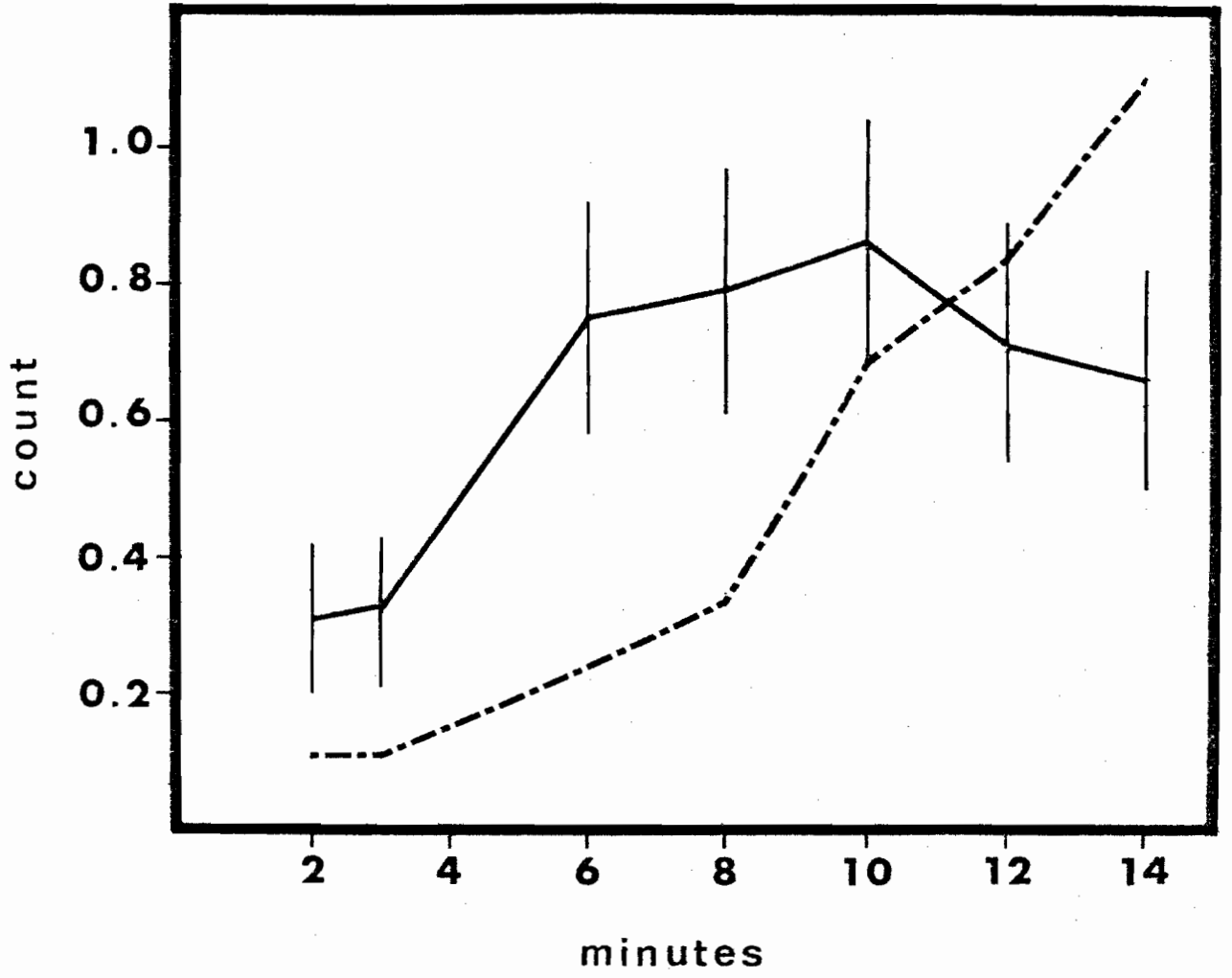
rapid stirring can result in separation of the emulsion from the slide. It is suggested that a small number of a test organism with known labelling be added to each slide as an internal check on the adequacy of the preparation and development.

Slides prepared as described above readily permit the examination of even delicate flagellates (fig.11) with minimal interference from the overlying emulsion.

Track counting

Track counting is a skill readily acquired. We define a track as a trace consisting of at least four silver grains arising within 5 μm of the cell (fig.12). The ease of discerning tracks is a direct function of the optical system used. We routinely use a Wild phase contrast microscope at 700-900x. With a similar quality Zeiss system the cell image interfered significantly with the resolution of the overlying tracks. This effect can be reduced by using the phase 3 condenser with the phase 2 objective for counting tracks followed by a return to phase 2 for locating the next organism.

Statistical analysis

If the carbon fixation rates of individual cells of a species reflect a normally distributed population mean the frequency distribution of the cellular disintegration rate will fit a Poisson model because the disintegrations are a random and rare occurrence. Analysis confirms that the experimental data fit the expected distribution (Table 2). The statistical significance can be tested with either a chi square or "G" computation (Sokal and Rohlf 1969). The confidence limits for the mean are determined following Elliott (1971) as:

$$\overline{x} \pm t \sqrt{\dfrac{\overline{x}}{n}}$$

$\overline{x}$ = mean tracks/cell

n = number of cells scored

t = Student t for n and significance level desired.

Since the data have a Poisson distribution they must be transformed
before statistical procedures requiring a normal distribution are applied.

Table 2. Statistical comparison of observed frequency

distributions with those expected from a Poisson

model showing that the deviations are not

significant (p > 0.1).

exposure (h)		class (tracks per cell)					G^*	$df^\dagger$	p	$x\pm95\%$ conf. limits
		0	1	2	3	4				
5.0	f obs.	446.0	52.0	2.0			0.207	0	----	0.112±0.029
	f exp.	447.0	50.1	2.8						
10.6	f obs.	406.0	94.0	7.0	0.0		1.656	1	0.1<p<0.5	0.213±0.040
	f exp.	409.7	87.3	9.3	0.7					
19.6	f obs.	339.0	140.0	27.0	3.0	0.0	0.172	1	0.5<p<0.9	0.399±0.055
	f exp.	341.6	136.2	27.2	3.6	0.4				
25.0	f obs.	294.0	150.0	49.0	7.0	0.0	1.476	2	0.1<p<0.5	0.538±0.064
	f exp.	292.0	157.1	42.2	7.6	1.0				
30.0	f obs.	217.0	178.0	82.0	20.0	3.0	0.540	2	0.5<p<0.9	0.828±0.080
	f exp.	218.5	180.9	74.9	20.7	4.3				

G test calculated with lumping of all low frequency classes so that no f exp. is less than 5.0

Degrees of freedom equals the number of classes in the G test minus two.

Figure 11. Representative algae on track autoradiography slides.
A. _Cryptomonas_ _rostrataformis_ (45 μm). B. _Dinobryon_
bavaricum (12 μm). C. Two _Rhodomonas_ _minuta_ (8 μm).
D. Four _Chrysochromulina_ _parva_ (4 μm). E. _Fragilaria_
crotonensis (60 μm) with epiphytes. All photographs
phase contrast & measurements represent cell lengths.
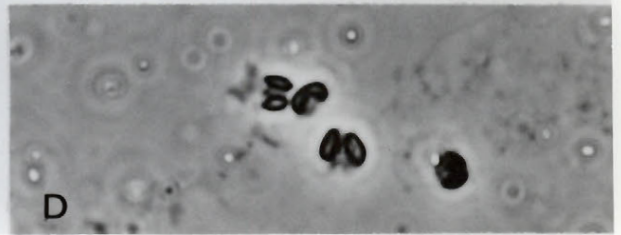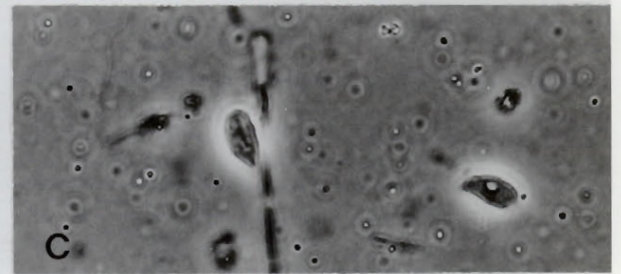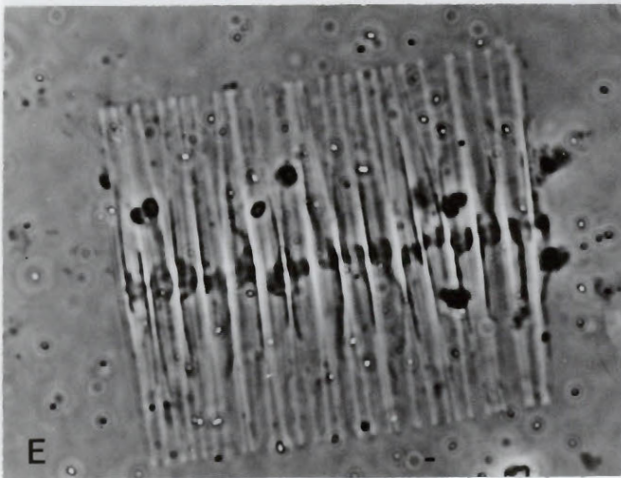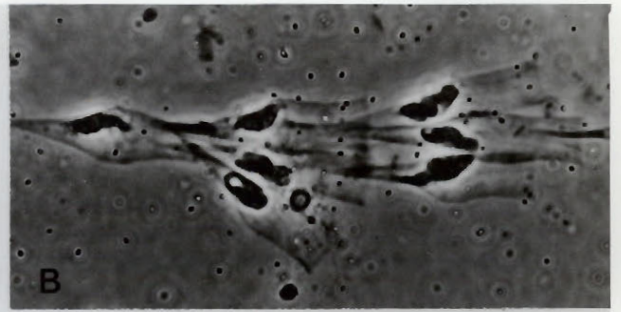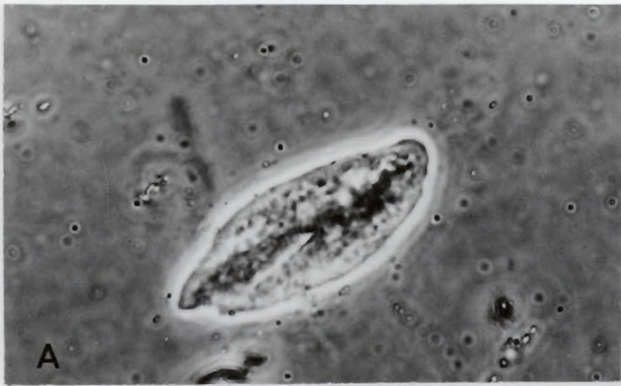
Figure 12. Two cells of _Tabellaria fenestrata_ with one track

each. Left track rising vertically and only partially

in focus.
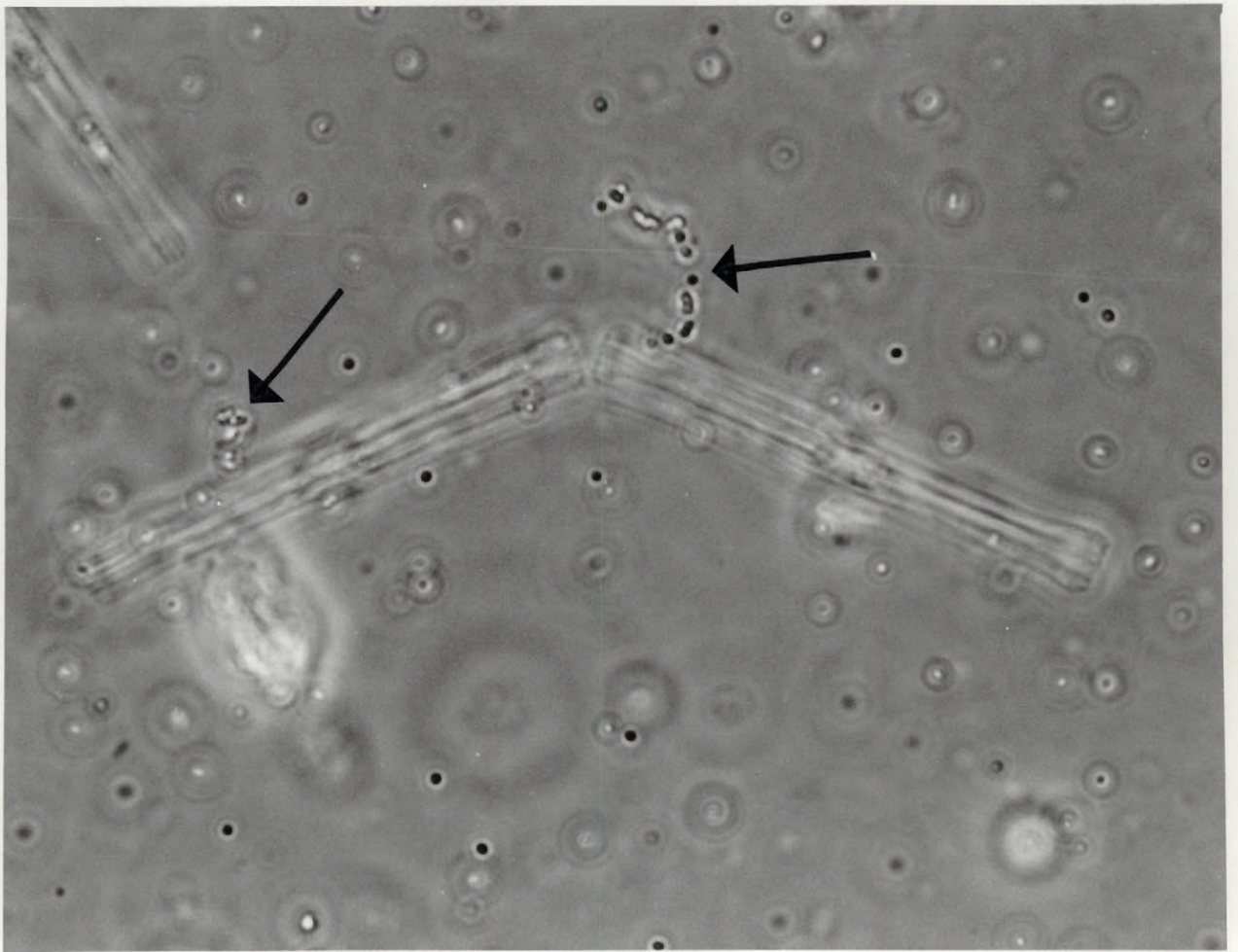
RESULTS

The track technique compared favorably with the ^{14}C filtration method using a non-axenic <u>Chlorella</u> culture in the laboratory. Determination of the filterable fraction by scintillation counting yielded an estimate of 2032 dpm ml^{-1}(n = 6). Linear regression analysis of the autoradiography results, consisting of track counts on 500 cells from each of five slides representing different exposure times, yielded y = 0.0268 x -0.0649 (fig.9, r = 0.97, p < 0.01). The intercept of the regression line was used as an adjusted estimate of zero time and the cellular disintegration rate was computed from the slope as:

$$\frac{0.0268 \ (\text{tracks cell}^{-1} \text{ hour}^{-1}) \times 2.0}{0.86 \times 0.98 \times 60 \ (\text{minutes hour}^{-1})} = 1.060 \times 10^{-3} \text{ dpm cell}^{-1}$$

The factor 2.0 corrects for the source:emulsion geometry and 0.86 is a factor correcting for the 14% of the beta particles with insufficient energy to produce a four grain track (Levi and Rogers 1963) while 0.98 corrects for a 2% loss due to self-absorption (see Part 1, this thesis) This cellular disintegration rate combined with the mean cell count of 1.88 x 10^{6} cells ml^{-1} (derived from counts of 10 Whipple fields from each of six replicate samples in a 0.1 ml nanoplankton counting cell) results in a volumetric disintegration rate of 1993 dpm ml^{-1} which agrees well with the above scintillation determined rate of 2032 dpm ml^{-1}.

In field experiments we use track autoradiography to determine individual species productivity during <u>in situ</u> incubations. The ideal ^{14}C dosage for 2 hour incubations and a total available inorganic carbon content of 6.4 mg l^{-1} is approximately 0.5 μCi per 265 ml sample.

A vertical _in situ_ incubation series permits the determination of the carbon fixation of a particular species as function of light and depth. The example shown (Fig. 13) is for the diatom _Tabellaria fenestrata_ on June 14, 1972 when the population was in early exponential growth. The response curve indicates an I_k and P_{max} of approximately 0.06 ly min^{-1} (PAR) and 0.4 pg C cell^{-1} hr^{-1} respectively.

In situ measurements can also elucidate algal dynamics. Thus, from measurements made at regular intervals during the summer season, we have been able to examine an algal succession in which _Tabellaria fenestrata_ was replaced by _Anabaena planctonica_ (see Part 3, this thesis). Comparative analysis of the growth rates for each species enabled us to determine that the cause of the succession was increased sedimentation of the diatom rather than a superior growth rate of the blue-green. We are now using the technique to elaborate the seasonal and diel dynamics of the common net and nanoplankton species in a north temperate zone lake. A second study in our laboratory presently is focusing on the phosphorus flux through the components of the phytoplankton community using ^{33}P as a tracer.

In conclusion, our results demonstrate the suitability of track autoradiography in obtaining accurate data on the activity of individual species within algal communities and thus permitting elucidation of the role of different algal components in energy flow as well as providing the means to investigate the causes of algal succession in nature.

Figure 13. Relation between in situ carbon fixation

(pg C cell^{-1} hr^{-1}) and light (ly min^{-1} P.A.R.)

for Tabellaria fenestrata on 14 June 1972.

Curve fitted visually.
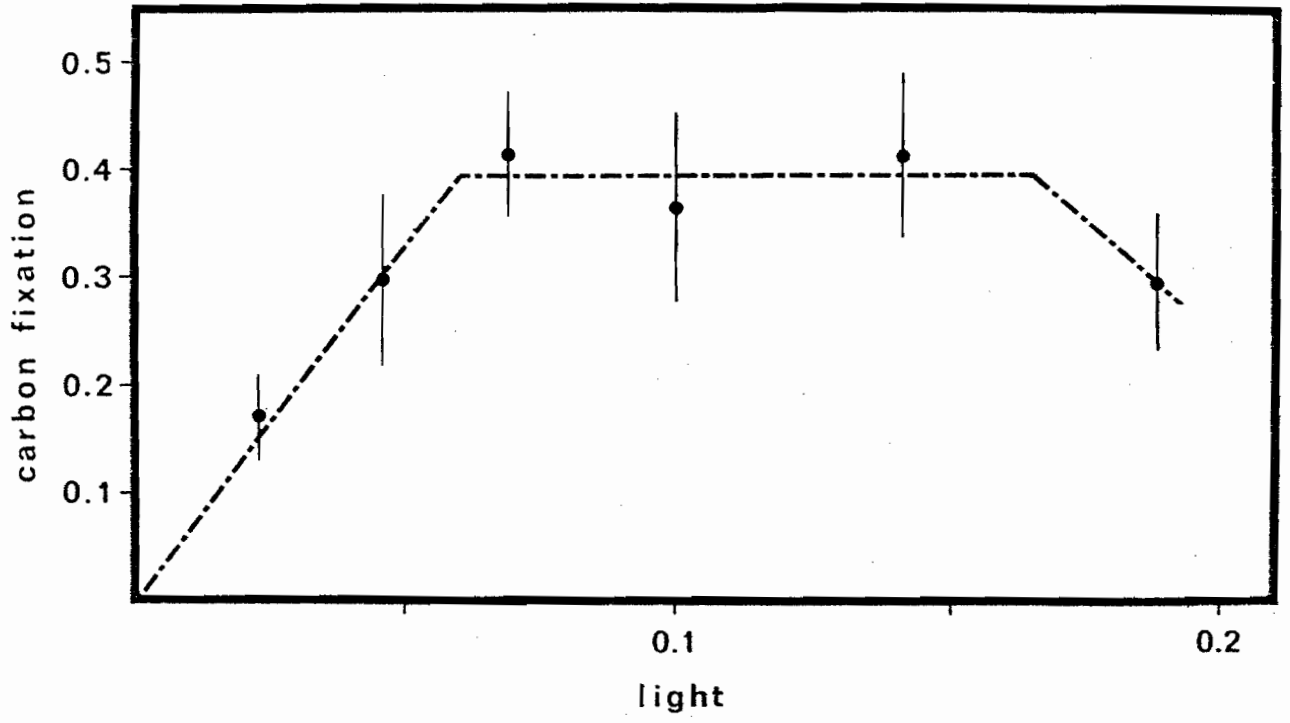
REFERENCES

Coulon, C. and V. Alexander. 1972. A sliding-chamber phytoplankton settling technique for making permanent quantitative slides with applications in fluorescent microscopy and autoradiography. Limnol. Oceanogr. 17: 149-152.

Elliott, J.M. 1971. Some methods for the statistical analysis of samples of benthic invertebrates. Freswat. Biol. Assoc. Publ. 25. 144 pp.

Knoechel, R. and J. Kalff. 1975a. Algal sedimentation: the cause of a diatom - blue-green succession. Verh. Internat. Verein. Limnol. 19: in press (Part 3, this thesis).

Knoechel, R. and J. Kalff. 1976. The applicability of grain density autoradiography to the quantitative determination of algal species production: a critique. Limnol. Oceanogr. in press (Part 1, this thesis).

Levi, H. and A.W. Rogers. 1963. On the quantitative evaluation of autoradiograms. Mat. Fys. Medd. Dan. Vid. Selsk. 33(11), 51 p.

Rogers, A.W. 1969. Techniques of autoradiography (revised ed.). Elsevier, Amsterdam-London-New York. 338 p.

Sanford, G.R., A. Sands and C.R. Goldman. 1969. A settle-freeze method for concentrating phytoplankton in quantitative studies. Limnol. Oceanogr. 14: 790-794.

Saunders, G.W., F.B. Trama, and R.W. Bachmann. 1962. Evaluation of a modified C-14 technique for shipboard estimation of photosynthesis in large lakes. Mich. Univ. Great Lakes Res. Div. Publ. 8. 61 p.

Sokal, R.R. and F.J. Rohlf. 1969. Biometry. W.H. Freeman and Co., San Francisco. 776 p.

Utermöhl, H. 1958. Zur Vervollkommnung der quantitativen Phytoplankton-Methodik. Mitt. Internat. Verein. Limnol. 9. 38 pp.

Vollenweider, R.A. (ed.). 1974. A manual on methods for measuring primary production in aquatic environments. I.B.P. handbook No. 23 (2nd. ed.). Blackwell Scientific Publications, Oxford. 225 p.

Part 3

Algal sedimentation: the cause of a diatom -

blue-green succession

ABSTRACT

The in situ carbon fixation of individual phytoplankton species was quantitatively determined through the application of track autoradiography in a small Quebec lake. The results enable the calculation of daily growth rates of the individual species. The decline of the summer diatom population (Tabellaria fenestrata) appears to be the result of a high sinking rate rather than a low production rate. In contrast the blue-green algal population (Anabaena planctonica) continues to increase despite a lower growth rate, and becomes dominant in the community, apparently due to a lower sinking rate.

INTRODUCTION

The mechanisms by which blue-green algae dominate eutrophic lakes during the summer have been a source of speculation (see Lund (1965) and Fogg (1969)). One major hypothesis holds that particular blue-green algal species are especially well adapted physiologically for photosynthesis under the high temperature and low nutrient conditions present while another suggests the possibility of a competitive advantage gained through the production of allellopathic substances. Both hypotheses require a higher growth rate of blue-greens than of their competitors. Alternatively it is possible that the blue-greens are favored by the elimination of other species through disease and parasitism or through limitation by a specific nutrient requirement such as that of diatoms for silica. However the decline of one or more species may also be due to a purely physical process such as sedimentation. Hutchinson, after considering the hydromechanics of the plankton, concluded that, "It is quite possible that much of the seasonal succession of the phytoplankton is due to this interrelation between turbulence and sinking speed." (Hutchinson, 1967, p. 287). Similarly, the nutrient limitation models constructed by O'Brien (1974) suggest that succession is primarily the result of species specific loss rates.

In order to determine whether the succession observed in a particular lake is the result of an active or passive process requires a knowledge of either the production or loss rates, or both, of the individual species. Although it is possible to obtain population estimates, measurements of in situ productivity and/or loss rates which

bring about the observed populations are difficult to obtain. Only during virtually monospecific blooms has it been possible to estimate productivity of a single species (Findenegg, 1971) while rate of loss can be estimated, as changes in standing crop, only during short periods when productivity is assumed to be zero or nearly so. These difficulties have prevented a thorough examination of the significance of factors such as sedimentation in succession.

In this study we examine a system where _Tabellaria_ _fenestrata_ (Lyngbye) Kutzing is replaced by _Anabaena_ _planctonica_ Brunnth. through application, for the first time, of _track_ autoradiography to the study of aquatic primary production. By this technique we have measured the _in_ _situ_ carbon fixation rates of both species allowing us to evaluate the major hypothesis-- actively or passively attained dominance. We conclude that in our case at least the observed dominance shift to the blue-green alga is the result of a passive decline of the diatom population through sedimentation.

METHODS

Experiments were carried out in Lac Hertel a small, undisturbed, naturally eutrophic lake near Montreal, Quebec of which the phytoplankton production and biomass have been reported upon (Kalff, 1972).

Samples were routinely collected from 0, 1, 2, 3, 4, and 6 meters at a fixed station in the deepest portion of the lake (8 m) with an opaque 1.5 liter PVC water bottle at approximately ten day intervals between 4 June and 12 September 1973. All sampling and handling procedures were performed inside a darkened enclosure extending over

the stern of the boat in order to minimize possible light shock. The samples were resuspended at depth in 265 ml pyrex bottles after inoculation with 0.48 μCi of ^{14}C - Na_2CO_3 as determined by Van Slyke combustion and gas-phase assay. After a two hour, midday incubation period subsamples were fixed with iodine-Lugol's solution for subsequent analysis by autoradiography.

Total incident solar radiation was measured at shoreside with either an integrating pyranometer (YSI model 67) or a direct reading pyranometer (YSI model 14138) with subsequent planimetry of the continuous chart record. Photosynthetic Available Radiation (PAR) was estimated as 46% of total incident radiation (Strickland, 1958). PAR at depth was computed after correction for extinction, measured with a submarine photometer (Rich and Wetzel, 1969) and an assumed 5% surface reflectance. Temperature profiles were taken with a YSI thermistor. Total available inorganic carbon was calculated from pH, alkalinity, and water temperature following Bachmann (Saunders et. al. 1962). Alkalinity was determined by titration to a pH of 4.8.

Permanent mount slides were prepared for phytoplankton counting by settling 5 ml samples onto slides which were then dried using ethanol-substitution (Sanford et al. 1969) and mounted in 30% glycerine. Cell number (Tabellaria) or filament lengths (Anabaena) were recorded for six crossed transects representing 3.6% and 9.8% of the slide area for Tabellaria and Anabaena respectively.

Cell volumes were estimated from formulae for simple geometric solids using cell measurements made with an ocular grid calibrated by stage micrometer. As there was no observed change in cell size with either

depth or date a mean volume for each species was computed from the pooled cell volumes for all 1 m samples. Cell carbon was estimated from the carbon content: cell volume regressions of Strathmann (1967).

The ^{14}C content of the individual cells was measured by track autoradiography wherein a thick layer(>30 μ) of photographic emulsion records the passage of a beta particle as a visible string of silver grains termed a track   (Rogers, 1967). Samples were concentrated on slides in a similar manner to those for cell counts and were then dipped in Kodak NTB-3 nuclear emulsion. Following exposure the slides were processed using Kodak D-19 developer (see Part 2, this thesis).. Track counts were normally made on at least 100 cells of Tabellaria per slide and on 25 cell sections of 20 Anabaena filaments.

The number of tracks per cell per day of exposure were converted into absolute disintegration rates through multiplication by a factor of 2.0 for the π geometry of the source plus correction for the 14% of the beta particles with insufficient energy to produce a track (Levi and Rogers, 1963) plus self-absorption factors of 4% for Tabellaria or 8% for Anabaena (Knoechel and Kalff, in preparation). Total carbon fixation was computed as total available carbon times that fraction of the ^{14}C assimilated with correction for the 6% isotope effect.

Intrinsic growth constants (k) based on observed changes in standing crop were calculated from the equation:

$$k = \frac{\ln (N_t/N_o)}{t}$$ (Eq. 1 a)

where N_o and N_t are the initial and final number of cells and t is the time interval measured in days. For Tabellaria (k_T) the assumption was made that only those cells in the epilimnion (0-4 m) at time zero were responsible for production of the total standing crop at time t, the remainder presumed lost through sedimentation, thus;

$$k = \frac{\ln (N_{t(0-8\ m)} / N_{o(0-4\ m)})}{t} \qquad \text{(Eq. 1 b)}$$

The growth constant of Anabaena was computed with equation 1 b and also with equation 1 c which assumes that the thermocline population is retained but is inactive, thus:

$$k = \frac{\ln (N_{t(0-8\ m)} - N_{o(5-8\ m)} / N_{o(0-4\ m)})}{t} \qquad \text{(Eq. 1 c)}$$

Population sizes were obtained through integration of curves of cell number versus depth (Fig. 15 and 16).

Values of the growth constant were also calculated from carbon fixation as:

$$k = 10 \ \ln \left[\frac{\bar{x} \text{ cell carbon} + \bar{x}_{(0-4\ m)} \text{ C fixation cell}^{-1} \text{ hr}^{-1}}{\bar{x} \text{ cell carbon}} \right]$$

$$\text{(Eq. 2)}$$

Mean carbon fixation rates were estimated as the unweighted mean of the 0-4 m values (Fig.18 and 19). The factor of 10 is based on our observation that approximately 20% of the total daily radiation was received during the 2 hr incubation period -- therefore 10% hr^{-1}.

We can relate the observed shift in dominance of one species over another to the difference in growth constant necessary to account for

Figure 14. Biomass versus time curves for <u>Tabellaria</u> <u>fenestrata</u> (————) and <u>Anabaena</u> <u>planctonica</u> (-----).
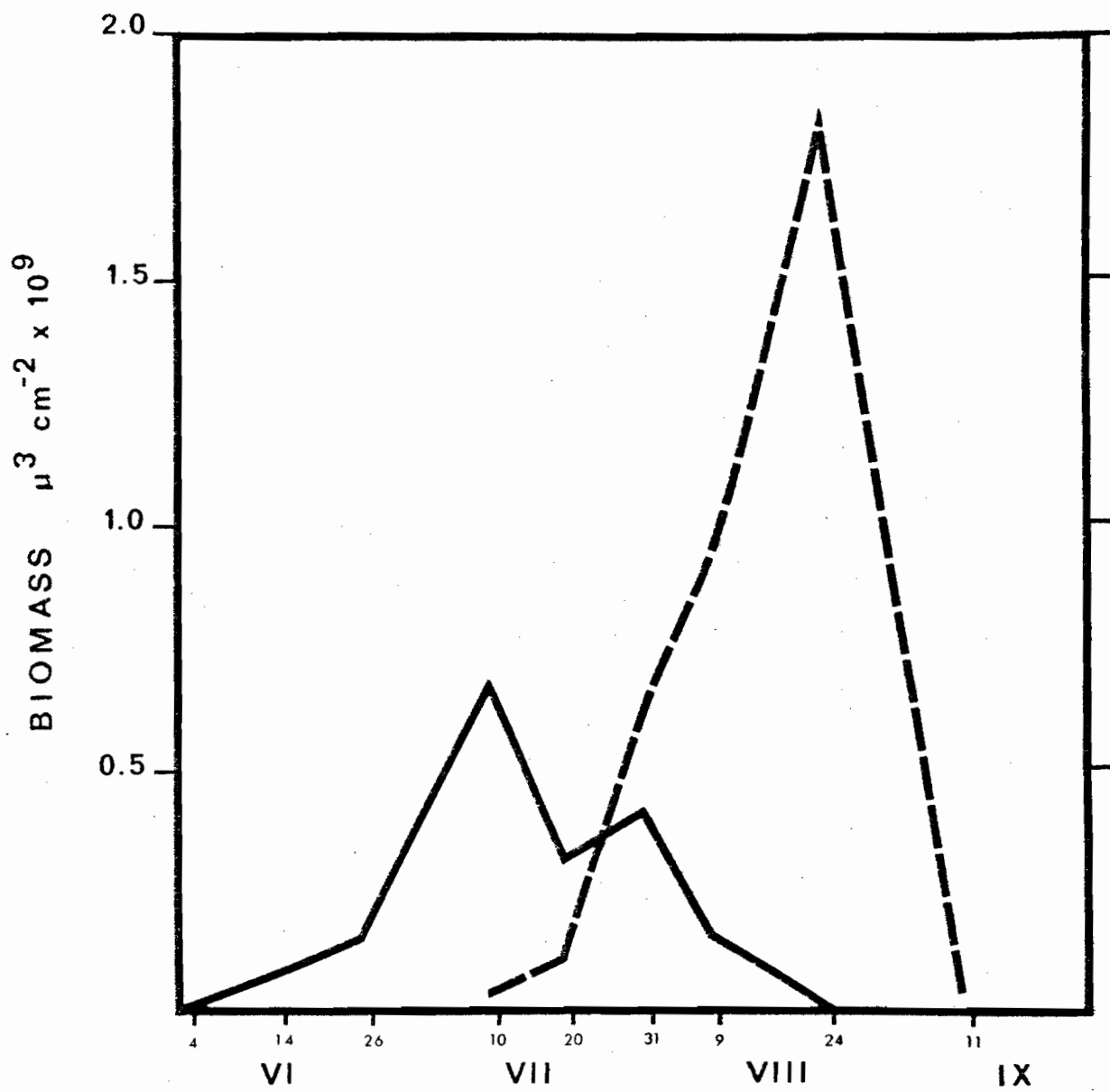
Figure 15. Depth distribution of <u>Tabellaria</u> <u>fenestrata</u>.
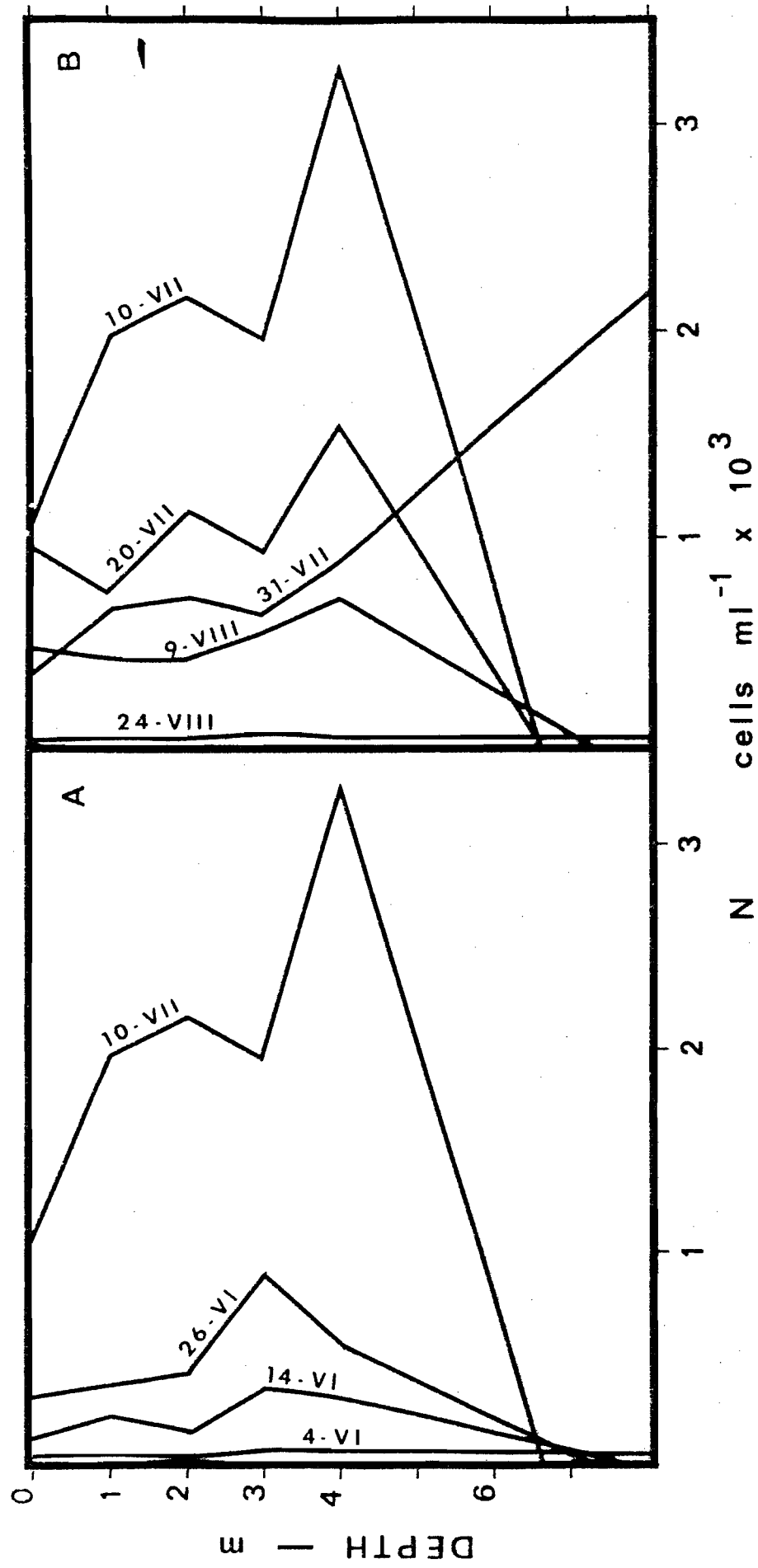
Figure 16. Depth distribution of <u>Anabaena</u> <u>planctonica</u>.
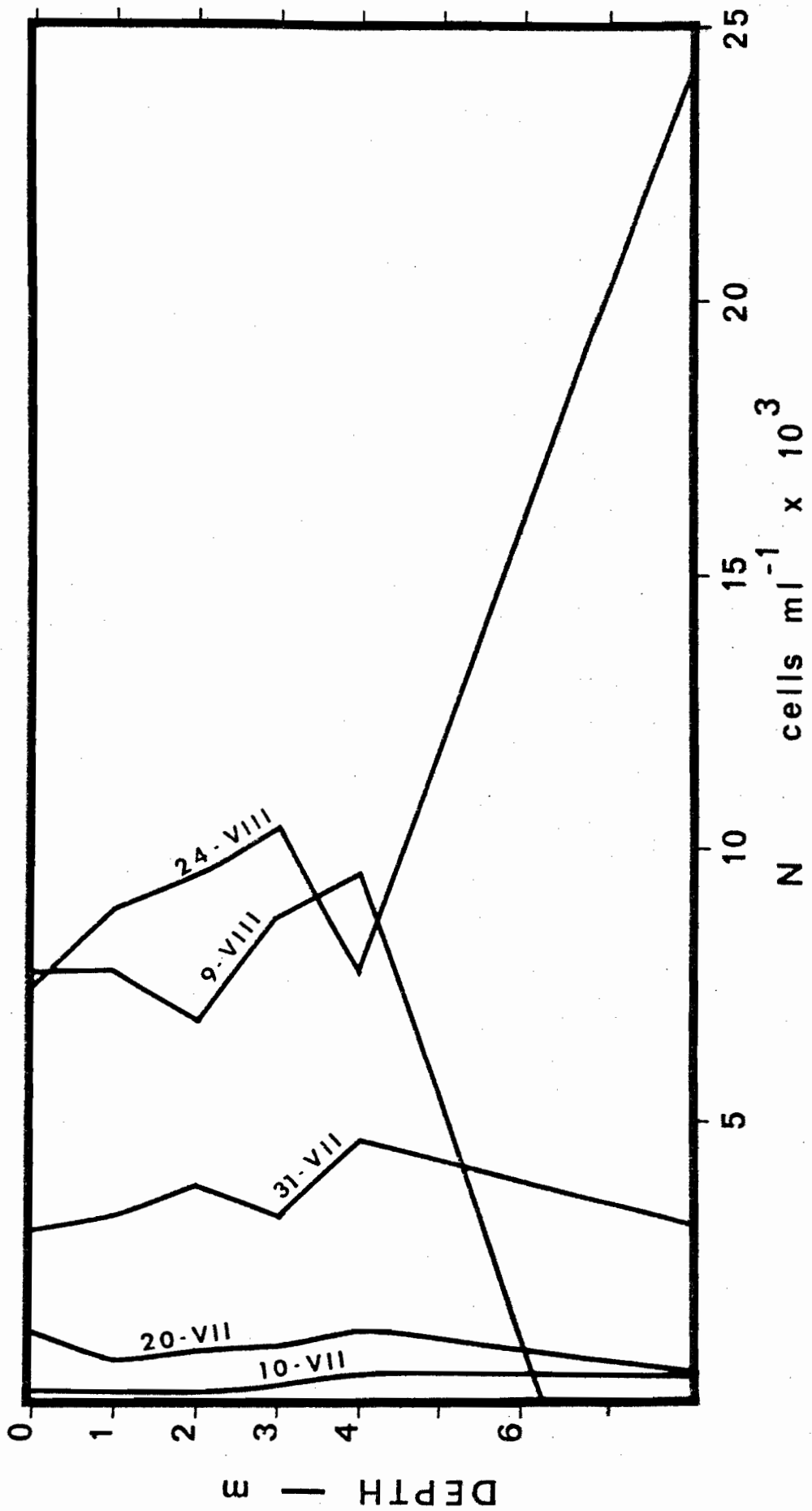
that change by differential growth through solving equation 1 a simultaneously for __both__ species, with the result:

$$k_A - k_T = \frac{\ln(1-f_o) - \ln((f_o/f_t) - f_o)}{t} \qquad \text{(Eq. 3)}$$

where f_o and f_t are the initial and final frequency of __Anabaena__ expressed as a fraction of the total __Anabaena__ plus __Tabellaria__ community and t is the time in days over which the change occurred.

The difference between the growth constant of __Tabellaria__ based on carbon fixation and that based on change in standing crop was used to calculate apparent sinking rates as:

$$v = (k_{Tc} - k_{Tn})z \qquad \text{(Eq. 4)}$$

where k_{Tc} and k_{Tn} are the growth constants estimated by carbon fixation and change in population size, z is the thickness of the epilimnion (cm) and v is the apparent sinking speed (cm day^{-1}).

RESULTS

The transition of dominance from __Tabellaria__ to __Anabaena__ occurred during late July (Fig.14). The distribution with depth of __Tabellaria__ (Fig.15) and __Anabaena__ (Fig.16) often reveals a population peak at the top of the thermocline (Fig.17, selected profiles).

Cellular carbon fixation rates of both species exhibited a consistent response to light on a day to day basis (Fig.18) despite large differences in the total incident radiation. A comparison of response curves for both species (Fig.19) reveals a general decline in the maximum fixation rates during the summer. However the reduction in carbon fixation of __Anabaena__ is greater so that its initially higher growth rate is exceeded by __Tabellaria__ during late July and August.

Figure 17. Selected temperature profiles. Thermocline depth

was unchanged on intervening sampling dates.
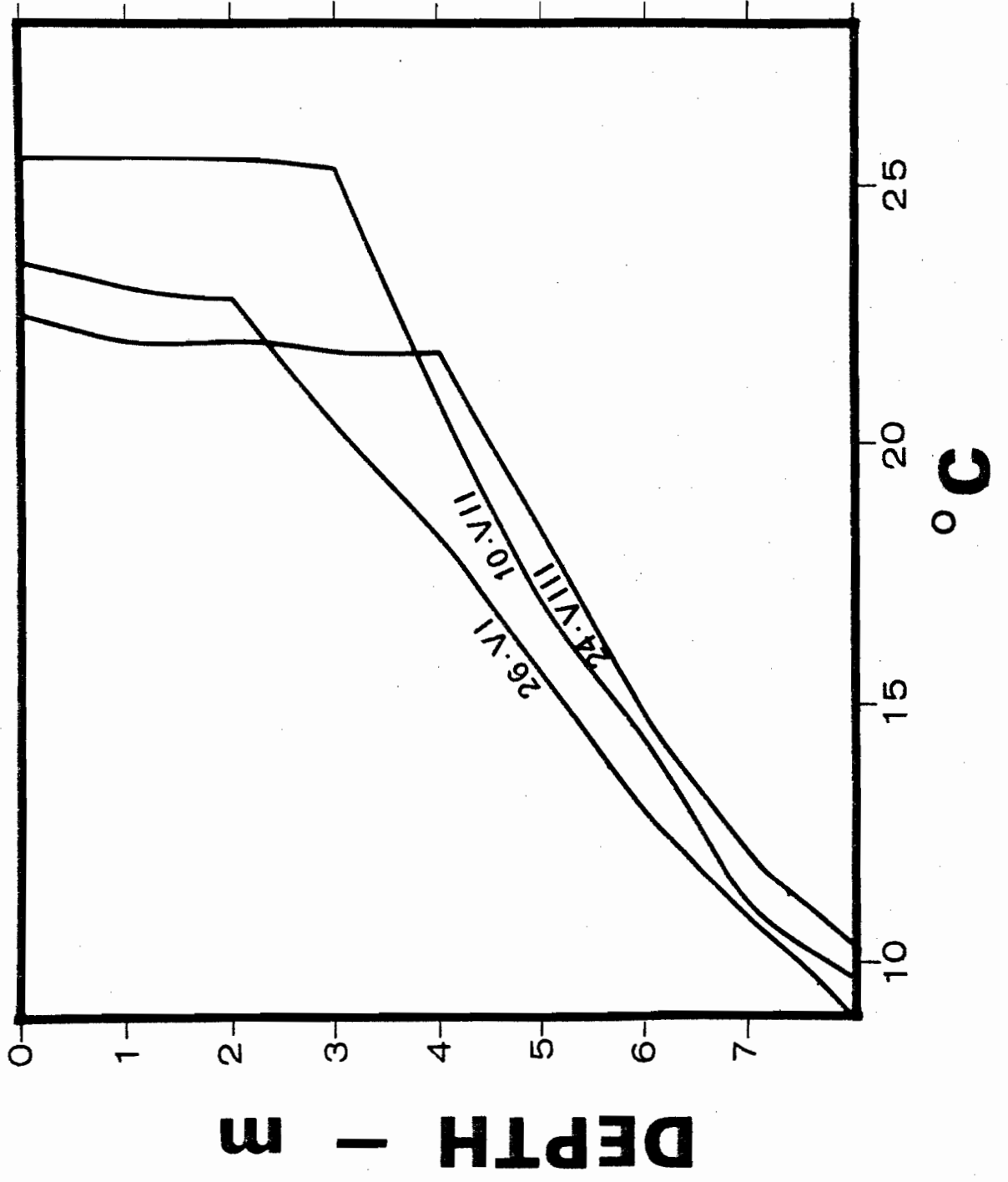
Figure 18. Carbon fixation rate on three consecutive days with widely differing total radiation values for <u>Tabellaria</u> (Fig. 18a) and for <u>Anabaena</u> (Fig. 18b) and 26 June results for <u>Tabellaria.</u>
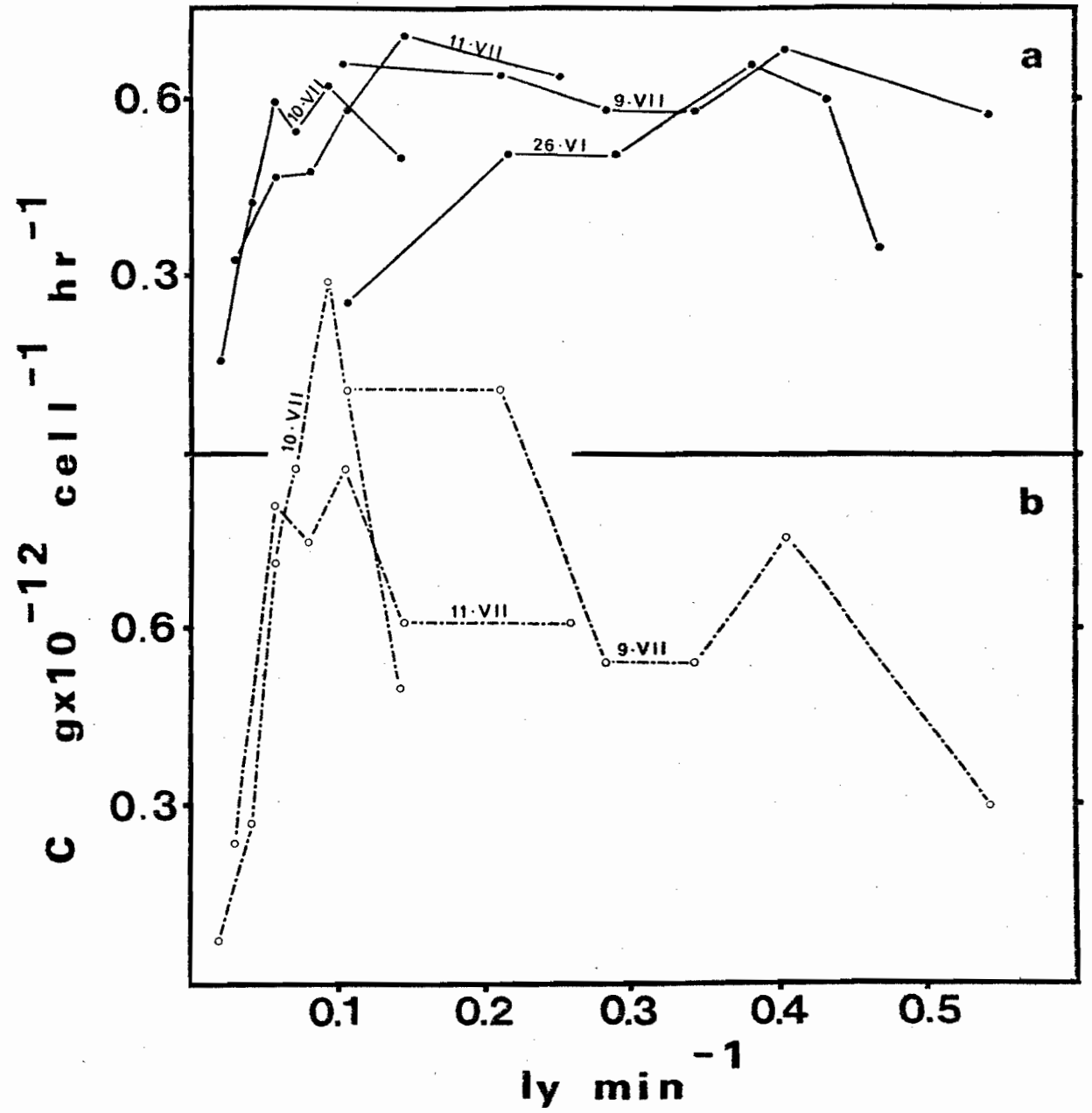
Figure 19.   Carbon fixation rates for Tabellaria (———) and
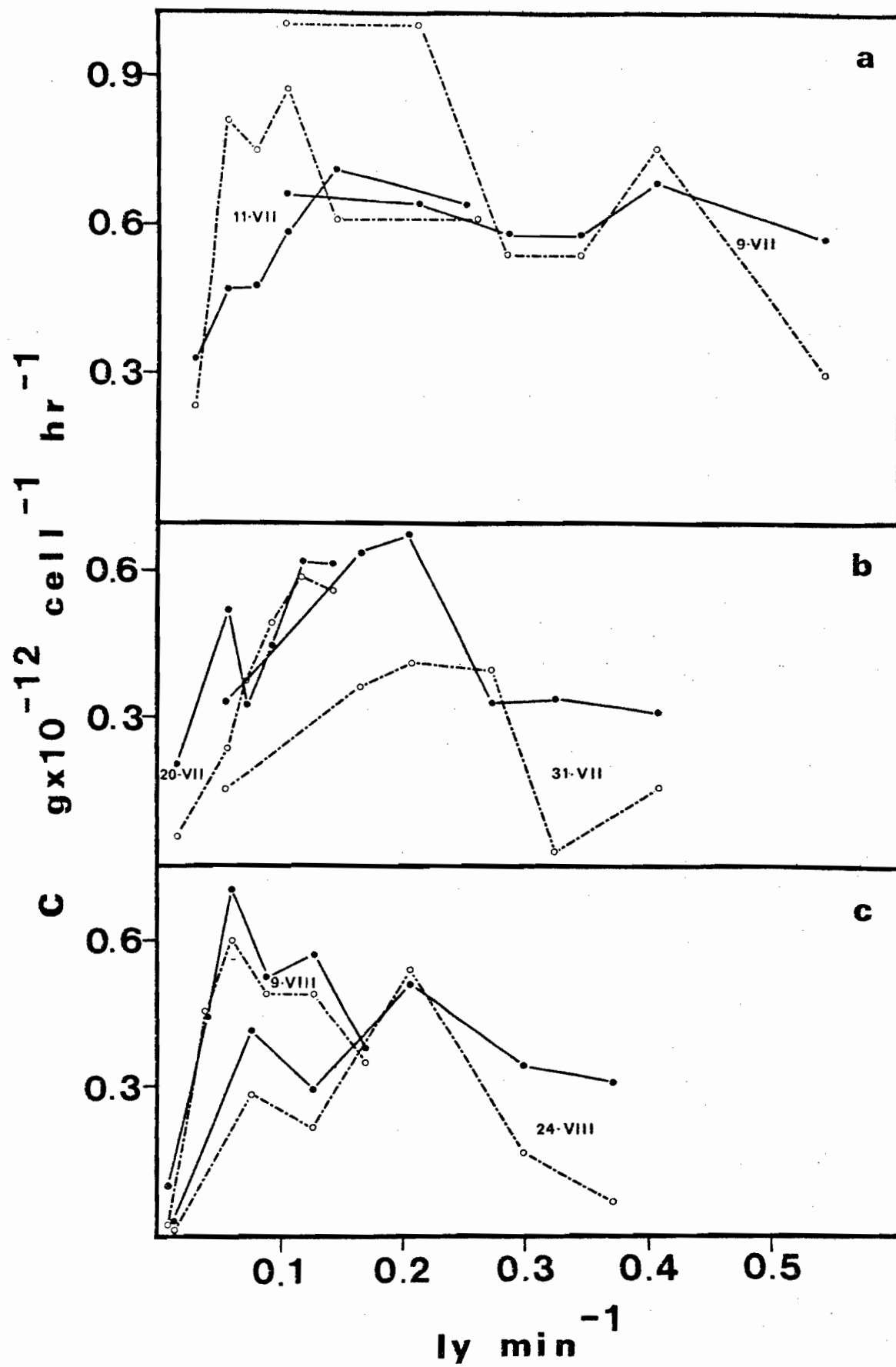
Anabaena (-----).

Mean cell volume estimates of 212 μ^3 for <u>Anabaena</u> and 528 μ^3 for

<u>Tabellaria</u> resulted in computed carbon contents of 36 and 44 picograms per

cell respectively.

Calculated values of the intrinsic growth constant (k) based on

observed changes in standing crop (Eq. 1b & 1c)and on carbon fixation

(Eq. 2) are similar for <u>Anabaena</u> throughout the sampling period while

<u>Tabellaria</u> estimates agree only during June. (Fig. 20). It should be

noted that values of k based on carbon fixation neglect the contribution

of the lower photic zone (see methods) and are thus conservative

especially in the case of <u>Anabaena</u> where buoyancy may prevent cells

produced in the thermocline from sinking to the bottom.

Comparing the necessary differences in growth constants between the

two species ($k_A - k_T$) to account for the observed shift in dominance

(Eq. 3) with those computed from carbon fixation (Table 3) indicates

that the required difference is always much greater than that which was

measured.

The estimated sinking speeds necessary to balance the observed and

measured values of k for <u>Tabellaria</u> (Fig. 20a) range from -0.5 to 85.1 cm

day^{-1} (Table 4) and show no significant correlation with the percentage

of dead cells in the population.

Figure 20. Computed growth constants based on carbon fixation

(———) and on change in standing crop (-----) for

Tabellaria (Fig. 20a) and Anabaena (Fig. 20b).

Anabaena estimates based on standing crop with

(-----) and without (-——- -——) sedimentation

(cf. Eq. 1b and 1c).
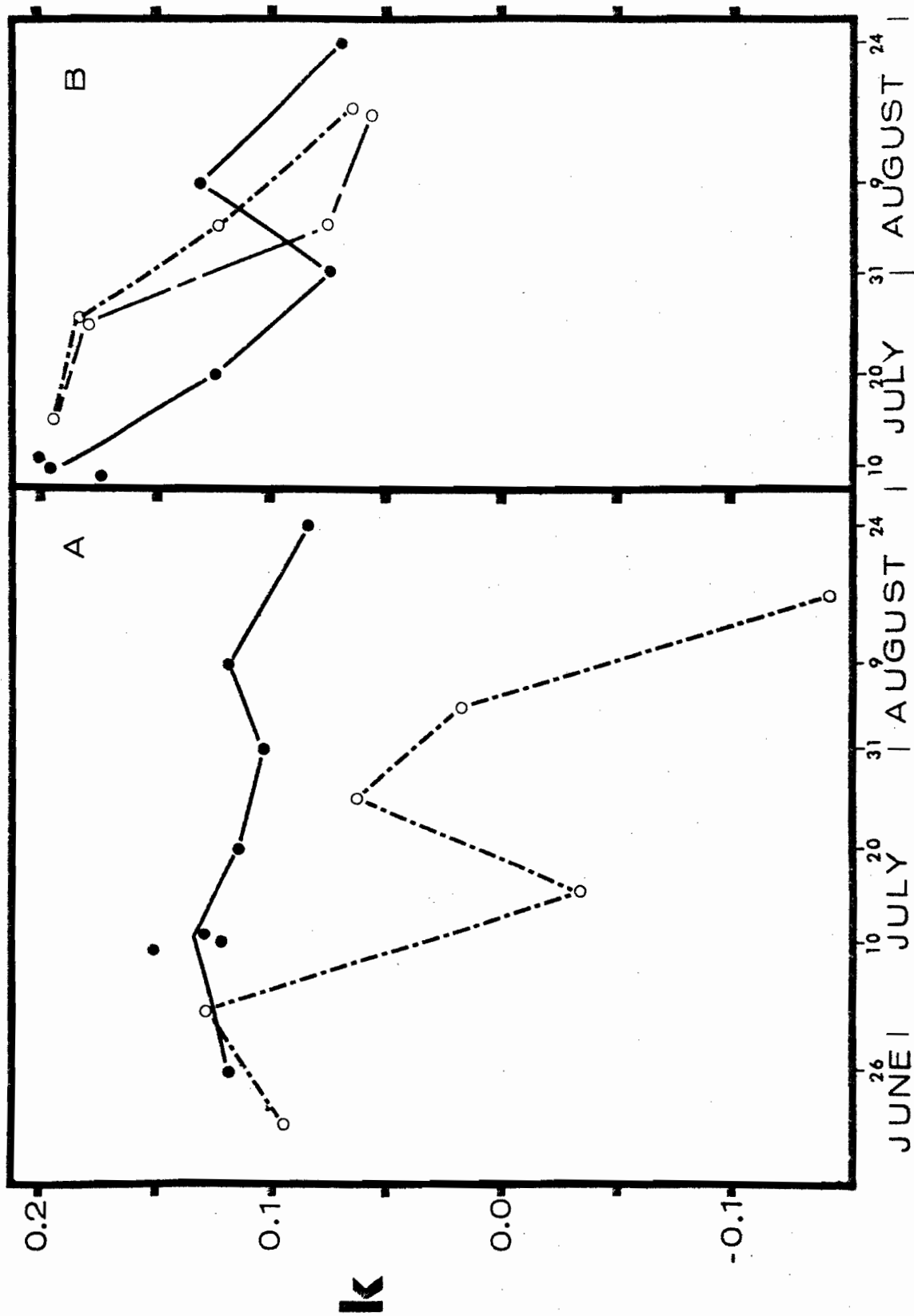
Table 3. Growth constant differences necessary to account for succession (Eq. 3) compared to the observed difference based on carbon fixation.

DATE	REQUIRED $k_A - k_T$	MEASURED $k_A - k_T$
9-11 July 1973		.056
	.176	
20 July 1973		.011
	.130	
31 July 1973		-.029
	.146	
9 August 1973		-.013
	.236	
24 August 1973		-.015

Table 4. Apparent sinking speeds necessary to balance observed

and measured rates of _Tabellaria_ growth and the

percentage of dead cells in the epilimnetic

population.

DATE	$k_{Tc} - k_{Tn}$	z	v	FRACTION DEAD
26 June 1973	.007	200	1.4	.041
3 July 1973	-.002	250	-0.5	
9-11 July 1973	.088	300	26.4	.031
15 July 1973	.157	300	47.1	
20 July 1973	.104	300	31.2	.155
25 July 1973	.045	300	13.5	
31 July 1973	.066	300	19.8	.072
4 August 1973	.094	300	28.2	
9 August 1973	.161	300	48.3	.065
16 August 1973	.243	350	85.1	

DISCUSSION

If the _Tabellaria_ decline (Fig.14) were due to either disease, parasitism, allellopathic interaction or interspecific competition we would expect its carbon fixation relative to that of _Anabaena_ to be severely lowered during the decline. This is clearly not the case (Fig.19) because the carbon fixation rate actually increases relative to _Anabaena_ as the summer progresses. The relatively greater decline in carbon fixation by _Anabaena_ may well be the result of the intraspecific competition being greater than the interspecific competition for nutrients. This decline can, however, also be the result of autoinhibition or of a change in the age structure of the population resulting from an increasing doubling time (Fig. 20b).

The mean growth constant of 0.10 for _Tabellaria_, based on carbon fixation, is similar to the 0.07 (7% per day) estimated for this species in Lake Constance (Grim, in Hutchinson, 1967) and the 0.10 for _Asterionella formosa_ (one doubling per week) in Windermere reported by Lund (Lund _et al._, 1963).

It is possible to compute the difference in growth constants necessary to account for the observed shift in dominance solely through possession of a growth rate advantage by _Anabaena_ (Eq.3). From comparison of these required values with those computed from carbon fixation (Table 3) we conclude that the shift in dominance is definitely not the result of _Anabaena_ outgrowing _Tabellaria_.

The decline of _Tabellaria_ cannot be attributed to a decline in its productivity since its growth rate remained relatively stable (Fig. 20a)

It is also not due to the sudden death of cells since the percentage of dead cells (Table 4) did not increase rapidly until the very end of the season. The approximate steady state observed can only be maintained by a death rate: total dead cell ratio that is the same as the growth rate: total live cell ratio (approximately 1:10, cf. Eq. 2). On this basis the death rate expressed as a negative growth constant would be on the order of 0.002 to 0.015 throughout June and July, clearly insufficient to account for much of the unrealized productivity. There is probably no grazing of this large diatom by zooplankton (Nauwerck, 1963) particularly in our lake where the zooplankton is dominated by rotifers. Therefore, sinking appears as the principal mechanism responsible for cell loss. A priori we would expect this factor to be an especially important mechanism of succession in our study since we are comparing species representing the two extremes in algal cell density. We can balance the difference between measured and observed growth constants (Fig. 20a) by postulating the daily sinking loss of a proportionate amount of the epilimnetic population (Eq. 3). For example, if the difference between measured and observed growth constants is 0.10 then sedimentation of approximately 10% of the epilimnetic standing crop per day would be required to balance the two estimates. Apparent sinking speeds calculated in this manner (Table 4) are negligible in June followed by a mean rate of 31 cm day^{-1} from 10 July through 9 August with a much higher rate occurring thereafter. The observed values are not extreme when compared to the 100 cm day^{-1} estimated by Grim for T. fenestrata in the epilimnion of Lake Constance and to his observed sinking speeds of 170 - 390 cm day^{-1} in capillary tubes at 17-18° (Grim, in Hutchinson, 1967).

There are several hypotheses that may be advanced to account for the dramatic increase in apparent sinking speed which occurred in early July. From Stoke's Law it is evident that the two primary variables affecting theoretical maximum sinking speed are cell density and water viscosity. The speed is a linear function of the difference between the density of the cell and that of the medium and is an inverse function of viscosity. Phytoplankton cell density has been observed to increase with decreasing growth rate (Steele and Yentsch, 1960) but as the Tabellaria growth constant remained stable throughout the summer a change in their cell density is improbable. The viscosity of the medium is an inverse function of temperature and thus decreased between 26 June and 10 July after which it slowly increased to the former level by 24 August (cf. temperature profiles, Fig.17). Thus the pattern of viscosity change is not in accord with that of apparent sinking speed. Lund (Lund et al., 1963) has advanced the hypothesis that the Asterionella formosa decline in Windermere is due to increased sinking speeds as a result of an increase in the number of dead cells in the colonies. If we compare the percentage of dead cells observed in our material with the apparent sinking speeds computed (Table 4) we see that the two values are not correlated and we therefore reject this hypothesis.* Instead, we propose that our Tabellaria decline, as well as that of Asterionella in Windermere, can be more adequately explained by the following hypothesis. The degree to which the theoretical maximum sinking speed is realized is primarily a function of turbulence. If we assume that turbulence in the epilimnion is an inverse function of depth then the critical zone is the epilimnion-

* However, see Part 4 of this thesis.

metalimnion interface and it follows that as the thermocline is depressed
to lower levels the apparent sinking speed will progressively approach
the maximum theoretical rate. We may thus explain our results as indicating
a near zero sinking speed when the epilimnion is only two meters thick
followed by a speed of approximately 30 cm day^{-1} when the interface is
at three meters succeeded by a speed of over 80 cm day^{-1} as this zone is
further depressed towards four meters.

In less well protected and deeper lakes with a thicker epilimnion we
would predict a greater sinking speed at the interface. However the
percentage of the population affected would be correspondingly lower due
to the increased thickness of the epilimnion so that the percentage loss need
be no greater than for a more protected lake. Our results indicate that
late summer net plankton succession from a diatom to a blue-green was
brought about, not by a greater growth rate of the blue-green alga , but by a
higher diatom sedimentation rate.

REFERENCES

Findenegg, I. 1971. Die Produktionsleitungen einiger planktischer
    Algenarten in ihrem naturlichen Milieu. Arch. Hydrobiol. 69, 273-293.

Fogg, G.E. 1969. The physiology of an algal nuisance. Proc. Royal
    Soc. B 173, 175-189.

Hutchinson, G.E. 1967. A Treatise on Limnology. Vol. II Wiley, New
    York-London. 1115 p.

Kalff, J. 1972. Net plankton and nanoplankton production and biomass in
    a north temperate zone lake. Limnol. Oceanogr. 17, 712-720.

Levi, H., and A.W. Rogers. 1963. On the quantitative evaluation of
    autoradiograms. Mat. Fys. Medd. Dan. Vid. Selsk. 33(11), 51 p.

Lund, J.W.G. 1965. The ecology of the freshwater phytoplankton. Biol.
    Rev. 40, 231-293.

Lund, J.W.G., F.J.H. Mackereth and C.H. Mortimer. 1963. Changes in
    depth and time of certain chemical and physical conditions of the
    standing crop of Asterionella formosa Hass. in the north basin of
    Windermere in 1947. Phil. Trans. B. 246, 255-290.

Nauwerck, A. 1963. Die Beziehungen zwischen Zooplankton und Phytoplankton
    im See Erken. Symb. Bot. Ups. 17(5), 163 p.

O'Brien, W.J. 1974. The dynamics of nutrient limitation of phytoplankton
    algae: a model reconsidered. Ecology 55, 135-141.

Rich, P.H., and R.G. Wetzel. 1969. A simple, sensitive underwater
    photometer. Limnol. Oceanogr. 14, 611-613.

Rogers, A.W. 1969. Techniques of Autoradiography. Elsevier, New York-
    Amsterdam. 338 p.

Sanford, G.R., A. Sands and C.R. Goldman. 1969. A settle-freeze method
    for concentrating phytoplankton in quantitative studies. Limnol.
    Oceanogr. 14, 790-794.

Saunders, G.W., F.B. Trama, and R.W. Bachmann. 1962. Evaluation of
a modified C-14 technique for shipboard estimation of photosynthesis
in large lakes. Mich. Univ. Great Lakes Res. Div. Publ. 8. 61 p.

Steele, J.H., and C.S. Yentsch. 1960. The vertical distribution of
chlorophyll. J. Mar. Biol. Ass. U.K. 39, 217-226.

Strathmann, R.R. 1967. Estimating the organic carbon content of
phytoplankton from cell volume or plasma volume. Limnol. Oceanogr.
12, 411-418.

Strickland, J.D.H. 1958. Solar radiation penetrating the ocean. A
review of requirements, data and methods of measurement, with
particular reference to photosynthetic productivity. J. Fish. Res.
Bd. Canada. 15, 453-493.

Part 4

An <u>in situ</u> study of the species productivity and

population dynamics of five planktonic diatoms

ABSTRACT

Species carbon fixation rates were measured in situ, using track autoradiography, during the wax and wane of five planktonic diatom species in a small, naturally eutrophic lake. The results indicate that photoinhibition of primary production in nature is much stronger than predicted from culture studies while, conversely, temperature effects are insignificant. Despite the severity of photoinhibition, maximum cell growth is attained at or near the surface in all species. The particular light intensity at which inhibition becomes evident is an inverse function of the maximum photosynthetic rate (P_{max}). The P_{max} of Tabellaria correlated well with combined meteorologic and geologic nutrient input, as estimated by precipitation. Population fluctuations are inadequately explained by growth rate estimates, as the latter always predict expansion. A strong interdependence exists between population growth and sinking which, in turn, is well correlated with death. These population fluctuations are primarily the result of variable loss rates.

INTRODUCTION

Although a great deal of information is available on the production dynamics of phytoplankton communities, virtually nothing is known about the quantitative behaviour of the component species due to the hitherto lack of suitable techniques. Information is available on the physiology of selected algae in culture but this contributes little to our understanding of events in nature (see review by Lund 1965). Not only are the species studied rarely planktonic but more importantly the media and environmental conditions deviate sharply from those found in nature and thus result in abnormal growth rates and behaviour. For example, the simple addition of a dark cycle to a laboratory culture had a dramatic effect on the photosynthetic light response (Jorgensen and Steemann Nielsen 1965). Similarly, Talling (1955, p. 334) found that late spring populations of Asterionella suspended in lake water died while those in culture media continued to grow. The significance of these and similar observations has been ignored in attempts to account for natural phenomena based on results in culture. In the present study we were able, through the application of track autoradiography, to investigate the photosynthetic behaviour of individual phytoplankton species in nature and to partially elucidate the mechanisms of diatom population dynamics.

Species carbon fixation rates were measured throughout the wax and wane of populations of Asterionella formosa Hassall, Fragilaria crotoensis Kitton, Melosira italica Ehrenberg, Synedra radians Kützing and Tabellaria fenestrata Kützing. The data were applied in a computer simulation model, allowing investigation of diurnal photosynthesis patterns, depth optima and photoinhibition as well as determining the relative importance to cell growth of maximum photosynthetic rate (P_{max}) and saturation intensity (I_k).

Comparing calculated cell growth rates with observed population growth in the lake permitted the simultaneous calculation of death and sinking rates. Correlation analysis revealed the great importance of loss rates in determining population fluctuations.

METHODS

Productivity experiments were carried out in Lac Hertel, a small, naturally eutrophic lake with an undisturbed forested watershed located near Montreal, Quebec, Canada ($45^{\circ}32'$ N, $73^{\circ}09'$W). At approximately ten day intervals throughout the spring and summer of 1972 and 1973 samples were collected with an opaque 1.5 liter PVC water sampler from 0, 1, 2, 3, 4 and 6 meters at a fixed station over the deepest portion of the lake (8m). Samples were inoculated with $Na^{14}CO_3$ (0.48 µCi per 265 ml bottle) and then resuspended at depth for a two-hour midday incubation following which the samples were transferred to storage bottles and preserved with acid Lugol's solution for later autoradiographic analysis.

Temperature profiles were recorded using a YSI thermistor. Total available inorganic carbon was calculated from pH, temperature, and alkalinity measurements following Bachmann (Saunders et al. 1962). Alkalinity was determined by titration to a pH of 4.8.

During the summer 1973 incubations, incident radiation was determined with either an integrating pyranometer (YSI model 67) or a recording pyranometer (YSI model 14138). Photosynthetic Available Radiation (PAR) was estimated as 46% of total (Strickland 1958). Hourly radiation for prior incubations as well as for general use in the photosynthesis model was computer estimated from Campbell-Stokes sunshine meter records (Appendix 2). This method of estimation was evaluated against a Kipp and Zonen pyranometer

yielding a correlation coefficient of 0.93 (n=2355, p<0.001). We thank Dr. B. Garnier, of the McGill University Geography Department for providing the sunshine and Kipp and Zonen records plus additional data on precipitation and wind.

Light at depth was calculated from the above light estimates by correcting for extinction, as measured by submarine photometer (Rich and Wetzel 1969), plus an assumed 5% surface reflectance. Direct measurements were made starting 26 June 1973. For prior dates the relationship between extinction and secchi disc readings was used to calculate the extinction coefficient $(a = -0.104 \ z_{sd} + 0.760 \quad n = 9, r = 0.85, p<.01 \ )$. In the photosynthesis model the percent light at each depth between sampling dates was estimated by arithmetic interpolation.

Phytoplankton populations and cell volumes were estimated from observations on 5 ml subsamples settled onto slides, dried by ethanol substitution (Sanford et al. 1969) and mounted in 30% glycerin. Cell numbers (Tabellaria, Asterionella and Synedra), filament length (Melosira) or colony width (Fragilaria) were recorded for six crossed transects (Margalef in Vollenweider 1974) each one centimeter in length, except for Fragilaria at its maximum abundance when only three transects were recorded. Counts using this method correlate very well with those using a 0.1 ml nanoplankton counting cell (r = 0.98, n = 49, p<<.001, slope = 1.06). Thorough shaking before settling disrupted the colonial aggregations of Asterionella, Tabellaria and Synedra thereby allowing cells rather than colonies to be enumerated (cf. Lund et al. 1958).

In the data analysis an estimate of the dead cell population proved especially important. Any frustule which was entirely empty or which contained only a trace of chlorophyll not in the shape of a normal chloroplast was classified as dead. This definition was supported by the general

observation on the autoradiography slides that such cells remained unlabeled while those with as little as one chloroplast of normal appearance were still capable of fixing carbon.

Cell volumes were estimated using length and/or width measurements from at least twenty cells of each species from the 1m sample for each date covered by autoradiographic analysis. This cell number was doubled for _Melosira_ as the filament width carried a double weight in the volume calculation. For the crucial valve view measurements of the pennate forms oil immersion was employed with a total magnification of 2250x. Under these conditions the small squares of a Whipple grid represented only 1.0 μm. Volumes were calculated individually for each cell before averaging. However, the daily means for individual size parameters (e.g. length, width) showed a seasonal range generally less than ± 5% of the mean, thus only the average seasonal volume of each species was employed in subsequent calculations.

The post-incubation ^{14}C content of each species was determined through track autoradiography. In this procedure a thick (>30μm) layer of photographic nuclear emulsion (Kodak NTB$_3$) is applied to specimens concentrated on slides similar to those for population counts. The emulsion records the passage of beta particles as tracks of silver grains arising from the source cell. A detailed account of this procedure is provided elsewhere (see Part 2, this thesis). Track counts were made on at least 100 cells from each sample for _Tabellaria, Asterionella_ and _Synedra_ and on twenty-five filaments or colonies of _Melosira_ and _Fragilaria_ respectively. Since the data follow a Poisson distribution (see Part 2, this thesis) the standard error was calculated as:

$$s.e. = \pm \ (m/n)^{1/2}$$

where m is the mean number of tracks per counting unit and n is the number

of units (cells, colonies or filaments) counted   (Elliott 1971). In only

the few instances where n was less than 30 (Fragilaria colonies and Melosire

filaments) and the product nm was also less than 30 was it necessary, follow-

ing Elliott, to take asymetric limits from the tables of Crow and Gardner

(1959).

Mean track counts per cell per day exposure were converted into absolute

disintegration rates through correction by a factor of 2.0 for the

geometry of the source plus correction for the 14% of the ^{14}C beta particles

with insufficient energy to produce a track (Levi and Rödgers 1963) plus

additional species specific self-absorption factors (Knoechel and Kalff 1976b)

based on cell thickness. This latter correction was only 1% to 2% for all

but Melosira which required a 6% factor. Net carbon fixation was calculated

as the fraction of the total ^{14}C assimilated times the total available in-

organic carbon corrected for a 6% isotope effect.

Observed species growth rates were calculated from live cell counts

as:

$$k = \frac{\ln(L_t/L_o)}{t}$$

where k is the observed growth rate and L_o and L_t are the number of live

cells present in the epilimnion at time zero and t respectively.

In order to compare modeled growth in units of carbon with observations

based on cell counts a conversion factor for cell carbon per unit volume is

required. Strathmann (1967) provides log:log regressions of carbon versus

volume for diatoms but the variance is large and thus the 95% confidence

limits for an organism such as Asterionella with a volume of 470 μ^3 span

a range from 3.4% to 21.4% with a regression value of 8.5%. Additionally,

Strathmann noted that the regressions were based on cultured populations

and there was field evidence (Antia et al. 1963) to suggest that nutrient limited natural diatom populations might possess less than one-half the carbon content of cultured cells. In the present study we were able to generate an internal estimate of carbon for each species. This was done by making the initial assumption that for some period in time the epilimnetic sinking losses for a particular species were negligible so that only loss due to death needed to be considered. The percent carbon was then set by successive approximation so that the model prediction for carbon fixation would equal the observed cell growth plus dead cell production at the point in time when this observed rate was maximal. Thus:

$$c(f) = k = \frac{\ln((L_t + D_t - D_o)/L_o)}{t}$$

where D_o and D_t are the number of dead cells in the epilimnion on day zero and day t, c is the model calculated carbon fixation and f is the correction factor for percentage cell carbon. To the extent that sinking might occur over the time involved these estimates are maxima. Carbon values estimated in this manner tended to be less than one-half that predicted by Strathmann's regressions except those for Tabellaria which were more nearly in agreement (Table 5).

The percent carbon factors were applied in the model, which calculated biomass accumulation at each depth on an hourly basis, thereby allowing "interest" to be earned on the biomass increments. Total daily growth estimated by the model is expressed as the cell growth rate (c) for mathematical comparison with the observed growth rate. Otherwise values are expressed as the cell division rate (μ, where $\mu = e^c$) as this linear transformation facilitates graphic comparison.

Equations used in the photosynthesis model were derived through correlation analysis with principal axis determination since linear regression

Table 5. Estimated percentage carbon of five diatom species in comparison with those predicted by Strathmann (1967).

Species	Year	Volume	% C This study	% C Strathmann
Asterionella	1972	434	3.0	8.7
Asterionella	1973	470	3.6	8.5
Fragilaria	1973	214	3.3	10.3
Melosira	1973	701	2.8	7.8
Synedra	1973	280	3.1	9.7
Tabellaria	1972	444	6.9	8.7
Tabellaria	1973	528	8.1	8.3

should not be applied to data where the independent variable (light in our case) is not under the control of the investigator (Sokal and Rohlf 1969). It should be noted that correlation analysis does not require a cause and effect relationship but at the same time it does not preclude one. Statements regarding causation must be based on knowledge of the biological processes involved and can never be proven through either correlation or regression.

Differences between observed and predicted growth rates are ascribable to losses from death, sinking and grazing. Due to their large size and colonial habit, these diatom species are largely unavailable to grazers (Nauwerck 1963) therefore, we consider here only death and sinking as discrete loss variables. Thus:

$$k = c + d + s$$

where k is the observed growth, c is the model calculated growth, d is the death rate and s is the sinking rate. Having observed and calculated growth rates it is possible to calculate both sinking and death rates through a procedure best explained by example. Examining the Asterionella population during the period from 24 May through 4 June 1973 (Table 6) the initial and final epilimnetic live cell population was 55 and 120 (mg m^{-2}) and that of the dead cells was 28 and 31. The live cell data yield an observed growth rate of 0.07 while the model predicts 0.333 (Table 6). Since the number of dead cells changed little we might first assume a zero death rate in which case:

$$s = k - c = -0.263$$

However, if this rate of sinking occurred then a portion of the dead cells initially present must have also been lost because both live and dead cells are associated together in colonies. At time t the dead cells remaining from those initially present would be:

$$D_o' = D_o e^{st} = 1.55$$

Table 6. Epilimnetic living (L) and dead (D) biomass (g m^{-2})

for five diatom species.

Date 1973	Asterionella L	D	Tabellaria L	D	Fragilaria L	D	Melosira L	D	Synedra L	D	Date 1972	Asterionella L	D	Tabellaria L	D
25 April	256	23					294	102	53	11	26 May	166	167	48	10
4 May	160	95					1063	290	125	61	2 June	236	60	65	0
14 May	50	59					946	220	88	44	8 June	2333	493	205	3
24 May	55	28			25	10	206	111	286	44	14 June	195	569	424	3
4 June	120	31	143	3	990	291			29	8	24 June	104	94	711	8
14 June	1052	393	491	7	3610	136					5 July	17	24	2678	58
26 June	59	83	1111	40	1480	460					14 July			6358	115
10 July			4658	127	118	64					23 July			5753	583
20 July			2088	363							3 Aug			2252	505
31 July			1372	95							14 Aug			3078	302
9 Aug			1076	73							23 Aug			2842	323
24 Aug			80	40							1 Sept			926	411

and the rate of "growth" of the dead cell population would be:

$$d' = \frac{\ln(D_t/D_o e^{st})}{t} = 0.272$$

From this "growth" rate for dead cells we can calculate the production of dead cells per day as:

$$DC = D_o(e^{d'}) - D_o = 8.76$$

This can be used to calculate a true death rate based on the live cell population at time zero as:

$$d = \ln\left(\frac{L_o - DC}{L_o}\right) = -0.174$$

This provides a preliminary estimate of the death rate but it is evident that, if this factor is now included in the analysis, the original estimate of sinking must be lowered as it assumed there was no loss due to death. Lowering the sinking rate will in turn necessitate recalculation of a lower death rate since not as many dead cells will have been lost as was previously estimated. This then requires a slight increase in the sinking rate and so on. The cycle of calculations is repeated until the one unique set of values for d and s where no further changes take place is obtained. In the special case where the initial dead cell population exceeds that of the live cells errors, resulting from applying estimates based on a smaller population to a larger one, cause these calculations to <u>diverge</u> from the correct result. This problem occurred once each year, only in <u>Asterionella</u>, making it necessary to perform a reverse calculation whereby sinking is first estimated from the change in the dead cell population, allowing a preliminary estimate of death by difference. The estimate is then applied to the live cell population in order to yield the production of dead cells per day. This factor is converted into a "growth" rate of dead cells which must be added to the original sinking estimate, thus making it necessary to

re-estimate death, etc. The basic rule to be followed is that calculations must be based on whichever cell type (live or dead) is largest at time zero. If the numbers are about equal then the one showing the greatest change with time should be chosen.

MODEL CONSTRUCTION

Carbon fixation data based on autoradiographic analyses are presented in terms of micro-nanograms (10^{-15}) of carbon fixed per cubic micrometer of cell volume per hour. This allows direct comparison between all species irrespective of their cell volumes. The results are used to construct carbon fixation:light curves for each species through correlation analysis.

Each sampling date has six data points, one for each incubation depth. The depths are not specifically noted but can be ascertained readily by locating the highest light level for the date, which is the 0m sample, and then proceeding to the next highest which is 1m and so on. The equations and statistical parameters are summarized in tabular form (Table 7). This table together with the following brief descriptions, allows the determination of the individual data points that yield each response curve.

The model does not provide for diurnal variation in the shape of the photosynthetic light response curve. In a study of Tabellaria on 9 August 1973 (Appendix 1), the P_{max} computed from five 2h incubations between 0445 a.m. and 1700 p.m. was 1.109 as compared to 1.084 based only on the standard, midday incubation. The observed difference of only 6% indicates a very small diel response pattern that is of insufficient magnitude to warrant the complexities required for inclusion in the model.

It was necessary to eliminate only three of the 252 data points from the correlation analyses. Two of these are 6m hypolimnetic values that did not reflect the epilimnetic response on the dates in question

Table 7. Data for carbon uptake curves shown in Figures 21 through

29.   The slopes and intercepts apply to the light

ranges and dates specified, "n" is the sample size

and "r" is the correlation coefficient.   The significance

level is indicated as: $* < 0.05$, $** < 0.01$, $*** < 0.001$.

Species/year	Sampling dates	Light range	Slope	Intercept	n	r
Synedra	all	<.258	2.69	0.10	16	.93***¹
1973	all	>.258	−2.32	1.39	11	−.93***¹
Melosira	all	low	9.05	−.24	10	.93***¹
1973	all but 14 May	>.135	−2.79	1.37	9	−.96***¹
	14 May	>.086	−0.81	0.61	5	−.99**
Tabellaria	all	low	19.94	−0.26	34	.83***¹
1972	boundary	.112 to .285	−6.73	2.72	10	−.99**¹
	boundary	>.285	0.00†	0.81	10	−.31ns
	8 June	.083 to .196	0.00	1.41	3	---
	14 June	.054 to .276	0.00	0.87	5	---
	24 June	.066 to .224	0.00	1.09	3	---
	14 July	.070 to .233	0.00	1.17	3	---
	14 August	.070 to .233	0.00	1.16	4	---
	23 August	.065 to .246	0.00	1.07	0	---
	1 September	.061 to .260	0.00	0.98	3	---
Tabellaria	all	low	20.98	−0.08	19	.88**
1973	4,14 June	>.044	0.00	0.81	5	---
	26 June	>.052	0.00	0.98	5	---
	9,10,11 July	>.058	0.00	1.11	13	---
	after 11 July	>.315	0.00	0.61	5	---
	after 11 July	inhibition‡	−6.73	2.72	0	---
	20 July	.049 to .266	0.00	0.95	5	---
	31 July	.063 to .221	0.00	1.24	2	---
	9 August	.053 to .254	0.00	1.02	4	---
	24 August	.039 to .293	0.00	0.76	5	---
Asterionella	before 24 May	<.133	3.67	0.04	10	.89**
1973	before 24 May	>.133	−0.95	0.65	8	−.81*
	after 14 May	low	22.26	−0.07	6	.95**
	24 May, 4 June	>.061	−2.24	1.42	5	−.99**
	14 June	.022 to .475	0.00†	0.36	5	---
Asterionella	all	low	19.70	−0.22	16	.91**
1972	2 June	>.112	−3.92	2.41	0	---
	8 June	.065 to .344	0.00	1.07	3	---
	14, 24 June	.036 to .490	0.00†	0.49	8	−.62ns
Fragilaria	all but 26 June	low	15.20	−0.02	8	.95*¹
1973	24 May	>.120	−3.82	2.26	5	−.86*
	4 June	.054 to .380	0.00	0.80	0	---
	14 June	.034 to .465	0.00†	0.49	5	.78ns
	26 June	<.428	1.46	−0.01	5	.99*¹

† A slope of zero is substituted for the principal axis when the correlation is non-significant.

‡ The inhibition response from Tabellaria in 1972 was used.

Figure 21. Photosynthetic carbon uptake ($gC \times 10^{-15} \ \mu m^{-3} \ h^{-1}$) by <u>Synedra</u> <u>radians</u> in 1973 as a function of light ($ly \ min^{-1}$ PAR) for the dates indicated. The lines of best fit represent the response used in the model. Refer to Table 7 for equations and statistical information. Vertical lines indicate standard errors.

Synedra
1973

C UPTAKE

0.8

0.4

▲ 25 April
■ 4 May
● 14 May
△ 24 May

LIGHT

.1 .2 .3 .4 .5

Figure 22. Photosynthetic carbon uptake (gC x 10^{-15} μm^{-3} h^{-1})

by <u>Melosira</u> <u>italica</u> in 1973 as a function of light

(ly min^{-1} PAR) for the dates indicated. The lines of

best fit represent the responses used in the model.

Refer to Table 7 for equations and statistical

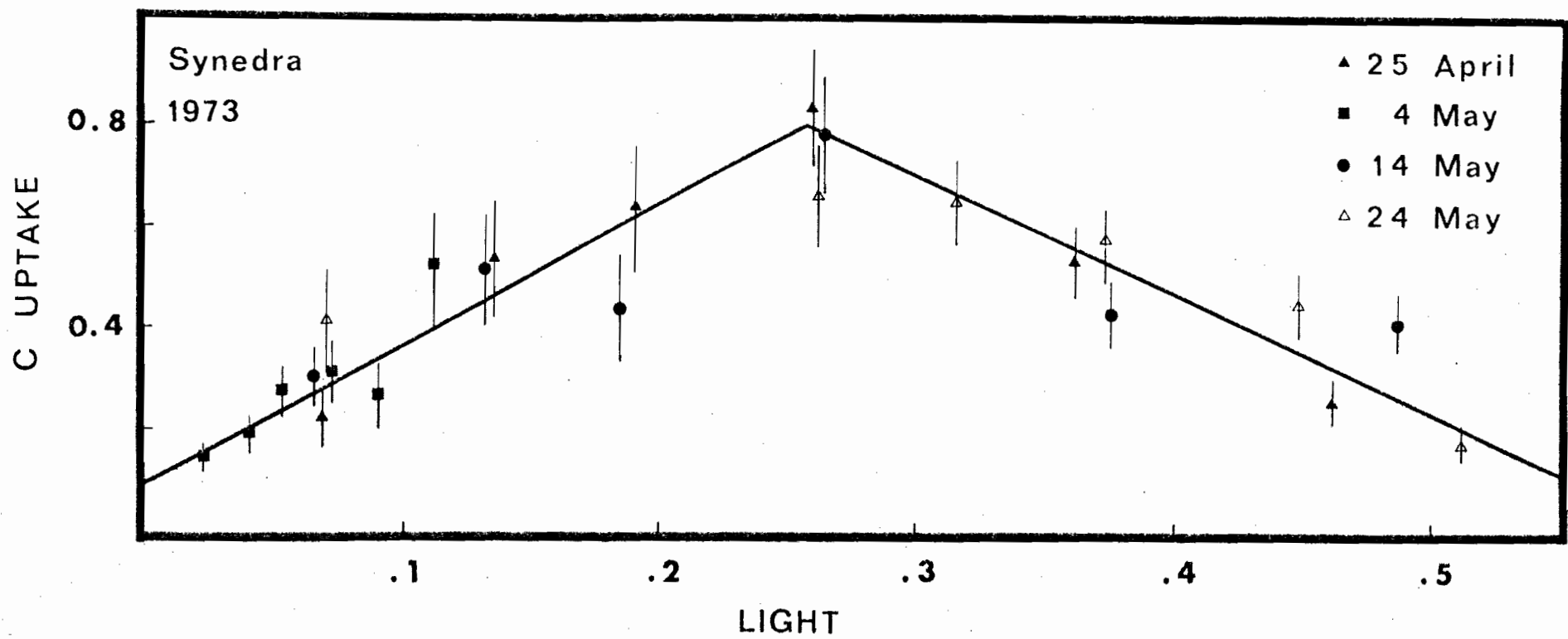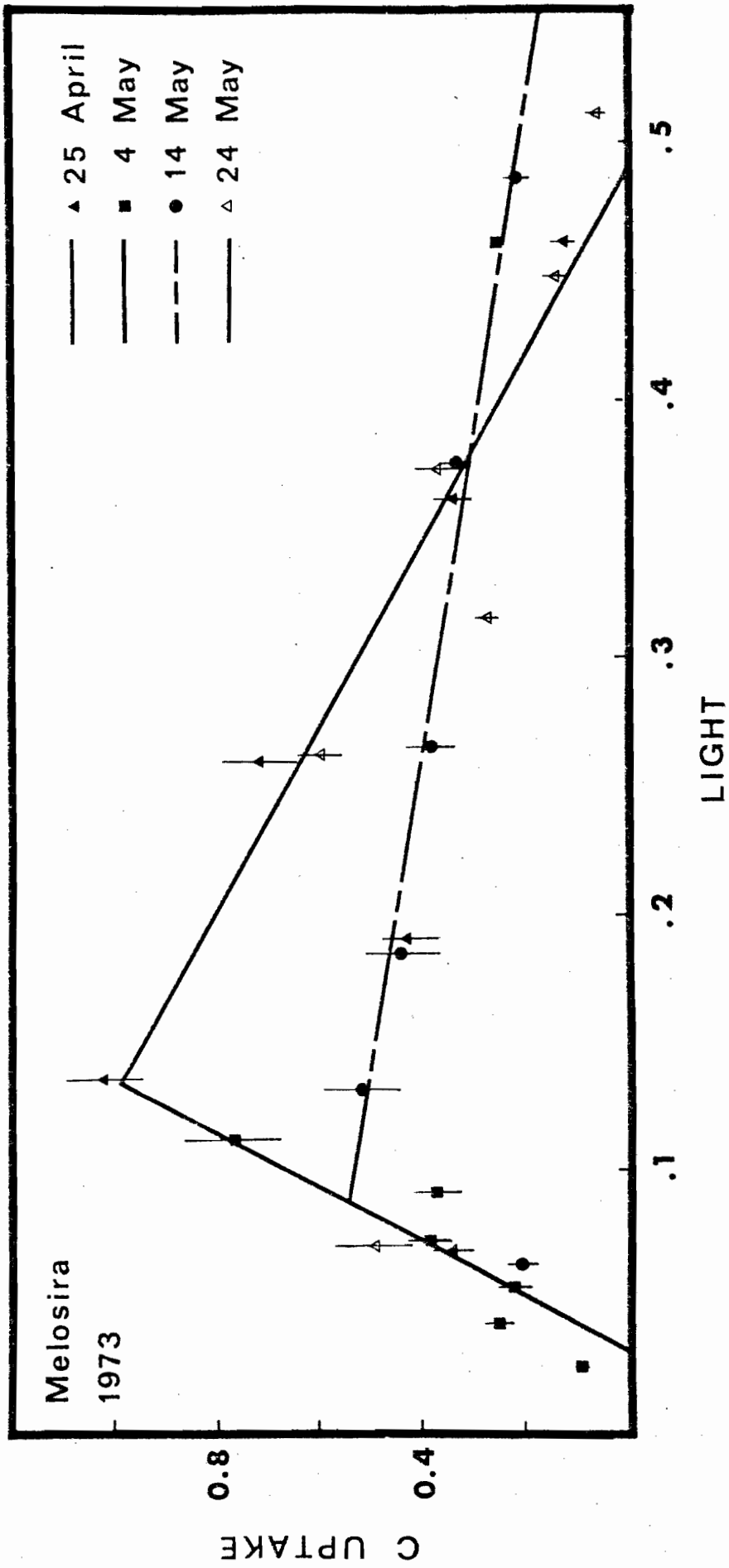information. Vertical lines indicate standard

errors.

(*Asterionella* 24 May 1973 and *Tabellaria* 26 June 1973). The third is a

Melosira datum (25 April, 3m) that is clearly anomalous but for no

apparent reason.

Synedra radians Kützing

Synedra was the simplest species to model as the light response remained

similar on each sampling date during the period from late April through

the end of May. Since the response indicated that light limitation was

followed immediately by inhibition (Fig. 21), the curve was constructed by

computing the principal axis for all light levels <0.28 ly min^{-1} and for

all light levels >0.24 ly min^{-1} (Table 7).

Melosira italica Ehrenberg

In contrast to *Synedra*, *Melosira* exhibited significant changes in its

high light response with time. The light limited response curve was

generated using data from all light levels <0.15 ly min^{-1} (excluding 14 May,

4m as that value was on the plateau of a reduced response at that time. A

high light curve was generated from the 25 April and 24 May data (Figure 22,

table 7) following the elimination of the anomalous 25 April, 3m datum.

The 14 May slope was calculated separately as it demonstrated a lesser

response.

Tabellaria fenestrata Kützing

The 1972 data for *Tabellaria* provide a longer record that exhibits an

extremely consistent response. The comparatively large number of observations

allowed the calculation of general boundary equations delineating three

regions of the light response (solid lines in Fig. 23 & 24). All data for

light values <0.10 ly min^{-1} were combined to form a single light limitation

equation (Table 3). A second section of the curve was calculated using the

data between 0.10 and 0.30 ly min^{-1}, eliminating those values which formed

Figure 23. Photosynthetic carbon uptake ($gC \times 10^{-15} \; \mu m^{-3} \; h^{-1}$)

by <u>Tabellaria</u> <u>fenestrata</u> in 1972 as a function of

light ($ly \; min^{-1}$ PAR) for the dates indicated. The lines

of best fit represent the responses used in the

model. The solid lines are the boundary response

and broken lines denote reduced P_{max} plateaus.

Refer to Table 7 for equations and statistical

information. Vertical lines indicate standard

errors.

Tabellaria
1972

2 June
8 June
14 June
24 June
5 July

LIGHT

C UPTAKE

Figure 24. Photosynthetic carbon uptake ($gC \times 10^{-15} \mu m^{-3} h^{-1}$)

by _Tabellaria_ _fenestrata_ in 1972 as a function of

light ($ly\ min^{-1}$ PAR) for the dates indicated. The lines

of best fit represent the responses used in the

model. The solid lines are the boundary response

and broken lines denote reduced P_{max} plateaus.

Refer to Table 7 for equations and statistical
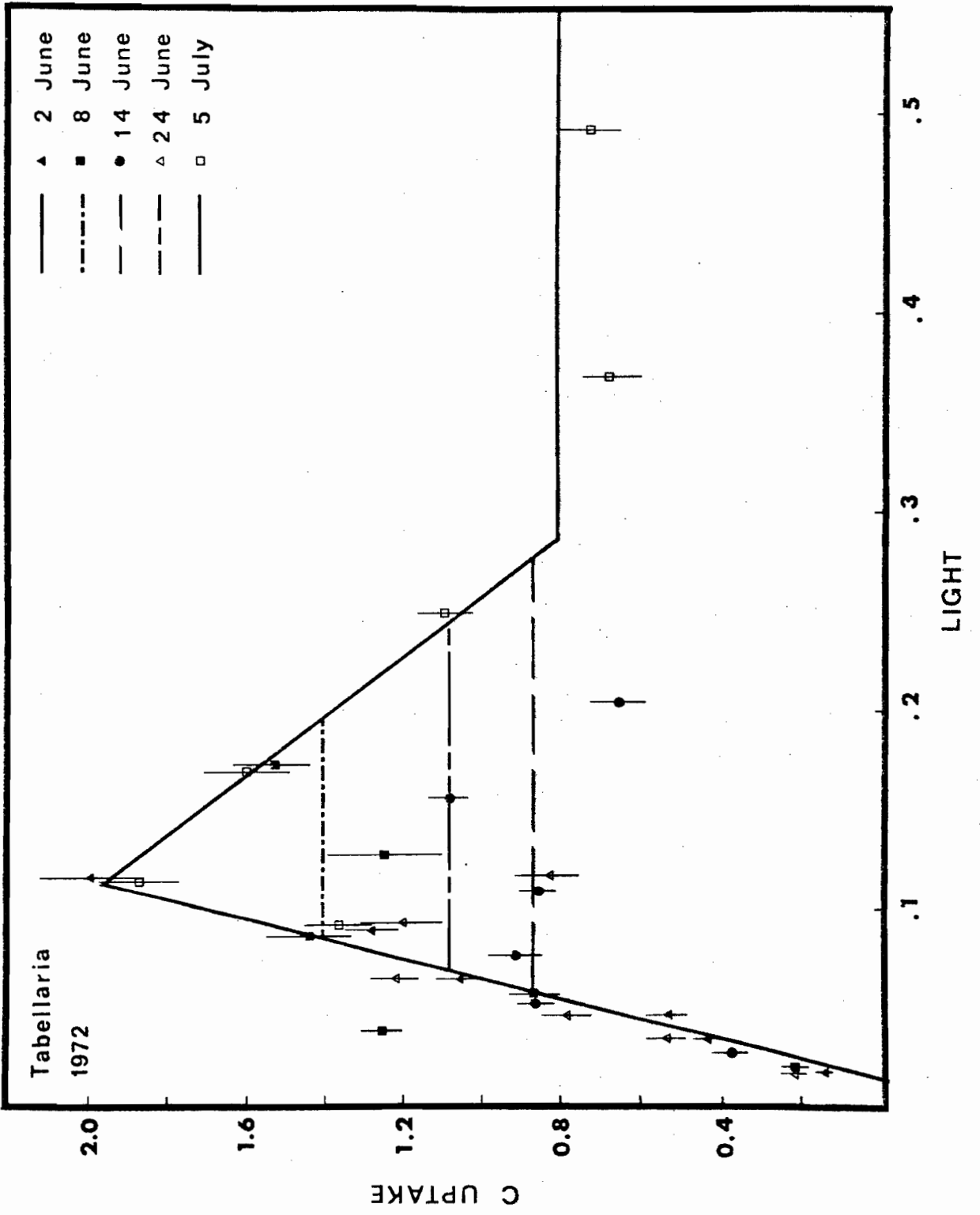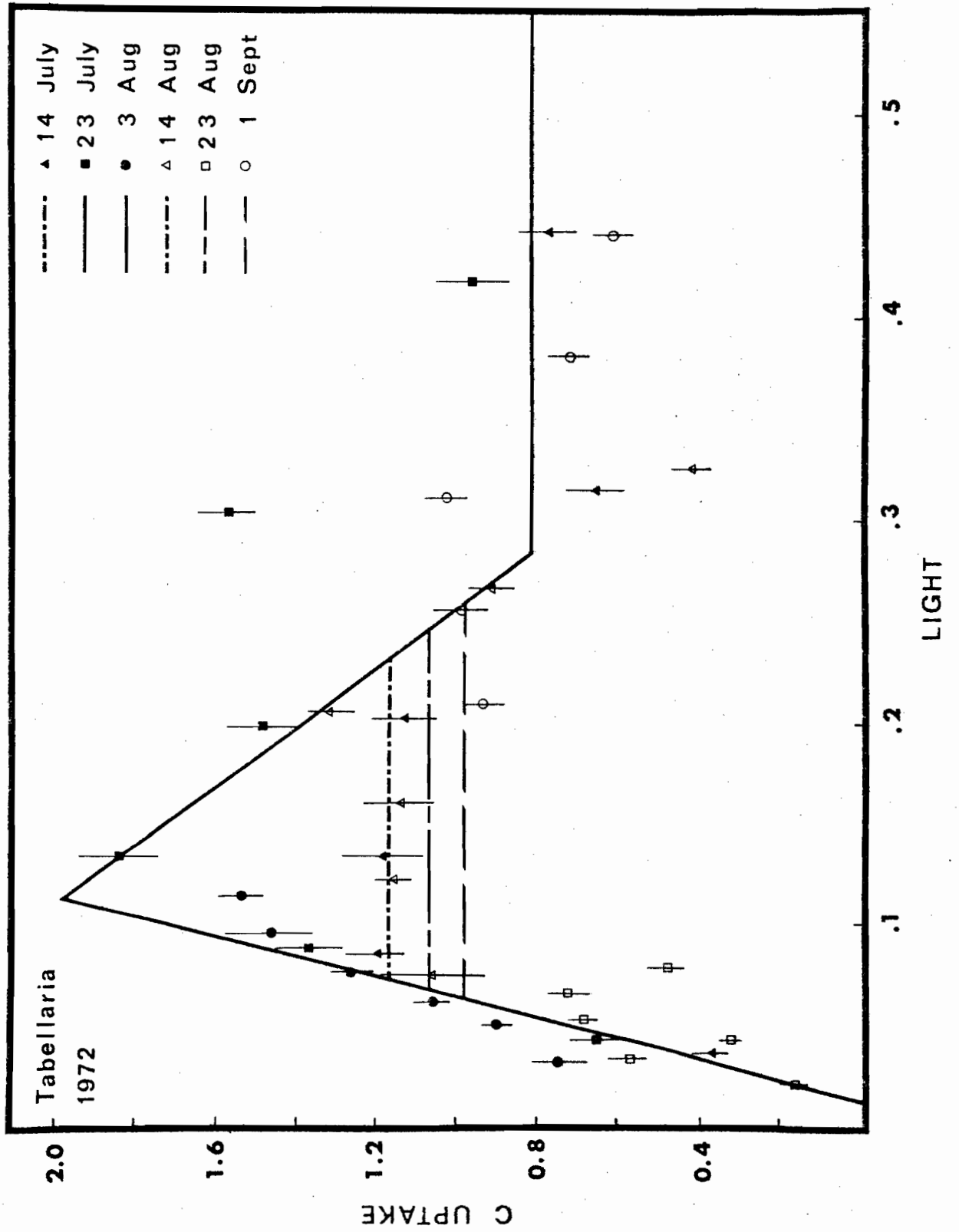
information. Vertical lines indicate standard

errors.

Tabellaria
1972

Legend:
▲ 14 July
■ 23 July
● 3 Aug
△ 14 Aug
□ 23 Aug
○ 1 Sept

LIGHT

C UPTAKE

the various response plateaus (see below). Finally, all of the values above 0.30 ly min^{-1} were considered but since the relationship with light was insignificant only the mean was used in the model. The resultant boundary curve was used to describe all data sets by simply establishing central plateaus, when necessary to fit the observations for a particular date (Fig. 23 & 24). Each plateau was calculated separately as the mean of all data for light levels extending between the boundary limits for the date in question. As the light level on 23 August was insufficient to establish a plateau, the mean of the 14 August and 1 September values was used.

The data from 1973 indicate a more variable response than was noted in 1972. At medium and high light levels the data prior to 20 July indicate a long plateau with no apparent inhibition (Fig. 25). The data for 20 July and after are more consistent with the shape of response curve found in 1972 (Fig. 26).

The light limited section of the response was calculated using all values for light <0.06 ly min^{-1} so as to avoid the region where the plateaus began. Since there was no significant correlation with higher light from 14 June through 11 July (Table 7), the mean of all epilimnetic values for each sampling date was used in the model. The light range on 4 June was insufficient to establish a plateau so that of 14 June was used.

The remaining dates were interpreted as in 1972. A high light plateau was established using the mean for all light levels <0.25 ly min^{-1} and this was joined to the light limited curve using the boundary equation from 1972 as there were insufficient data to calculate one solely for 1973. Between the two boundary limits plateau regions were again established using means.

Asterionella formosa Hassall

The Asterionella data for 1973 represent a two month record that spans from ice-out until mid June. The data prior to 24 May show no consistent

Figure 25. Photosynthetic carbon uptake ($gC \times 10^{-15} \mu m^{-3} h^{-1}$)

by <u>Tabellaria</u> <u>fenestrata</u> in 1973 as a function of

light (ly min^{-1} PAR) for the dates indicated. The

lines of best fit represent the responses used in

the model. Refer to Table 7 for equations and

statistical information. Vertical lines indicate

standard errors.

Tabellaria
1973

C UPTAKE

1.2

0.8

0.4

.1   .2   .3   .4   .5

LIGHT

- - - - ▲ 4 June
- - - - ■ 14 June
-·-·-·-· ● 26 June
———— △ 9 July
———— □ 10 July
———— ○ 11 July

88

Figure 26. Photosynthetic carbon uptake ($gC \times 10^{-15} \; \mu m^{-3} \; h^{-1}$)

by <u>Tabellaria</u> <u>fenestrata</u> in 1973 as a function of

light ($ly \; min^{-1}$ PAR) for the dates indicated. The

lines of best fit represent the responses used in

the model. Refer to Table 7 for equations and

statistical information. Vertical lines indicate

standard errors.
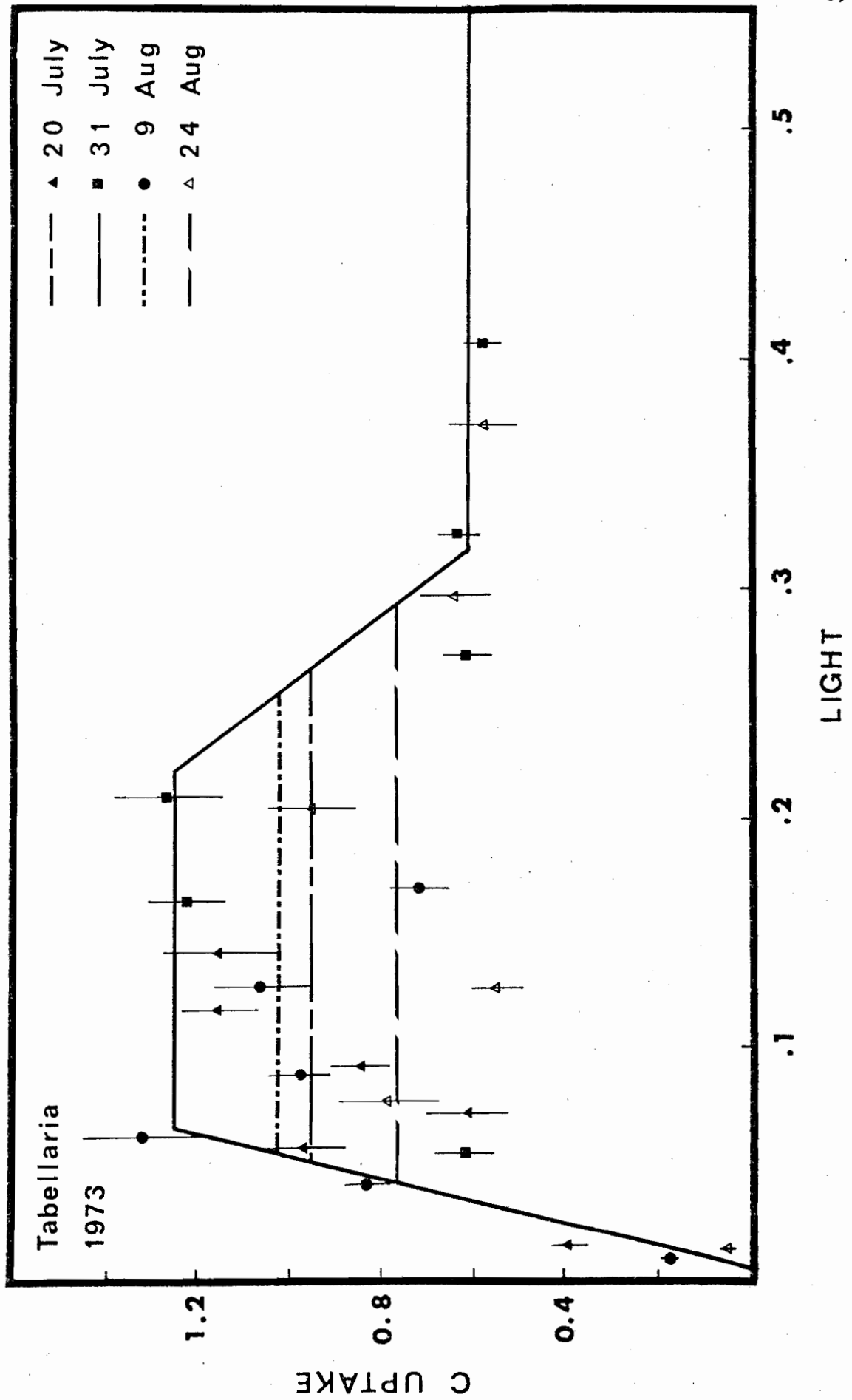
differences so the light limitation curve was calculated from data for all light levels <0.15 ly min^{-1} while the inhibition curve used all values above that range (Fig. 27a). The 24 May and 4 June data provide a striking change in response (Fig. 27b). A low light slope was calculated from all of the 4 June data while the 24 May epilimnetic data were used for the high response curve. The 6m depth on the latter date was excluded because it still exhibited the lower response of the previous period. The 14 June data demonstrated a much reduced response which was modeled as its mean, extending between the boundaries established by the previous two dates.

The sample record for Asterionella in 1972 begins later in the season with the response already at peak (Fig. 28). A light relationship was established using all data for each date up to the respective plateaus. The high light record was deficient as none of the sampling days were clear and sunny (it rained on all but the 14th). It was impossible to determine the 2 June maximum uptake rate since the incident light was insufficient to provide saturation. The high light slope was thus estimated by extending a line between the highest observed value and the point at which carbon uptake declined to zero in 1973 (0.63 ly min^{-1}). The 8 June response was modeled as a plateau between these light limitation and inhibition curves while the remaining two dates were combined to form another plateau (Fig. 28).

Fragilaria crotonensis Kitton

The light limited response for Fragilaria was calculated from all data for light levels <0.10 ly min^{-1} (Fig. 29). A high light response for 24 May was calculated from all of the epilimnetic data while for 14 June the correlation proved negligible so only the mean was used. Modeling the response of 4 June presented a problem as the light received was insufficient to delineate a high light response, but the 14 June response was probably

Figure 27. Photosynthetic carbon uptake ($gC \times 10^{-15} \mu m^{-3} h^{-1}$)

by Asterionella formosa in 1973 as a function of

light ($ly\ min^{-1}$ PAR) A. Early spring. B. Late spring.

The lines of best fit represent the responses

used in the model. Refer to Table 7 for equations

and statistical information. Vertical lines
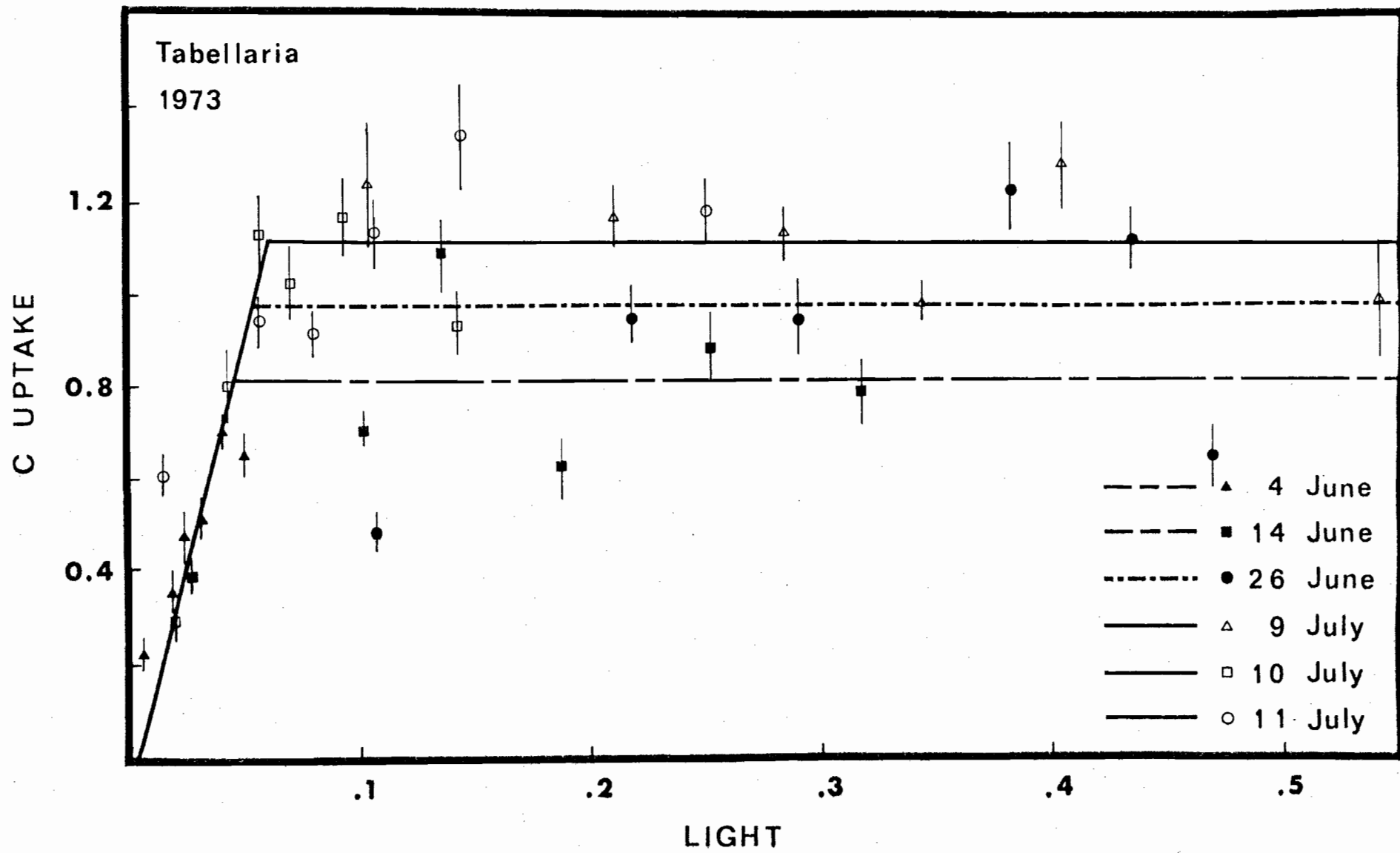
indicate standard errors.
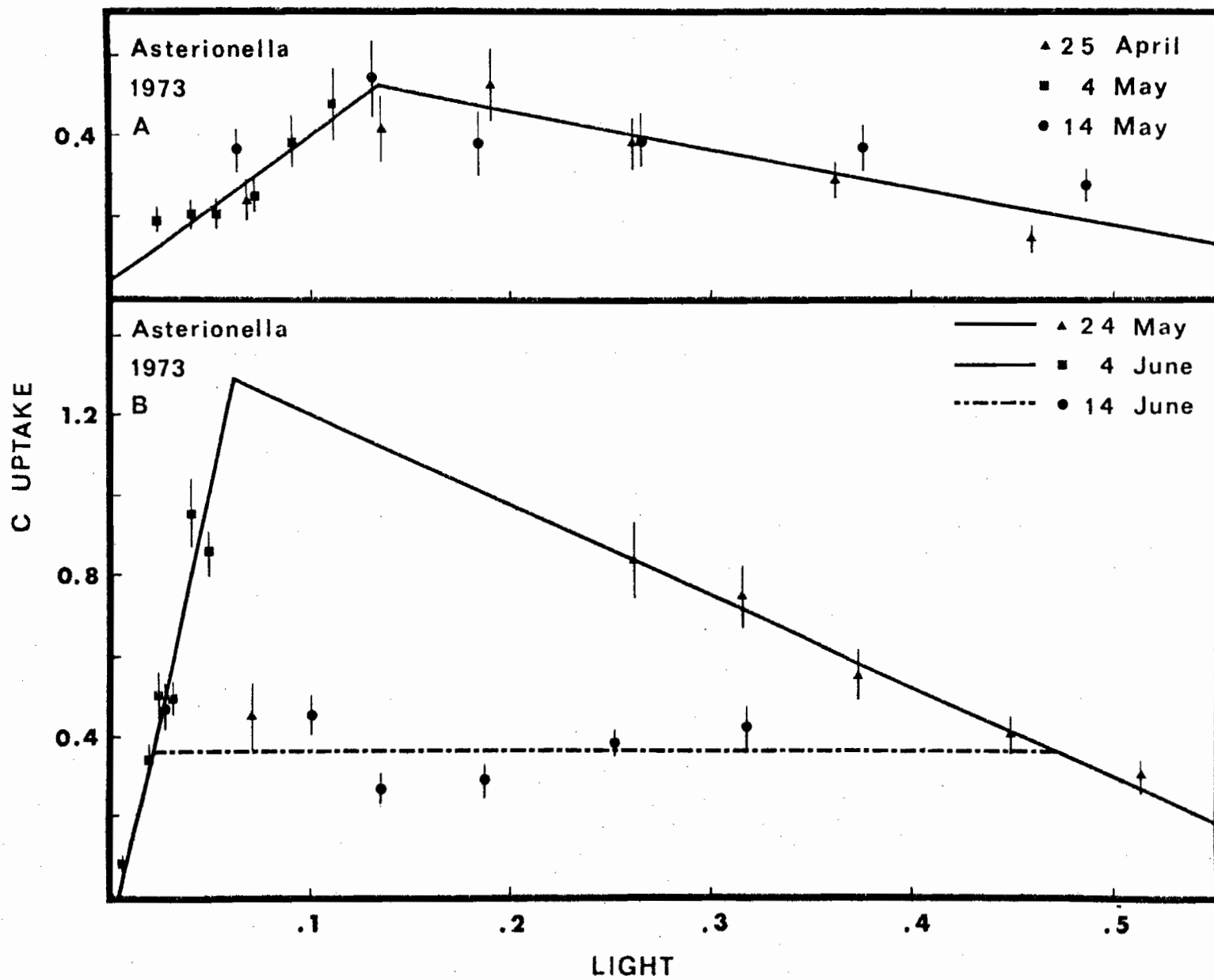
Figure 28. Photosynthetic carbon uptake (gC x 10^{-15} μm^{-3} h^{-1}) by <u>Asterionella</u> <u>formosa</u> in 1972 as a function of light (ly min^{-1} PAR) for the dates indicated. The lines represent the responses used in the model. Refer to Table 7 for equations and statistical information. Vertical lines indicate standard errors.

Figure 29. Photosynthetic carbon uptake ($gC \times 10^{-15} \mu m^{-3} h^{-1}$) by <u>Fragilaria</u> <u>crotonensis</u> in 1973 as a function of light ($ly\ min^{-1}$ PAR) for the dates indicated. The lines represent the responses used in the model. Refer to Table 7 for equations and statistical information. Vertical lines indicate standard errors.

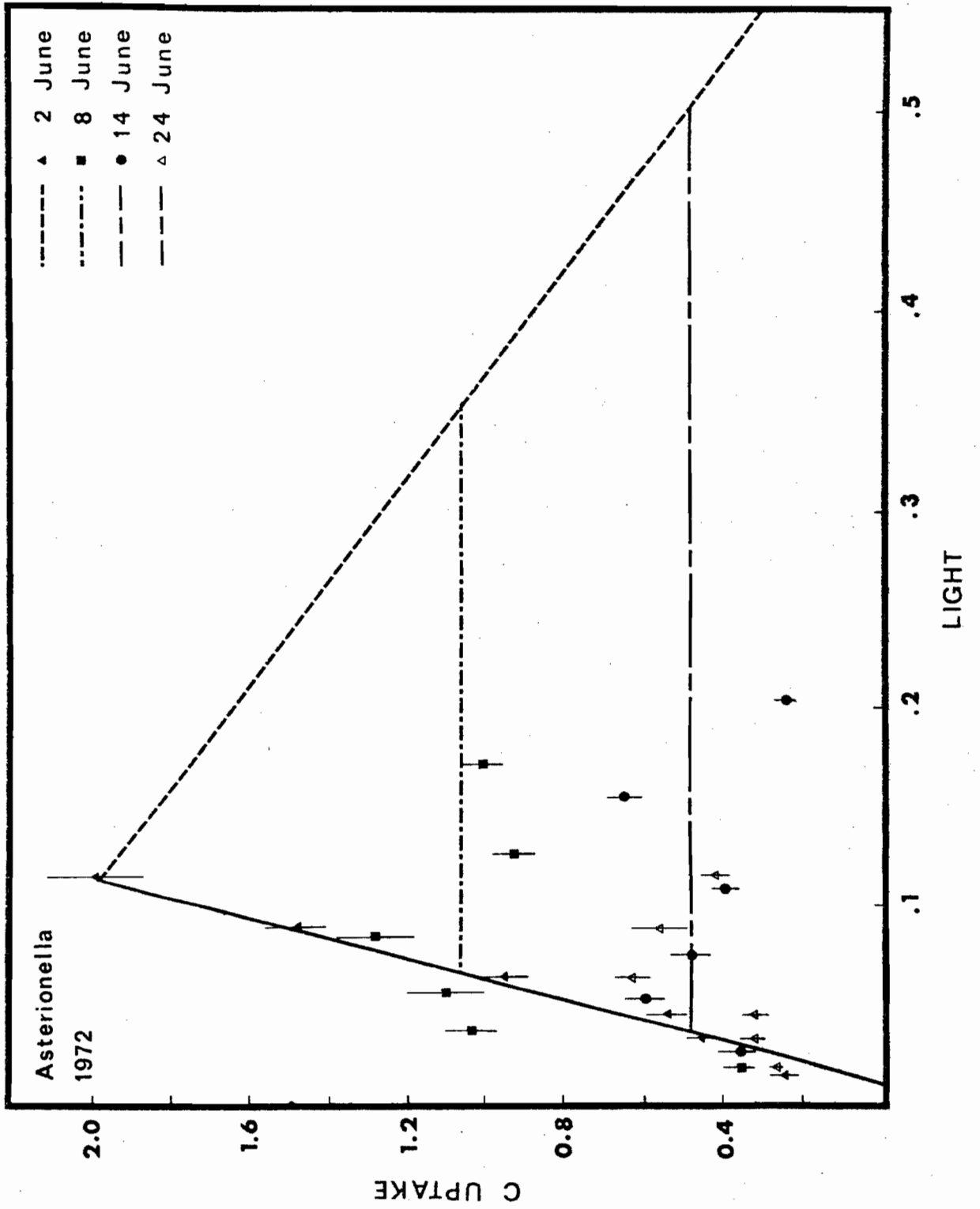Fragilaria
1973

▲ 24 May
■ 4 June
● 14 June
△ 26 June

LIGHT

C UPTAKE
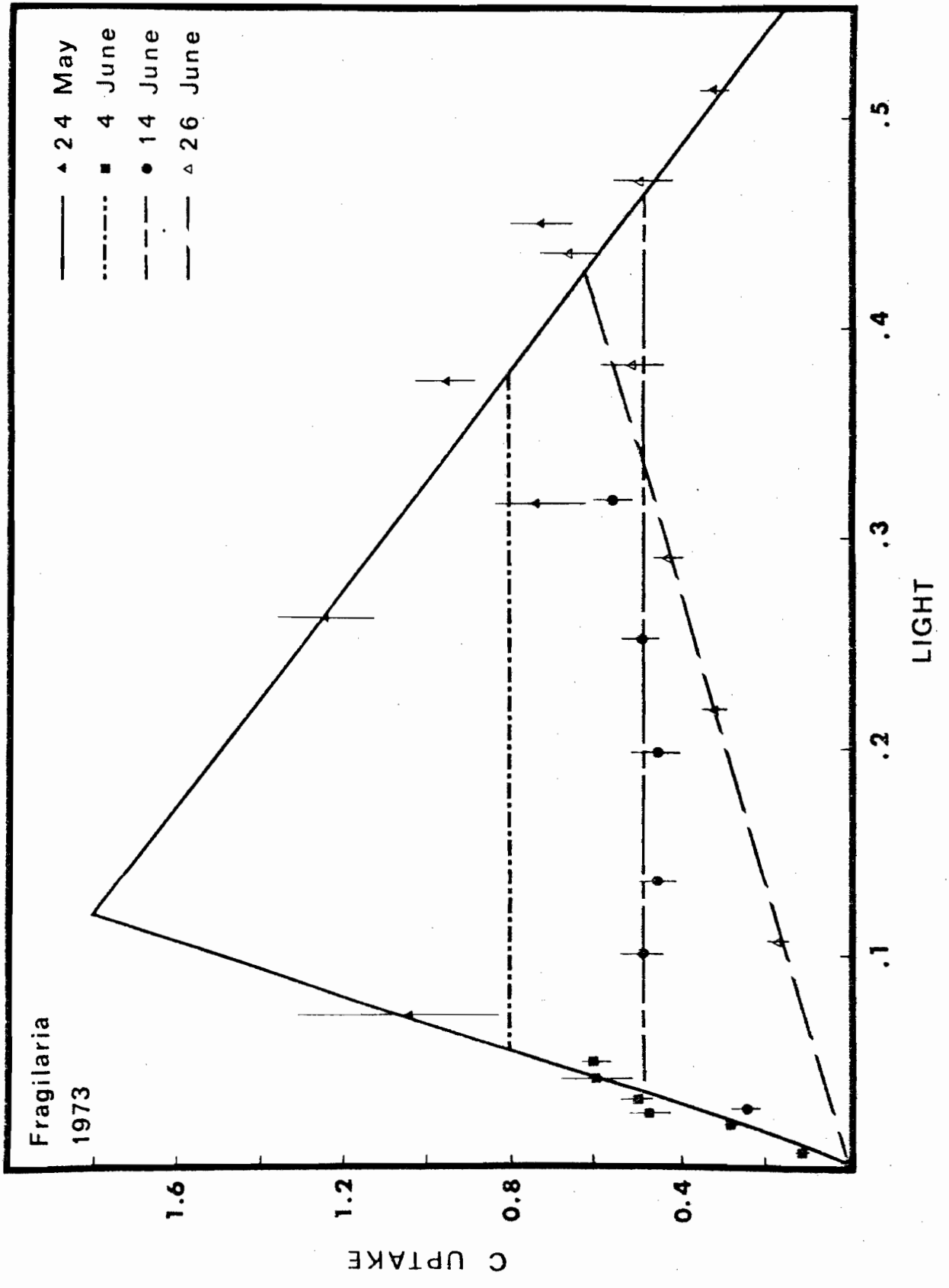
exceeded. As a compromise, a plateau was established part-way between this latter response and that of the previous sampling date. The data for the end of June indicated a large decrease in the light limited slope while the inhibition slope remained unchanged.

RESULTS

Our model is intended to deal primarily with events in the epilimnion. Analysis of temperature profiles using McEwen's method (see Hutchinson 1941) indicates that this zone extends to 4m in depth over most of the study period with a tendency towards further depression in August (Fig. 30, 31). We have elected to treat the epilimnion as always extending from 0m to 4m for this study in order to simplify model construction and analysis. From a theoretical viewpoint it is more important that our model epilimnion does not extend into the thermocline (Hutchinson's clinolimnion) that that it include all of the true epilimnion at all times.

Population data are presented in terms of biomass to allow direct comparison between species. Data from 1973 are presented for the five most common diatom species: Asterionella formosa, Fragilaria crotonensis, Melosira italica, Synedra radians, and Tabellaria fenestrata (Fig. 32). Data from the previous year are presented only for Tabellaria and Asterionella and are intended to extend the autoradiographic analysis for these species rather than to provide a complete lake analysis for that year.

Secchi disc readings (Fig. 33) provide a general measure of trends in lake transparency associated with changes in total algal biomass.

The purpose behind our model is twofold. First, we want to summarize the photosynthetic niche of each species. We do this by comparing model results for sunny and cloudy days in terms of the hourly diurnal patterns and the depth profile of integrated daily carbon fixation. Most importantly,

Figure 30. <u>Left</u>. Water temperature (^{o}C) at 5 sampling depths

between May and October 1972. Determining slopes

by regression permits analysis of the stratification

pattern. <u>Right</u>. Semi-logarithmic plot of rate of

temperature change (^{o}C per day) at each depth (m)

over time showing that the thermocline begins at

approximately 4 m.

Figure 31. <u>Left</u>. Water temperature (^{o}C) at 5 sampling depths
between May and October 1973. Determining slopes
by regression permits analysis of the stratification
pattern. <u>Right</u>. Semi-logarithmic plot of rate of
temperature change (^{o}C per day) at each depth (m)
over time showing that the thermocline begins at
approximately 4 m.
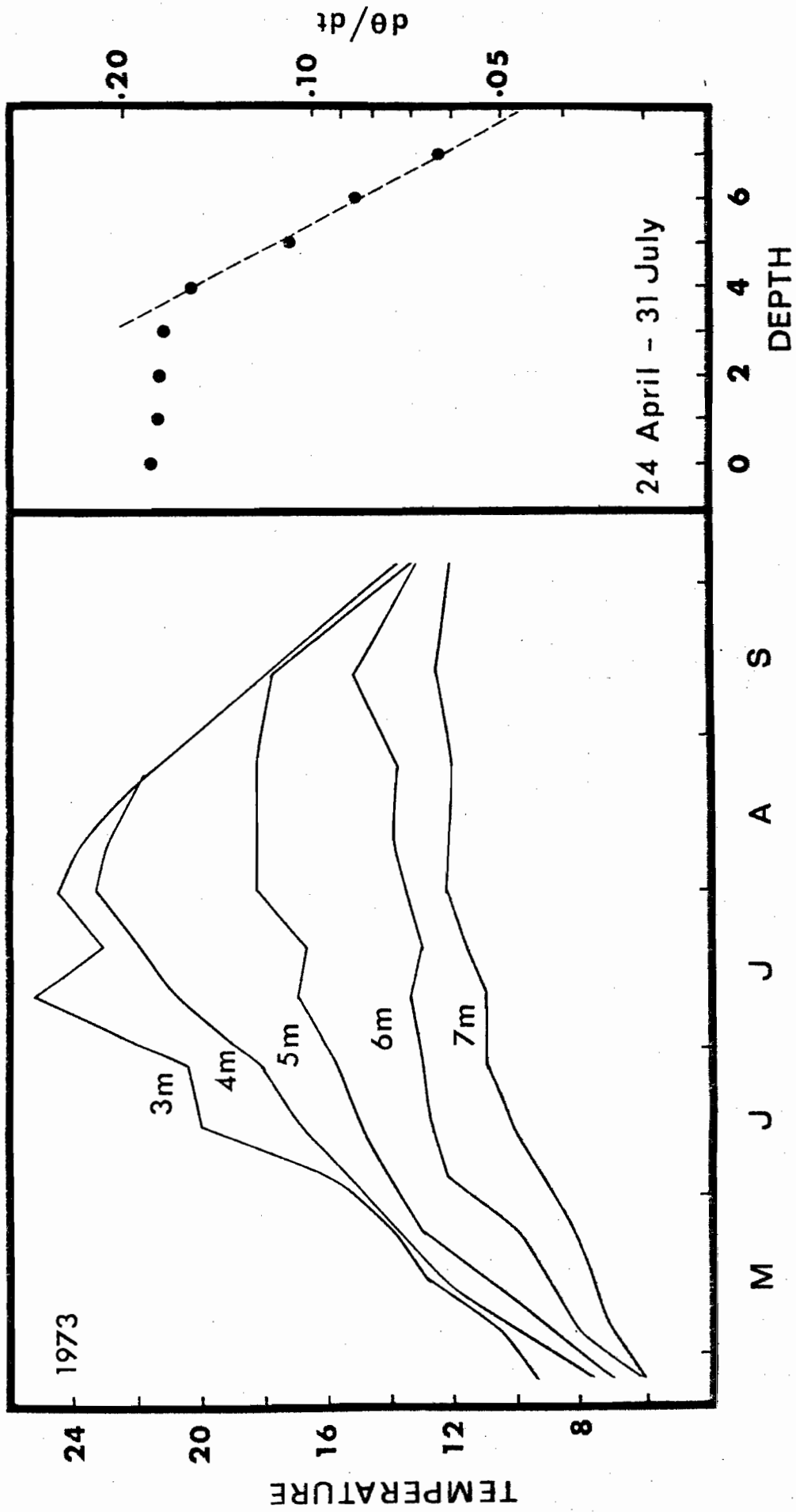
Figure 32. Seasonal pattern of epilimnetic diatom biomass

(mg m^{-2}) changes in Lac Hertel during 1972 and

1973.   a, Asterionella; f, Fragilaria; m, Melosira;

s, Synedra; t, Tabellaria.
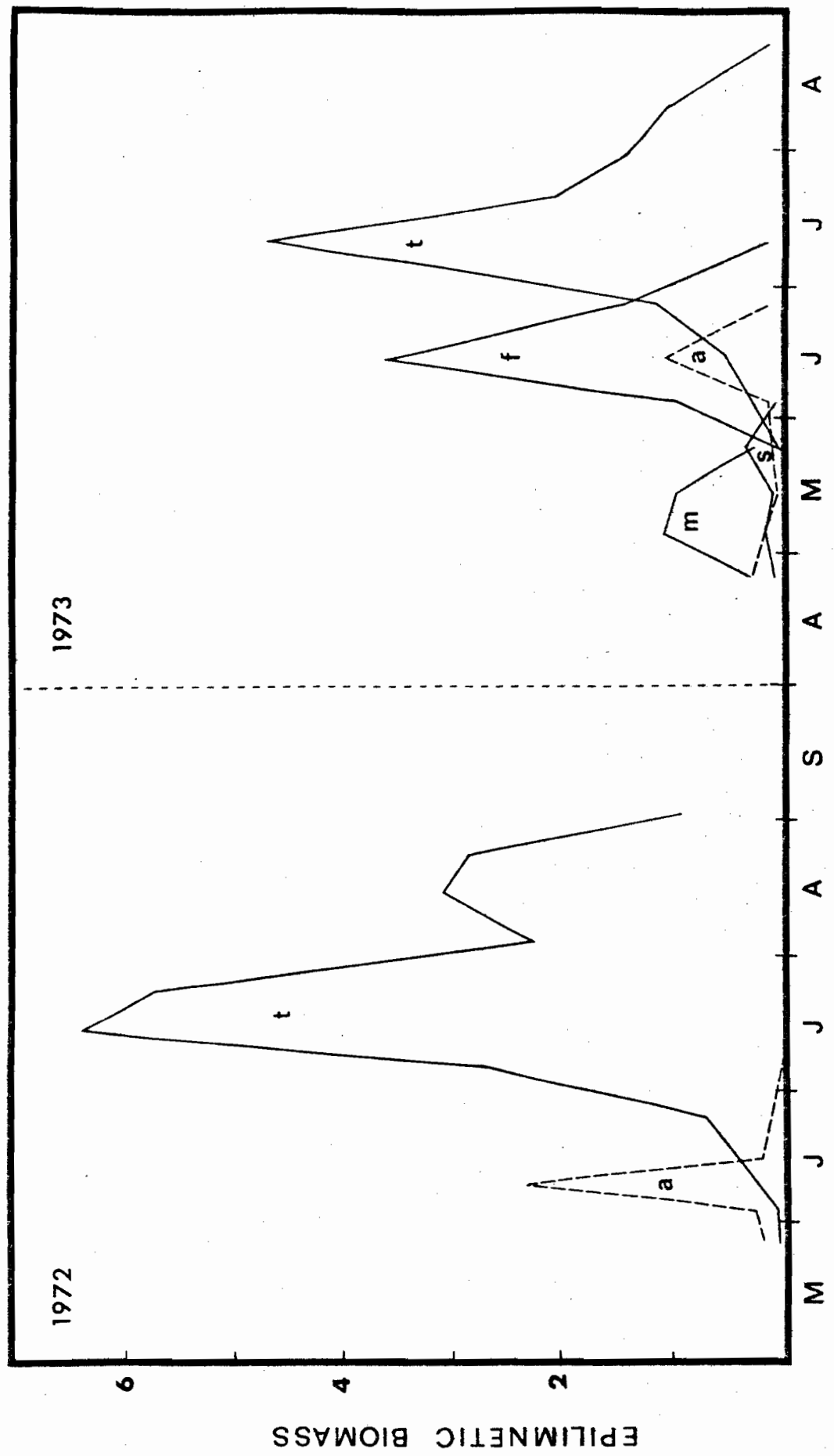
Figure 33. Seasonal pattern of secchi disc depth, reflecting

transparency changes in Lac Hertel. The June

and July peaks each year reflect the Asterionella/

Fragilaria and the Tabellaria blooms respectively.

The May 1973 peak was caused primarily by

flagellates while that of August was brought

about by blue-greens.
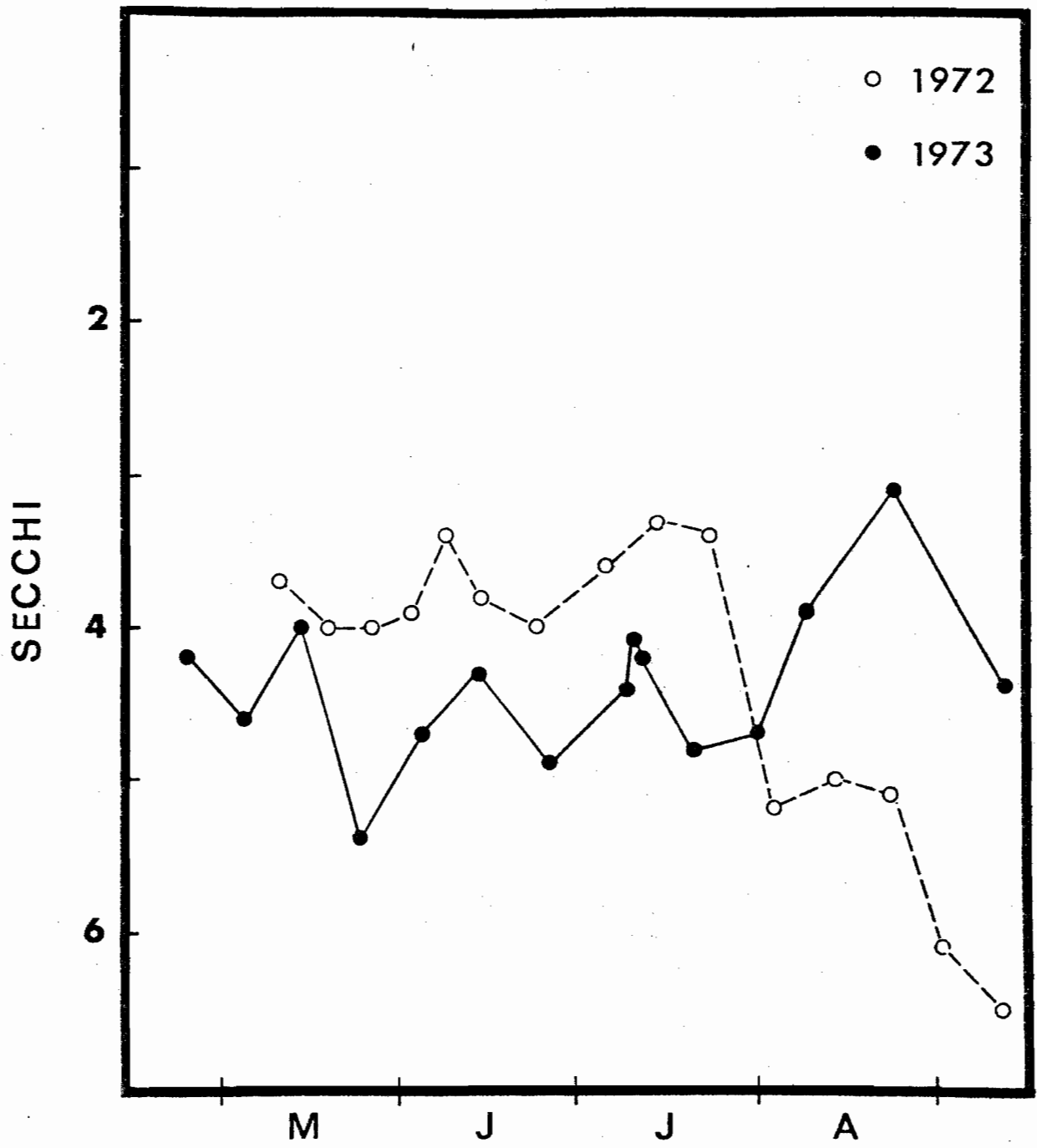
the model allows determination of the mean response of each species integrated over weekly or longer periods, based on the actual light history of the lake. This mean response indicates where each species grows best overall and provides a quite different picture from what one finds based only on sunny, midday incubations.

Second, we want to compare modeled population growth with that actually observed in order to investigate the dynamic processes affecting population success in the lake. To do this it is necessary to construct full light range response curves for each sampling date even when the incident light during a particular experiment was low. Whenever it was necessary to extrapolate the data to higher light this was done on the basis of the pattern exhibited on bright days. While the exact position of a particular curve remains uncertain, numerous model runs show that mean epilimnetic production is relatively insensitive to moderate changes in the high light section of the response curve and thus the precise location is not critical. This is because on bright days the effects of such changes are restricted to the upper epilimnion only and they do not apply at all on cloudy days. As a further precaution, whenever extrapolations were made the data are presented only as means of the entire epilimnetic population. When describing the photosynthetic niche of each species (see above) we consider only those response curves based on complete high light data.

Synedra radians Kützing

The light response data for this species (Fig. 21) suggest a curve with a nearly symmetric shape. While there is severe surface inhibition on bright sunny days this effect is nearly eliminated by 2m (Fig. 34c), due to an extremely high light saturation level (0.26 ly min^{-1}), and is not present at all on days with complete cloud cover (Fig. 34b). Photosynthesis versus depth curves (Fig. 34a) show that the depth of optimum photosynthesis

Figure 34. Model results for _Synedra radians_ in 1973.

A. Depth (m) profiles of daily carbon uptake ($gC \times 10^{-15} \mu m^{-3} day^{-1}$) on a sunny and a cloudy day plus the 30 day mean response (dashed line). Radiation data ($I_o = 1y \ day^{-1}$) and mean epilimnetic carbon uptake ($\overline{epi}$) are presented in the figure. B,C. Diurnal pattern of carbon uptake ($gC \times 10^{-15} \mu m^{-3} h^{-1}$) at various depths (m) for the above dates.

TOTAL DAILY C UPTAKE

A   Synedra

		I_0	$\overline{epi}$
1	19 May	158	3.6
2	$\overline{x}$ n=30	363	5.2
3	16 May	656	7.8

B   19 May

C   16 May

HOUR
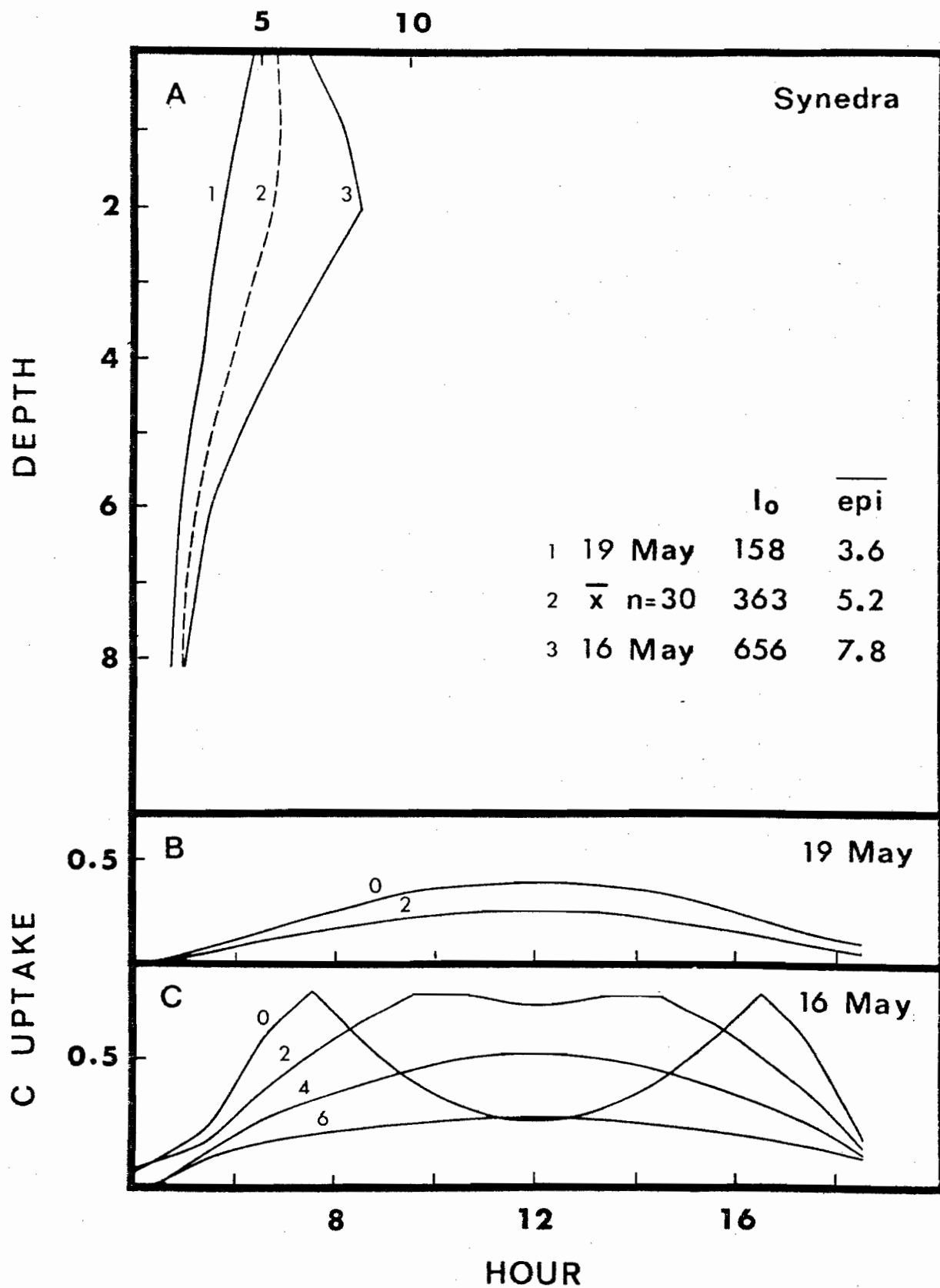
(z_{opt}) always remains in the upper epilimnion even on the brightest days. The average response for the 30 day period emphasizes the near surface optimum.

Melosira italica Ehrenberg

Melosira contrasts sharply with Synedra as its high light response varies considerably with time (Fig. 22). However, the light limited response remains constant and indicates light saturation at levels far below those for Synedra. Since this portion of the curve remains fixed, a decline in the maximum photosynthetic rate (P_{max}) is accompanied by both a decrease in the inhibition slope and a lowering of the light saturation point (I_k). The high P_{max} type curve provides a high growth potential but leads to extremely severe inhibition on clear days (Fig. 35c) resulting in almost total inhibition at the surface during midday. Due to the low I_k and the severity of inhibition, photosynthetic depression extends deep into the epilimnion. In contrast, there is no inhibition at all under cloudy conditions (Fig. 35d) so that photosynthesis decreases exponentially with depth (Fig. 35a). In mid May the greatly decreased P_{max} and I_k result in less severe midday inhibition (Fig. 35e) yet total daily production does not exceed the previous response (Fig. 35b) even at the surface. Although the depth optima are at 3m on sunny days, the mean response for all dates combined still indicates that the surface is more favorable for growth (Fig. 35a,b).

Tabellaria fenestrata Kützing

The model results for 1972 Tabellaria emphasize the contribution of the peak in the boundary response curve (Fig. 23, 24) to high rates of epilimnetic production. Comparison of daily production versus depth for periods covered by the boundary curve with that of a plateau response (Fig. 36a vs. b) indicates the advantage of the former at all levels of daily

Figure 35. Model results for _Melosira italica_ 1973. A,B.

Depth (m) profiles of daily carbon uptake

(gC x 10^{-15} μm^{-3} day^{-1}) on a sunny day and a

cloudy day for high P_{max} (A) and low P_{max} (B)

response dates (see Figure 22 for light

responses) plus the means (dashed lines) for

all dates. Radiation data (I_o = ly day^{-1})

and mean epilimnetic carbon uptake ($\overline{epi}$)

are presented in the figure. C,D,E. Diurnal

pattern of carbon uptake (gC x 10^{-15} μm^{-3} h^{-1})

at various depths (m): C. sunny day with high

P_{max} response, D. cloudy day with high P_{max}

response, E. sunny day with low P_{max} response.

Figure 36. Model results for <u>Tabellaria</u> <u>fenestrata</u> 1972 and

1973. A,B,C. Depth (m) profiles of daily carbon

uptake (gC x 10^{-15} μm^{-3} day^{-1}) on a sunny day

and a cloudy day for a plateau light response (A),

the boundary response (B), and the no inhibition

response (C) plus the means (dashed lines) of all

dates covered by these responses (see Figure

24 and 25 for light responses). Radiation data

(I_o = ly day^{-1}) and mean epilimnetic carbon uptake

($\overline{epi}$) are presented in the figure. C,D,E. Diurnal

pattern of carbon uptake (gC x 10^{-15} μm^{-3} h^{-1})

at various depths (m) for the above sunny days.

TOTAL DAILY C UPTAKE

A 1972

B Tabellaria 1972

C 1973

		I_0	$\overline{epi}$
1	16 July	210	8.2
2	$\overline{x}$ n=47	447	11.8
3	11 July	690	15.2

		I_0	$\overline{epi}$
1	7 August	146	11.5
2	$\overline{x}$ n=35	453	15.5
3	30 July	602	17.4

		I_0	$\overline{epi}$
1	10 July	180	10.1
2	$\overline{x}$ n=43	479	12.1
3	5 July	620	14.1

D July 11, 1972

E July 30, 1972

F July 5, 1973

DEPTH

C UPTAKE

HOUR
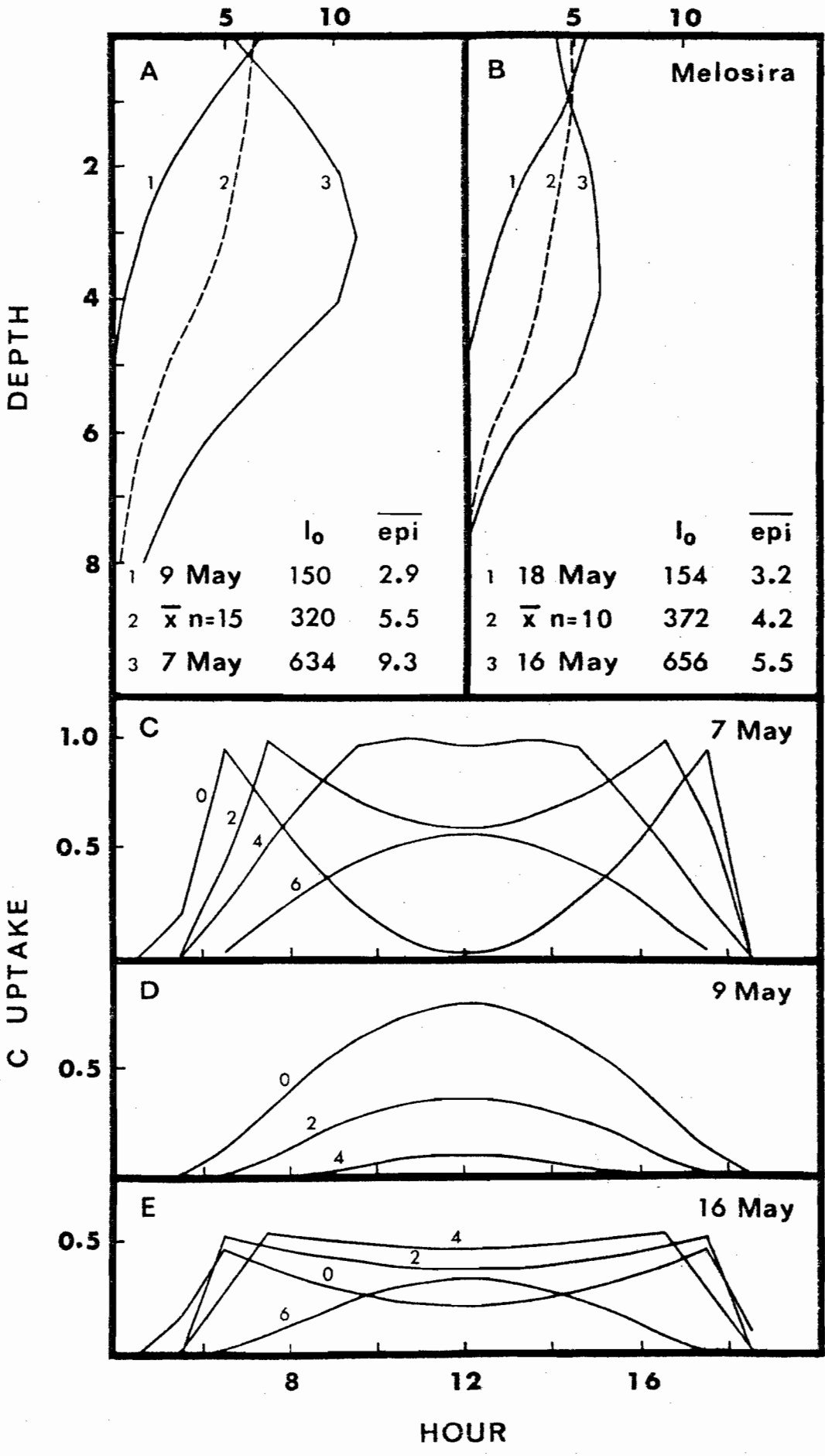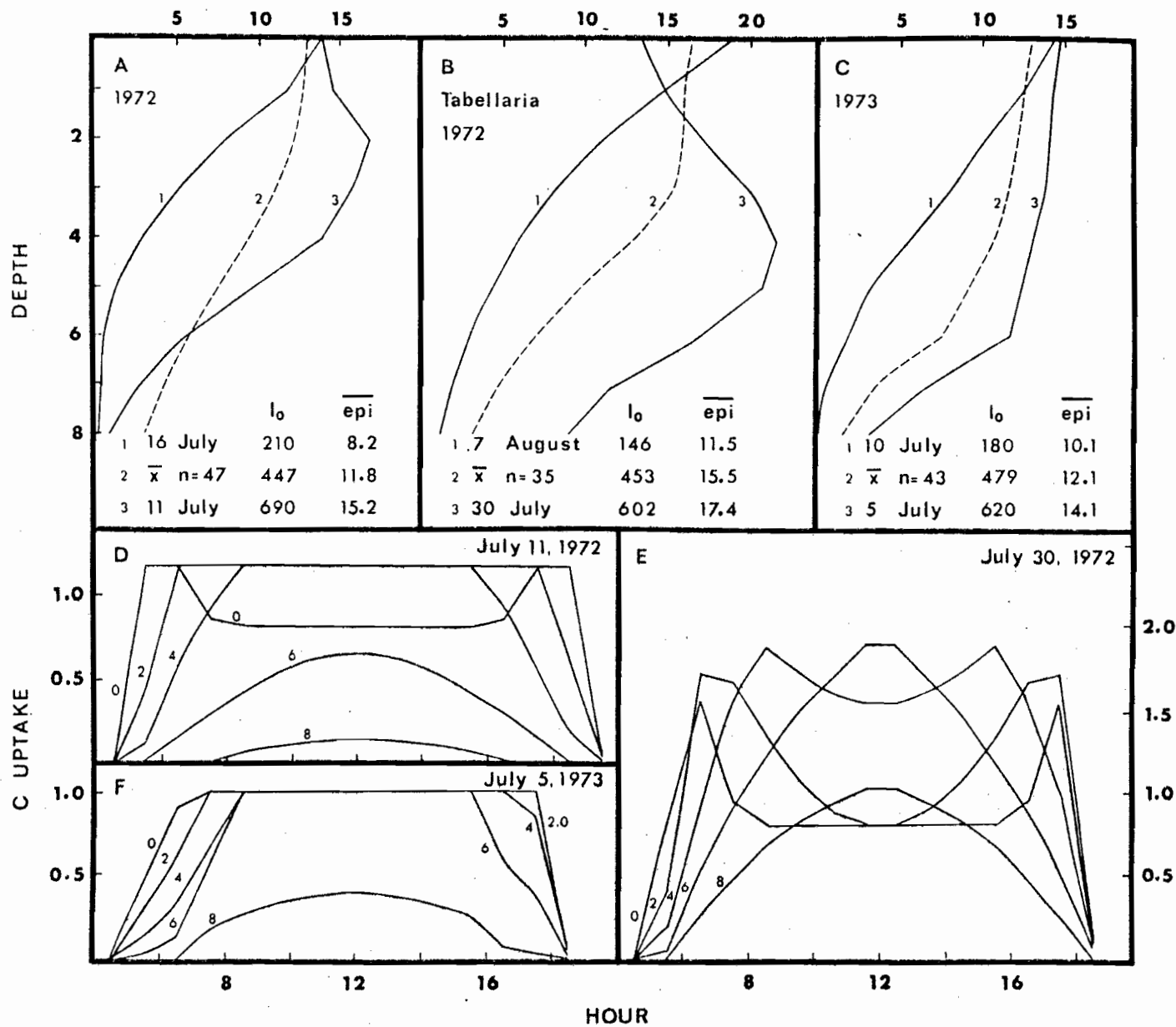
radiation. On bright days the boundary response curve results in depression of the z_{opt} to the bottom of the epilimnion (4m). Despite this depression to 4m, the 35 day mean (Fig. 36b) shows that the optimum growth zone is still at the surface. This is also true of the plateau response (Fig. 36a).

The high light plateau (cf. Fig. 23, 24) is advantageous as it reduces the severity of midday inhibition. This is evident from comparison of Tabellaria's diurnal curves (Fig. 36d, e) with those of Melosira (Fig. 35c).

In 1973 the early season light response was markedly different from that of the previous year as well as from that of any other species examined in this study. The mid to high light response consisted of a single plateau without inhibition (Fig. 25). As a result there was no surface depression under any light condition (Fig. 36c) and the diurnal pattern was simple even on sunny days with all epilimnetic depths saturating in quick succession early in the morning and remaining that way until near dusk (Fig. 36f).

Asterionella formosa Hassall

The 1973 data for Asterionella present an interesting dichotomy between early and late season response. The results up to the middle of May (Fig. 27a) represent a period when the population size was minimal (Fig. 32). The carbon fixation rate is similar to that of Synedra although the saturation intensity is lower thus leading to a deeper z_{opt} (Fig. 37a) on bright days but with generally less severe midday depression (Fig. 37c). At the end of May the slope of the light limited response increased dramatically and was accompanied by a large increase in P_{max} (Fig. 27b) with the overall result being an even lower I_k than earlier which, combined with increasing water transparency, depressed the sunny day z_{opt} to below the epilimnion (5m) (Fig. 37d). This effect is so strong that, for the only time in this study, the mean epilimnetic carbon fixation was considerably greater on cloudy days than on sunny ones (Fig. 37b). The bright day

Figure 37. Model results for _Asterionella formosa_ 1973. A,B.

Depth (m) profiles of daily carbon uptake

(gC x 10^{-15} μm^{-3} day^{-1}) on a sunny day and a

cloudy day for the early spring light response

(A) and the late spring, high P_{max} response (B)

plus the means (dashed lines) of all dates

covered by these responses (see Figure 27 for

responses). Radiation data (I_o = ly day^{-1}) and

mean epilimnetic carbon uptake $\overline{(epi)}$ are

presented in the figure. C,D,E. Diurnal pattern

of carbon uptake (gC x 10^{-15} μm^{-3} h^{-1}) at

various depths (m) for the early spring response

on a sunny day (C) and for the late spring, high

P_{max} response on a sunny day (D) and a cloudy day

(E).

TOTAL DAILY C UPTAKE

105
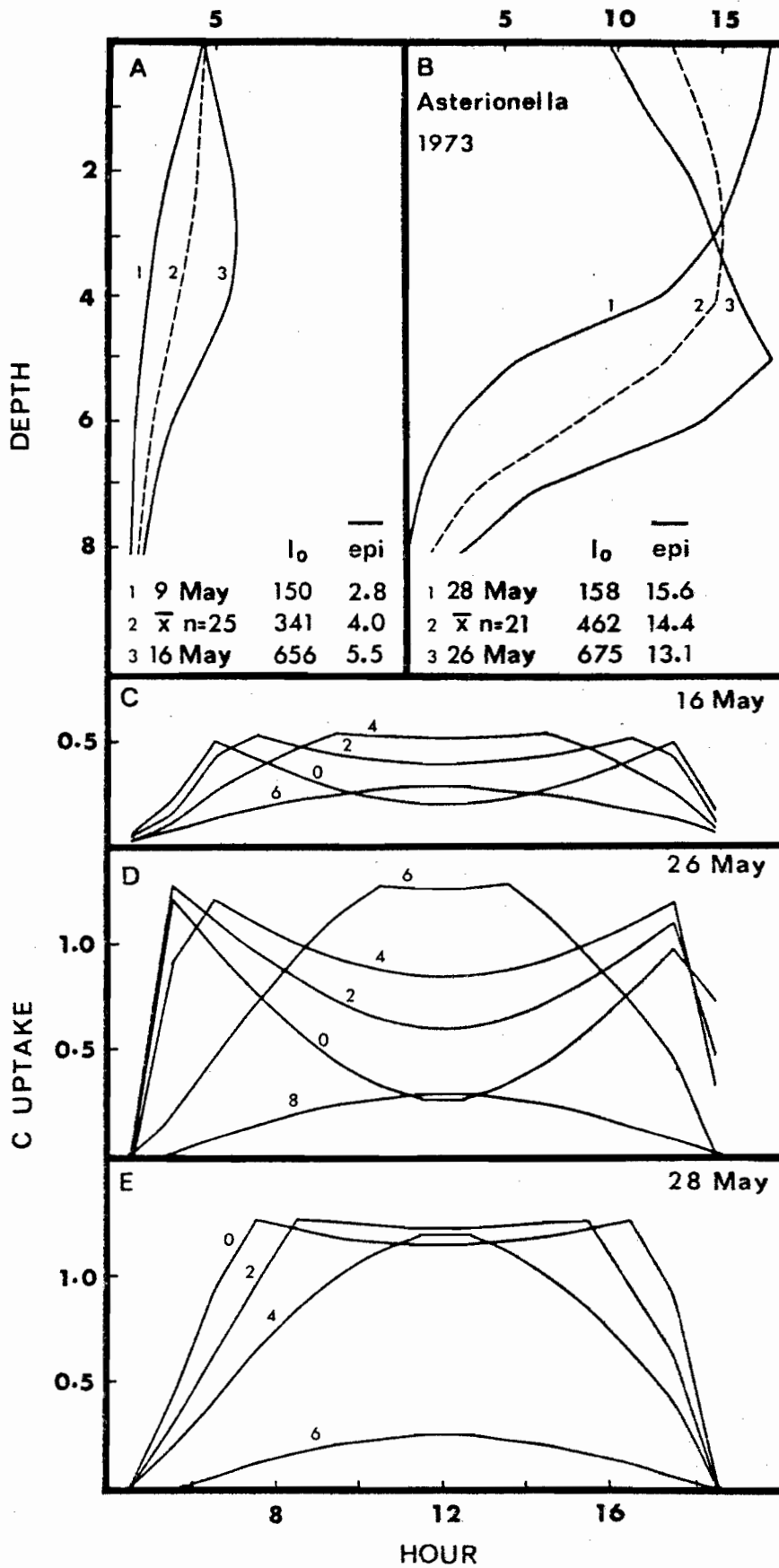
surface inhibition (Fig. 37d) with this response is similar in pattern to that of _Fragilaria_ and _Melosira_, while on cloudy days the epilimnion as a whole is saturated for most of the day without ever experiencing severe inhibition (Fig. 37e). By mid June the response flattened out to a broad plateau with very low P_{max}. Diurnal and depth profiles are not presented for this response because they are essentially of the same pattern as for _Tabellaria_ (Fig. 36a).

The early June data for 1972 exhibit an even higher P_{max} than in 1973 but rapidly declined to low levels by the middle of the month (Fig. 28). Since the high light section of these curves all involved extrapolation the diurnal and depth patterns are not presented in detail although it can be noted that they are similar to those of 1973.

Fragilaria crotonensis Kitton

The P_{max} of _Fragilaria_ changed very rapidly with time (Fig. 29). We present depth profiles for sunny days only (Fig. 38a) as cloudy days all indicated simple exponential declines. The high P_{max} curve provides a high growth potential but results in strong surface inhibition on bright days (Fig. 38b) as was also the case in _Asterionella_ (Fig. 37d). The z_{opt} with this type of response is at the bottom of the epilimnion (4m) on bright days (Fig. 38a). Under such conditions the low P_{max} plateau response of mid June yields nearly constant growth rates throughout the epilimnion. Diurnal curves are not presented for this response as they are similar in pattern to those of _Tabellaria_ (Fig. 36f). The greatly reduced light limited slope at the end of June gives a depth profile (Fig. 38a) and a diurnal pattern (Fig. 38c) most similar to that of _Synedra_ due to a high I_k value.

It is not possible to present representative mean depth responses for long periods as the light response changed too rapidly. However, from comparison with other species it is clear that the z_{opt} will be near the surface.

Figure 38. Model results for _Fragilaria crotonensis_ 1973.

A. Depth profiles of daily carbon uptake
(gC x 10^{-15} μm^{-3} day^{-1}) on sunny days with

three different light response curves (see

Figure 29) representing high slope, high

P_{max} (1); high slope, low P_{max} (2); and low

slope, low P_{max} (3). Radiation data (I_o = ly day^{-1})

and mean epilimnetic carbon uptake ($\overline{epi}$) are

presented in the figure. B,C. Diurnal pattern

of carbon uptake (gC x 10^{-15} μm^{-3} h^{-1}) at

various depths (m) for the high slope, high

P_{max} response (B) and the low slope, low P_{max}

response (C).

TOTAL DAILY C UPTAKE

A — Fragilaria

1	26 May	635	19.5
2	13 June	655	6.9
3	25 June	686	5.2

B — 26 May

C — 25 June
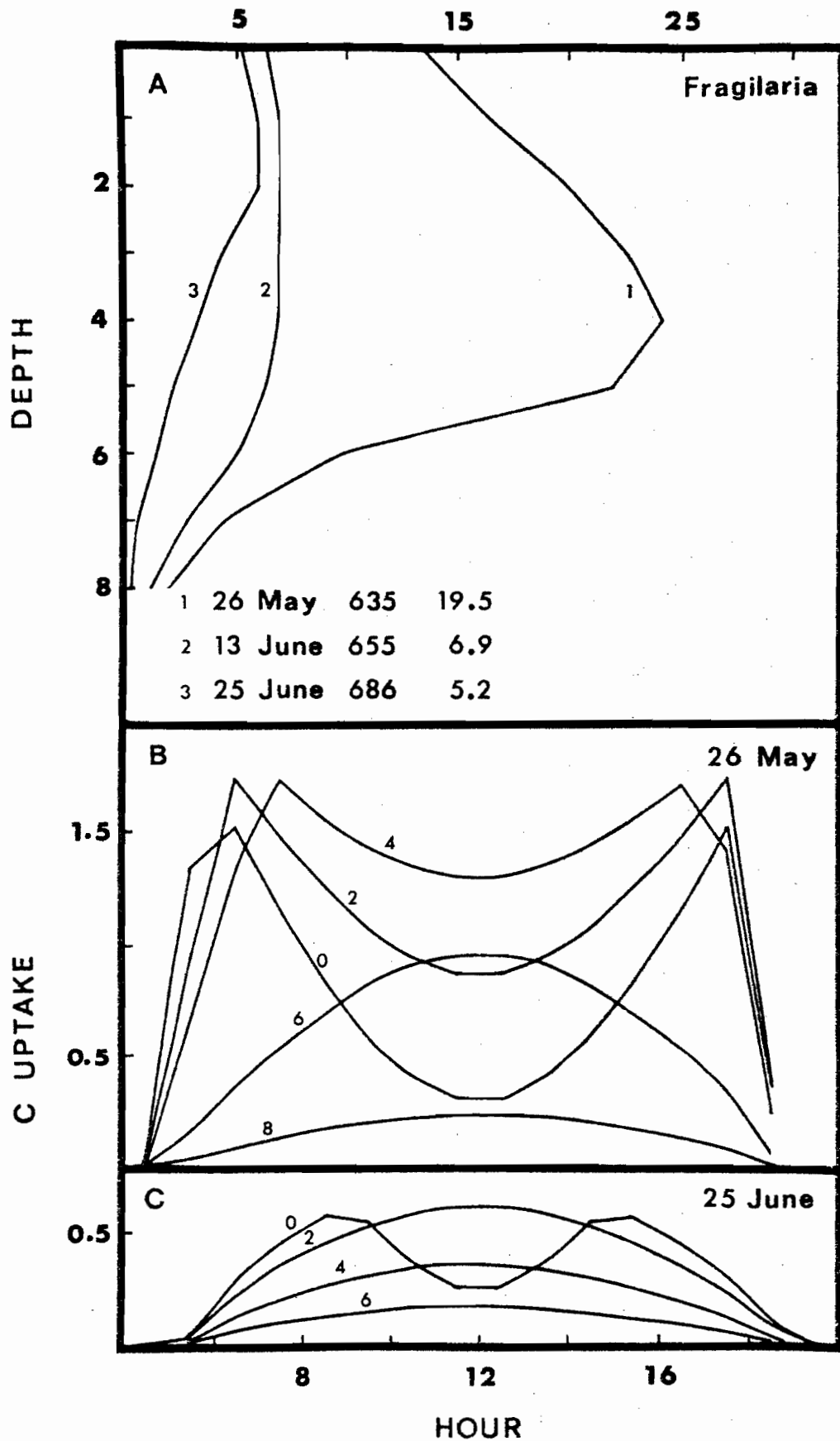
Seasonal summaries

Cell division rates (see Methods) are summarized on a seasonal basis
to facilitate comparison with biomass changes observed in the lake (Fig. 39,
40,41). The arrows in these figures delineate the points at which the
equations in the model were allowed to change if required by the light
response data (Table 7). In the absence of equation changes the variation
noted is due only to varying light conditions. Long term trends can result
from changing daylength, which accounts for the gradual seasonal decline of
Tabellaria's division rate (Fig. 40, 41). Trends can also result from
changes in lake transparency. For example, the division rate of Synedra
and Melosira were equivalent at the end of May while Melosira was highest
early in the month (Fig. 40). This change was the result of increased
transparency at the end of May (Fig. 33) which favored the higher I_k of
Synedra.

Comparing cell division rates during early Spring 1973 (Fig. 40) we
observe that Melosira and Synedra both have a cell divison rate distinctly
higher than that of Asterionella. Near the end of May, both Asterionella and
Fragilaria commence rapid growth at similar rates while neither Melosira or
Synedra respond. During the period of rapid growth, which extended until
early June, the average division rate of Asterionella was 0.40, similar to
the value of 0.47 (3.3. divisions per week) reported by Talling (1955) for
a natural population suspended in a bottle at 1m for one week. The maximum
division rate of Tabellaria is less than half that of Asterionella and
Fragilaria, primarily because of its higher carbon content. Talling (1955)
noted a similar relationship in cultures of these three genera suspended in
Lake Windermere, although the Tabellaria species was T. flocculosa rather
than T. fenestrata.

Combining the estimates of cell growth and population growth with data
on the proportion of dead cells present enables the simultaneous calculation

Figure 39. Comparison of model predicted mean epilimnetic

division rates (divisions day^{-1}) of <u>Asterionella</u>

<u>formosa</u> and <u>Tabellaria</u> <u>fenestrata</u> in 1972.

Figure 40. Comparison of model predicted mean epilimnetic

division rates (divisions day) of <u>Asterionella</u>

<u>formosa</u>, <u>Fragilaria</u> <u>crotonensis</u>, <u>Melosira</u>

<u>italica</u> and <u>Synedra</u> <u>radians</u> in spring 1973.

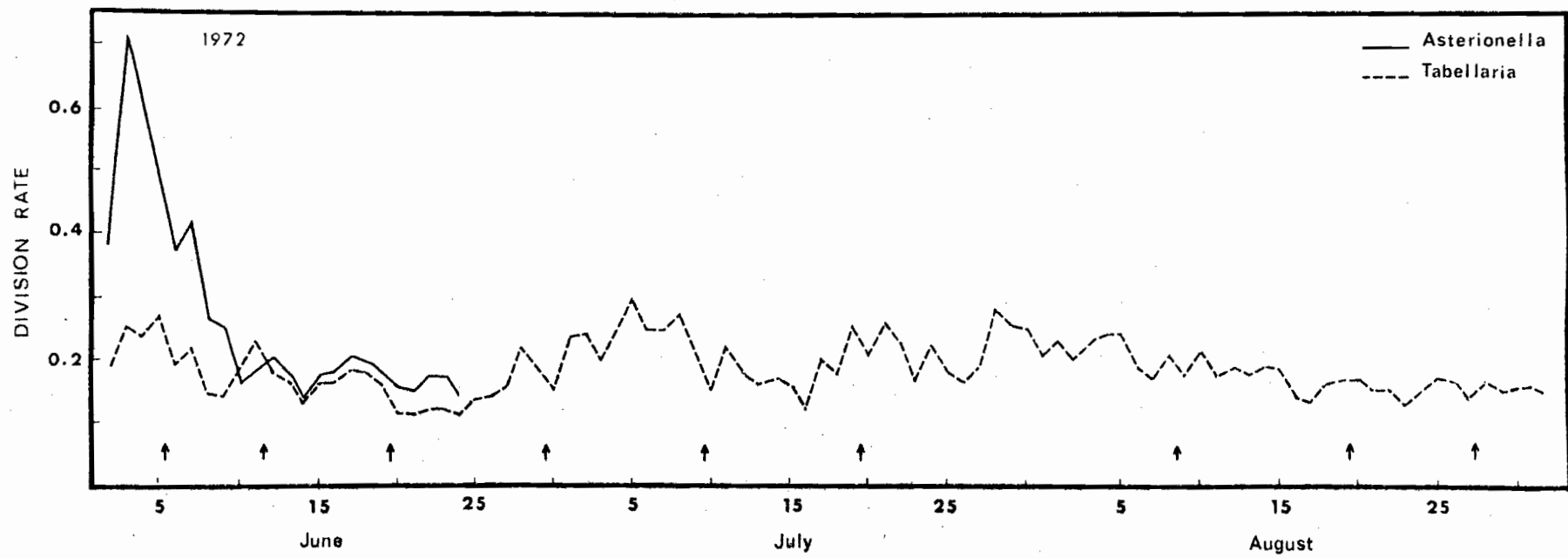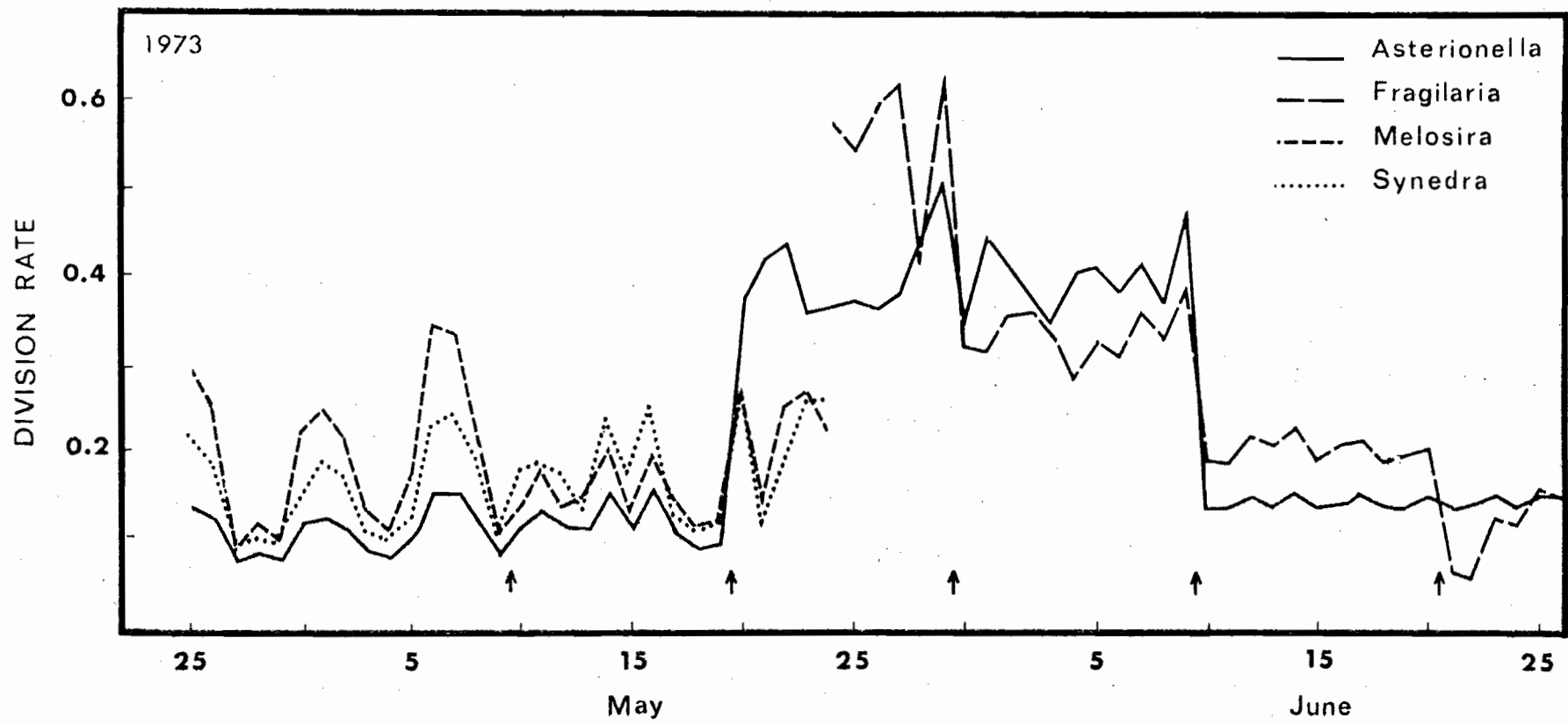Figure 41. Comparison of model predicted mean epilimnetic division rates (divisions day^{-1}) of <u>Asterionella formosa</u>, <u>Fragilaria crotonensis</u> and <u>Tabellaria fenestrata</u> in late spring and summer 1973.
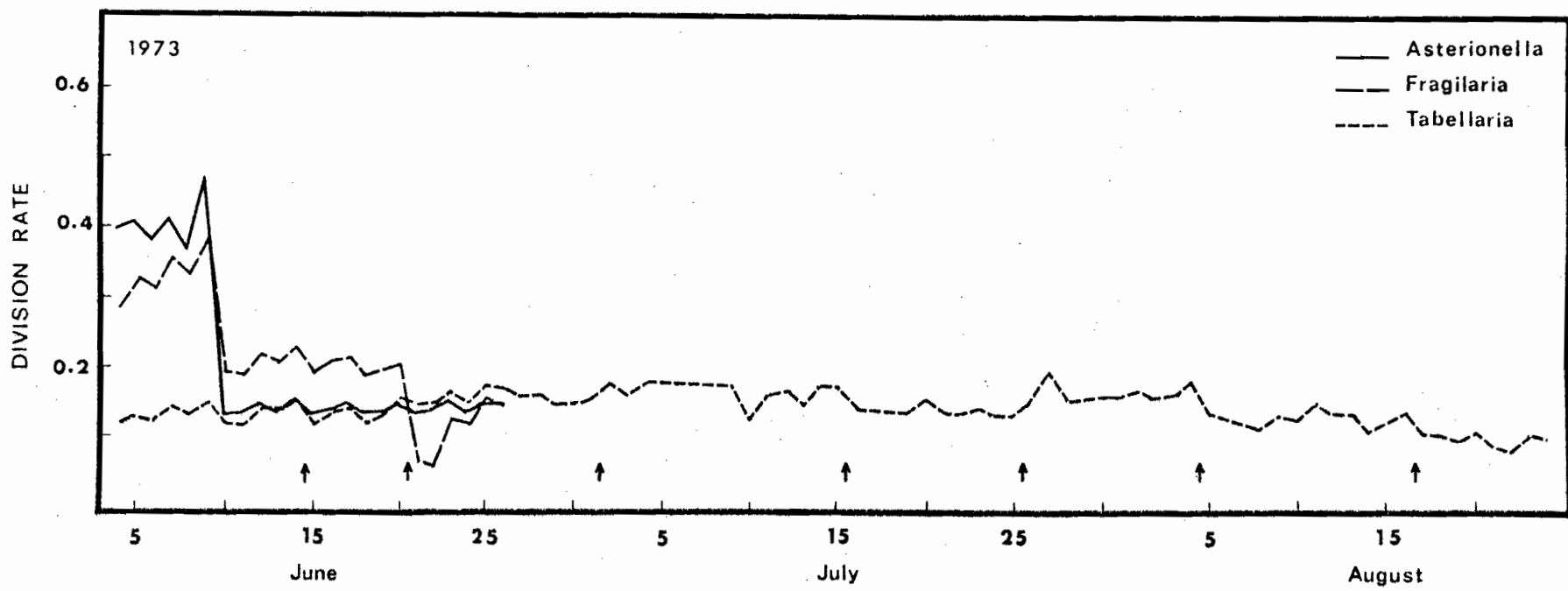
Table 8. Cell growth (c), death (d), sinking (s) and population

growth (k) rates computed for five diatom species. The

values apply to the sampling interval preceding

the indicated dates.

Species/date	c	d	s	k	Species/date	c	d	s	k
Tabellaria					Asterionella				
1972					1972				
2 June					2 June				
8 June	.193	-.001	-.000*	.192	8 June	.410	-.028	-.000*	.382
14 June	.154	-.000	-.033	.121	14 June	.219	-.150	-.483	-.414
24 June	.152	-.002	-.099	.052	24 June	.198	-.060	-.200	-.062
5 July	.176	-.003	-.053	.120					
14 July	.195	-.004	-.095	.096	Asterionella				
23 July	.177	-.007	-.159	.011	1973				
3 Aug	.195	-.011	-.269	-.085	25 April				
14 Aug	.182	-.009	-.144	.028	4 May	.094	-.029	-.118	-.052
23 Aug	.149	-.016	-.142	-.009	14 May	.110	-.070	-.156	-.117
1 Sept	.144	-.034	-.234	-.125	24 May	.209	-.068	-.130	.011
					4 June	.333	-.100	-.163	.070
Tabellaria					14 June	.246	-.030	-.000*	.217
1973					26 June	.133	-.072	-.301	-.240
4 June									
14 June	.124	-.001	-.000*	.123	Melosira				
26 June	.136	-.003	-.064	.068	1973				
10 July	.151	-.005	-.044	.102	25 April				
20 July	.139	-.010	-.209	-.080	4 May	.161	-.018	-.000*	.143
31 July	.140	-.008	-.169	-.038	14 May	.170	-.035	-.147	-.012
9 Aug	.135	-.009	-.153	-.027	24 May	.170	-.053	-.270	-.153
24 Aug	.087	-.016	-.244	-.173					
					Synedra				
Fragilaria					1973				
1973					25 April				
24 May					4 May	.132	-.037	-.000*	.095
4 June	.357	-.024	-.000*	.334	14 May	.157	-.055	-.137	-.035
14 June	.242	-.008	-.105	.129	24 May	.172	-.019	-.036	.117
26 June	.150	-.014	-.210	-.074					

* Defined to enable percent carbon calculation (see Methods).

of death and sinking rates (see Methods). Death rates of Tabellaria,
Melosira, and Fragilaria are generally much lower than their sinking rates
(Table 8). There is less disparity in Asterionella and Synedra, although
death losses still average less than half the sinking losses.

DISCUSSION

The results can be interpreted at two levels. First, they provide basic
information on the nature of light inhibition, the factors controlling the
P_{max}, and the role of the I_k in optimization of growth. Secondly, the results
elucidate the population dynamics through analysis of the relative contribut-
ions of growth, sinking and death to population fluctuations observed in
nature.

Light Inhibition

The absence of inhibition in Tabellaria during early summer 1973 (Fig.
25) is typical for algal cultures (e.g. Jorgensen 1969, McAllister et al.
1964) but, according to our results, is clearly exceptional in nature where
diatoms normally show a strong decline in net carbon fixation with increasing
light beyond the I_k. Thus Asterionella exhibits only mild inhibition in
culture (Talling 1966) while we find severe in situ inhibition (Fig. 27).

Postulating a light dependent inhibition function (Fig. 42) produces the
simple pyramid shaped curve noted for Asterionella, Fragilaria, Melosira and
Synedra at peak production. As these species exhibit plateaus during
periods of lowered P_{max} this implies that the light level at which inhibition
is initiated is inversely related to the P_{max}. Consequently, when the P_{max}
is low inhibition begins at a higher light intensity than when the P_{max} is
high (Fig. 42). When Tabellaria is inhibited the net photosynthetic rate
becomes re-stabilized at a lower plateau (Fig. 23, 24, 26) indicating that
inhibition reaches a maximum which is less than the gross photosynthetic rate.

Figure 42. Schematic diagram of photoinhibition function

hypothesized on the basis of the observed carbon

uptake: light responses. The slope of the

photoinhibition function remains constant but the

induction light intensity is an inverse function

of P_{max}. Thus when $P_{max}1$ is lowered to $P_{max}2$,

Photoinhibition 2 is initiated at a higher light

intensity than was Photoinhibition 1. The dotted

lines represent gross photosynthesis while the

solid lines represent net photosynthesis resulting

from the hypothesized photoinhibitory effects

(dashed lines).
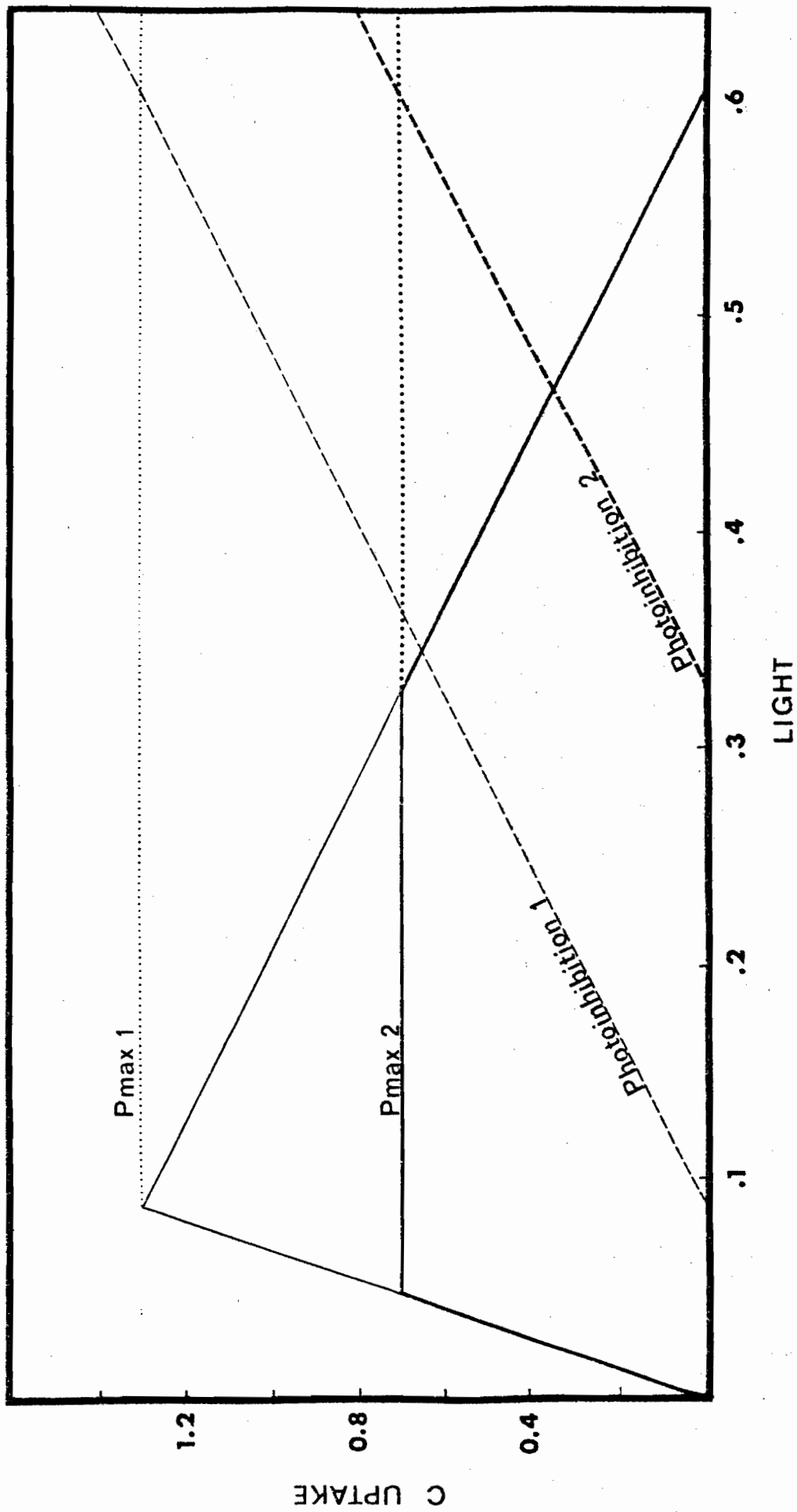
For the other four species this maximum must be higher than gross photo-synthesis because net carbon fixation goes to zero at high light.

The inhibition function we postulate is dependent on light for both induction and rate and thus has the characteristics of biochemical processes collectively included under the terms photorespiration and photooxidation. It is improbable that the latter accounts for the observed inhibition because Tabellaria showed no post-inhibition depression of the P_{max} or low light slope during the late afternoon incubation of a diurnal study (9 August 1973, Appendix 1). Photooxidation would have resulted in a lasting depression because damage to the photoreceptor system is not immediately reversible (Steemann Nielsen 1962). Furthermore the very low light levels at which inhibition is initiated also argue against photoinhibition. Research with algal cultures has demonstrated the occurrence of photorespiration in many species including Ankistrodesmus, Chlamydomonas, Chlorella and Ochromonas (Brown and Weis 1959, Hiller and Whittingham 1959, Weis and Brown 1959, Zelitch and Day 1968). The first three studies found an enhancement of photorespiration with increasing light similar to the inhibition process we observed and the experiments with Ankistrodesmus clearly showed that photo-respiration was absent under low light and was induced at higher intensities (Fig. 7 in Brown and Weiss 1959). We postulate that the observed relation-ship in our work between P_{max} and induction intensity is mediated through the stimulatory effect of O_2 on photorespiration (Tregunna et al. 1966) with higher rates of photosynthesis leading to higher internal oxygen levels which hasten the induction of photorespiration. If this mechanism applies photorespiration can be treated as a special case of end-product inhibition in phytoplankton growth models (e.g. Lehman et al. 1975). There clearly is a need for further work on both photorespiration and photooxidation in algae. Such research can be most readily done in the laboratory, but cultures should

be operated at _in situ_ production levels if the results are to be directly
applicable to nature.

Factors controlling the P_{max}

The basic light response parameters are the light limitation and
inhibition slopes and the P_{max}. As we have observed that both slopes remain
constant for long intervals, changes in growth rate result primarily from
changes in the P_{max}. The principal factors which can control the P_{max} are
photoreceptor capacity, temperature and nutrients.

The magnitude of the P_{max} is not likely due to photoreceptor saturation
because its level varies considerably without affecting the light limitation
slope. For example, the _Tabellaria_ plateau of 14 June 1972 is only 45% of
the peak response noted on 2 June and yet the low light slopes are essentially
identical (Fig. 23) indicating that photoreceptor efficiencies are equivalent.

Culture studies have demonstrated the potential role of temperature in
determining the P_{max} (e.g. Talling 1955, Steemann Nielsen and Jorgensen
1968), however our results indicate no significant temperature effects. For
example, despite a $13^{o}C$ temperature differential, _Tabellaria_ at 6m on July
1973 showed the same P_{max} as the epilimnetic samples (Fig. 25). Similarly,
Synedra exhibits a consistent light response independent of depth and
seasonal temperature variation (Fig. 21, range from $6^{o}-14^{o}C$). The rapid
growth of _Asterionella_ and _Fragilaria_ at the end of May (Fig. 40) similarly
is not related to temperature change. The discrepancy between these obser-
vations and those in culture results from the wide disparity in nutrient
conditions. Temperature effects are important under the nutrient sufficient
conditions of batch culture but are insignificant under the natural conditions
we have studied over a $6^{o} - 25^{o}C$ temperature range. Therefore, the indis-
criminant application in primary production models of temperature functions,

as well as other functions for practically every effect ever observed in culture, appears unwarranted. Without field data, models become little more than curve fitting exercises.

With the elimination of both temperature and photoreceptor capacity, nutrients remain as the principal factor controlling P_{max}. The epilimnetic population is reliant upon four principal nutrient sources: meteorologic input, geologic input, vertical entrainment and epilimnetic recycling. Precipitation records from the nearby (1 km) weather station provide an indirect estimate of combined meteorologic and geologic input. Analysis shows that the correlation of P_{max} in Tabellaria reaches a maximum with the rainfall for the three day period preceding the sampling date (Fig. 43). Graphic presentation indicates a linear relationship up to a rainfall total of about 2.5 cm, above which the P_{max} does not increase further. Up to this precipitation level the linear correlation accounts for 62% of the variance in P_{max} (Fig. 44). As Stauffer and Lee (1973) provided strong evidence for the importance of wind induced vertical entrainment, following a severe storm in Lake Mendota, an attempt was made to analyze these effects in Lac Hertel using wind records as an indirect measure. However, the correlation was both statistically insignificant and negative, possibly because of the well protected nature of the lake basin.

Data for the other four species are insufficient to allow as complete an analysis as for Tabellaria. Incidental observations on Asterionella and Fragilaria in 1972 and 1973 show that the periods of rapid growth were always preceded by substantial rainfall. However, the pigment and/or enzyme levels are not always sufficient to respond to nutrient inputs as demonstrated by the low slope of Asterionella's light limitation response in early spring 1973 (Fig. 27a). The factors which increased Asterionella's photoreceptor capacity at the end of May (Fig. 27b) and decreased that of Fragilaria at the end of June (Fig. 29) remain obscure.

Figure 43. Correlation coefficient (r) for $\underline{Tabellaria}$ P_{max}

vs (total) precipitation in 1972 as a function

of the number of days prior to the incubation for

which the total is integrated. The maximum

correlation with rainfall occurs upon integration

for the previous three days. The supra-optimal rain-

fall value (see Fig. 43) is not considered in

these calculations, although the correlation is

still significant ($p \leq 0.05$) if it is included.
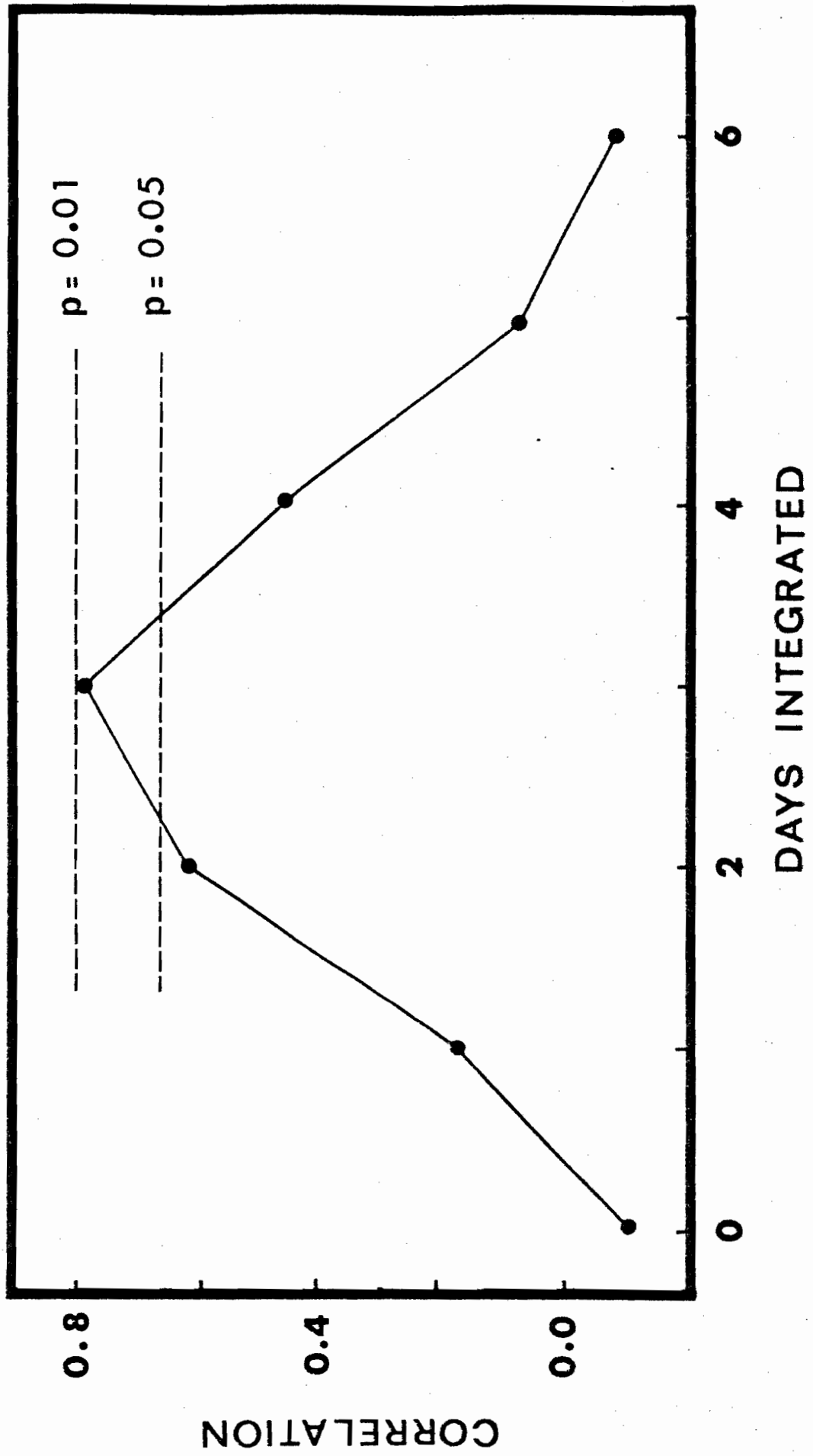
Figure 44. Correlation between <u>Tabellaria</u> P_{max} (gC x 10^{-15} μm^{-3} h^{-1}) and three-day integrated precipitation (cm). The solid line is the principal axis, excluding the supraoptimal rainfall value (open circle). There is a significant correlation ($r = 0.79$) indicating a linear response up to a total precipitation level of at least 2.5 cm. ($y = 0.96 + 0.42$ x, $n = 9$, $p < 0.05$).

Tabellaria
1972
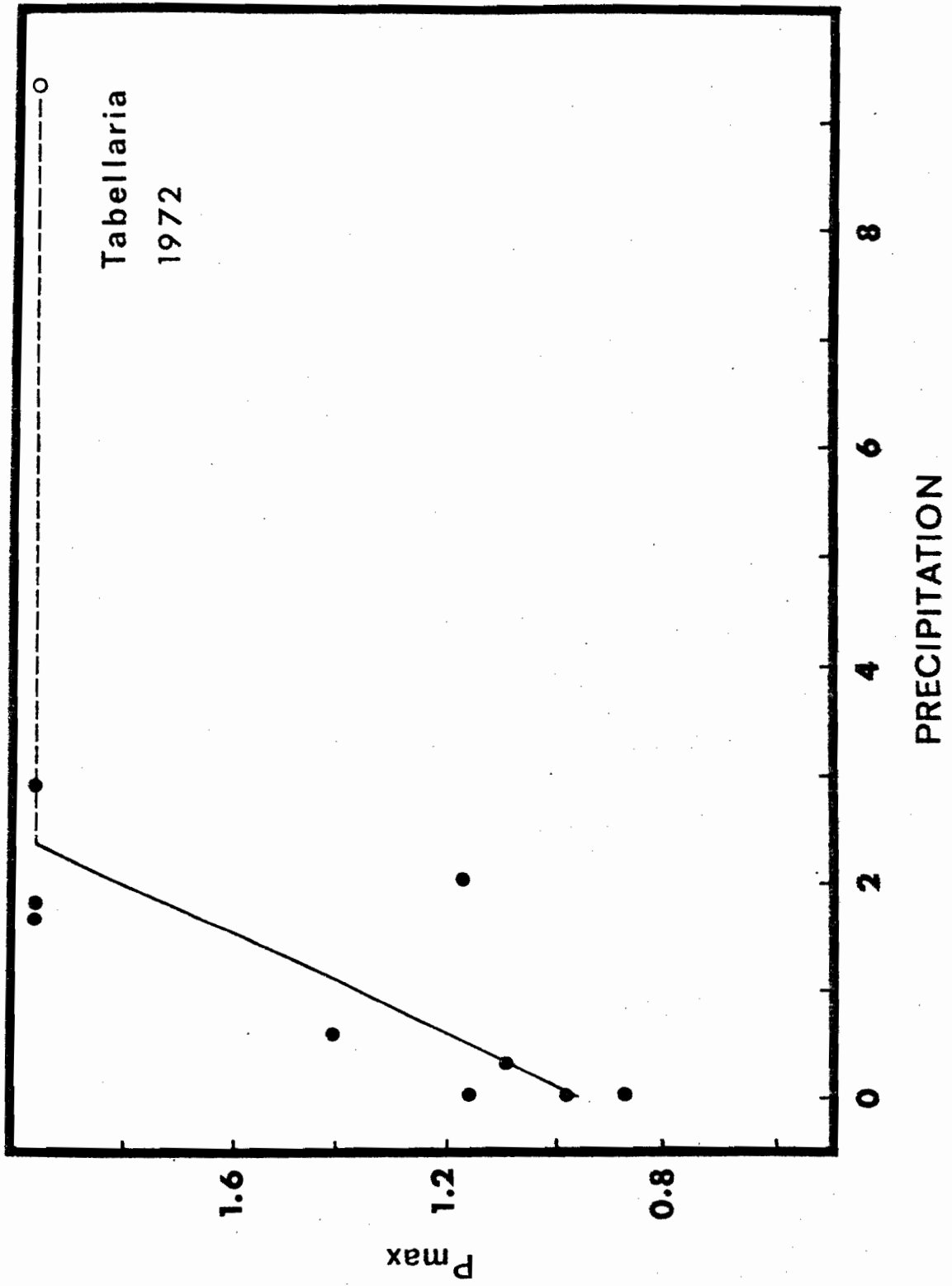
Role of the I_k
_____

While it is evident that the P_{max} determines the general magnitude of cell growth, the ecological significance of the I_k is less clear because all species show optima at or near the surface when growth is averaged over several days (Fig. 34-37, dashed lines).

Presenting the epilimnetic cell division rate as a function of daily incident radiation provides an integrative measure of how well the species light response is adapted to the environment. If the I_k is too high for average lake conditions then cell division will tend to be light limited. This is most notable in <u>Synedra</u> and <u>Melosira</u> (Fig. 45 a,b). An I_k that is too low will result in inhibition with increasing radiation. This was noted only in <u>Asterionella</u> during a period of rapidly increasing lake transparency (Fig. 45 c, '■' symbols). <u>Fragilaria's</u> division rate exhibited a flat response to light over a wide range of P_{max} values (Fig. 45 d) until the light limitation slope changed at the end of June (Fig. 29). <u>Tabellaria's</u> response was similarly flat in 1973 (Fig. 45 f) and was only slightly light limited in 1972 (Fig. 45 e) despite much lower lake transparency.

The advantage of a flat response can be readily demonstrated by re-simulating the growth of <u>Synedra</u> using the original P_{max}, x and y intercepts but with an I_k lowered from 0.248 to 0.120 ly min^{-1}. This change yields a 32% increase in epilimnetic growth.

There are two ways to achieve a lower I_k. One is to leave the light limitation slope unchanged but to lower the P_{max} (see Fig. 42). While this does maintain a flat response during changes in lake transparency, the lower P_{max} results in a lower division rate. Thus growth is <u>optimized</u> in terms of the given P_{max}, but is not <u>optimal</u> with respect to population success because the P_{max} is lower. Conversely, if the P_{max} is left unchanged, lowering the I_k requires an increase in photoreceptor capacity (Fig. 27a vs b)

Figure 45. Relationship between epilimnetic mean cell

division rate (divisions day^{-1}) and daily

incident radiation (ly day^{-1}). A. Synedra

radians. B. Melosira italica. C. Asterionella

formosa. D. Fragilaria crotonensis. E,F.

Tabellaria fenestrata. The various symbols

for each species represent results of different

response curves (see Table 7). The dashed lines

are fitted visually to show trends. A positive

slope indicates that epilimnetic growth is

light limited whereas a negative slope indicates

light inhibition. In the case where epilimnetic

mean cell division is independent of daily

radiation over the range encountered, the slope

is zero.
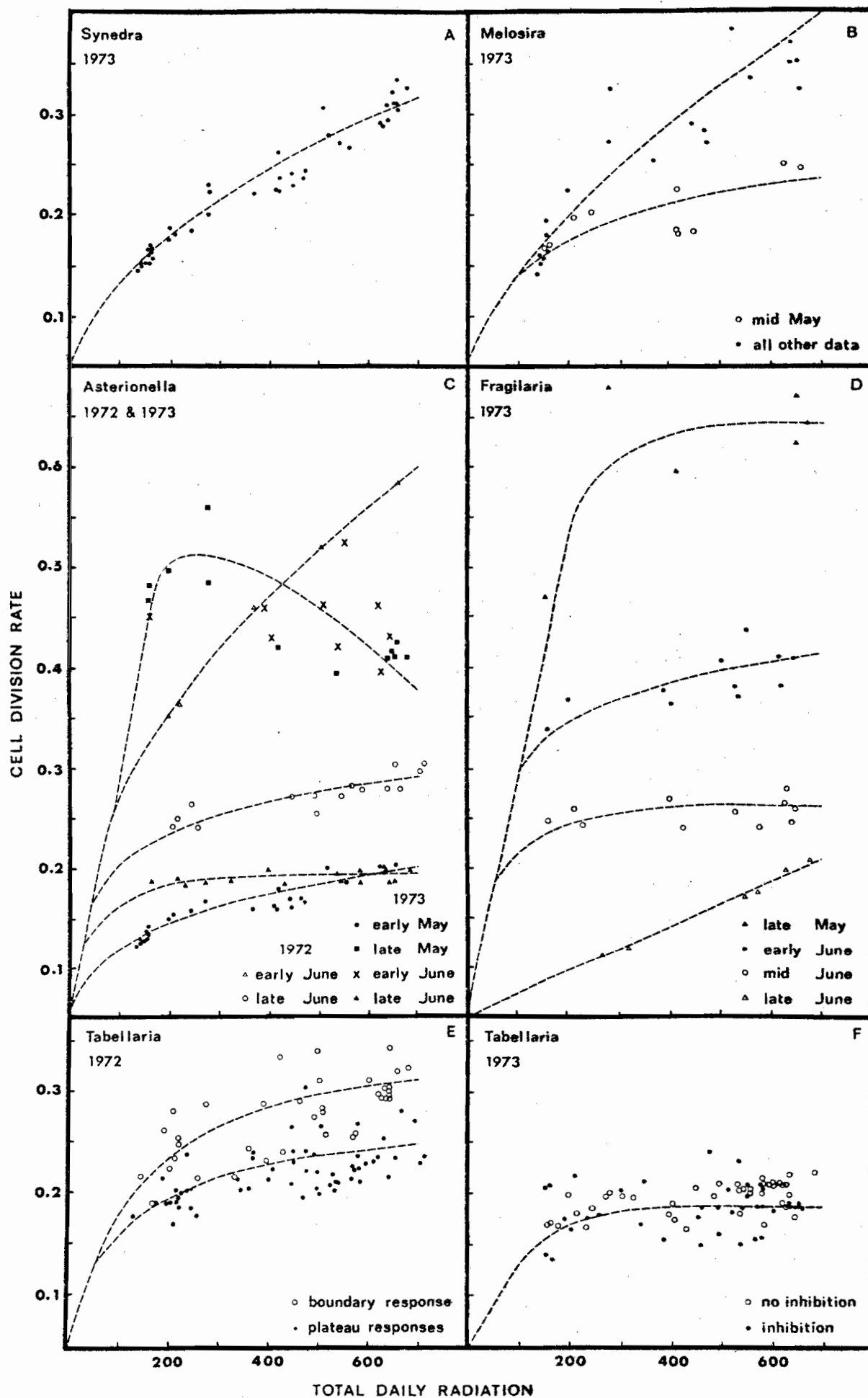
through increased pigment and/or enzyme levels (e.g. Jorgensen 1969). The species in this study tend to be light limited (Fig. 45), indicating that their photoreceptor capacity is not fully optimized. It thus appears that the physiological "cost" of achieving a lower I_k must often outweight the benefits.

Asterionella's division rate was mildly light limited but for two interesting exceptions. In early June 1972 cell division was strongly light limited concurrent with a rapid decline in lake transparency. An unusually high carbon fixation rate was observed at very low light (Fig. 28, 8 June, 4m),however, suggesting that the population was in the process of adjusting its photoreceptive capacity to the new growth conditions. Secondly, in late May of 1973 the Asterionella population appeared to be temporarily light inhibited (Fig. 27b) concurrent with rapidly increasing transparency but, during this period, the low light slope and thus the I_k changed dramatically making precise analysis difficult. Clearly further work is required to determine both the adaptive range of the I_k in nature and the time required for the adjustment of photoreceptor capacity.

Population dynamics

The population data for 1973 (Fig. 32) show that both Asterionella and Fragilaria decline quickly as soon as rapid growth terminates. They are replaced by Tabellaria even though they have equivalent or greater cell division rates (Fig. 41). Similarly, in 1972 Asterionella was replaced even though it possessed the higher division rate (Fig. 39). It is obvious that the various causes of cell loss need to be explored if diatom succession is to be explained.

The combined 1972 and 1973 results provide sufficient data to examine the contributions of cell growth, death and sinking to the population dynamics

Table 9. Matrix of correlation coefficients between cell
          growth (c), death (d), sinking (s), and observed
          population growth (k) for Asterionella (n = 7,
          upper right values) and Tabellaria (n = 15,
          lower left values). The significance level is
          indicated as: $* < 0.05$, $** < 0.01$, $*** < 0.001$.

ASTERIONELLA

	c	d	s	k	
c		.57	-.12	.27	c
d	.27		.81*	.59	d
s	.20	.70**		.92**	s
k	.49	.75**	.95***		k
	c	d	s	k	

TABELLARIA

of both <u>Tabellaria</u> and <u>Asterionella</u>. Although cell growth is obviously

necessary for population growth, changes in its magnitude are insufficient

to fully explain population fluctuation (Table 9). Living cells (with

chloroplasts) were always fixing carbon and thus cell growth estimates

point to population expansion and can never predict a decline. There is

a very strong correlation between observed population growth and sinking

in both <u>Asterionella</u> and <u>Tabellaria</u> (Fig. 46, 47, Table 9) indicating that

population fluctuations primarily result from variability in loss rates.

This finding supports the theoretical model of O'Brien (1974) in which

loss rates were predicted to be of major importance.

The high correlation found between population growth and death in

<u>Tabellaria</u> (Table 9) is at first surprising, since the death rate is almost

negligible. The correlation exists because sinking is also strongly

correlated with death. The data suggest a hyperbolic relationship with

maximal sinking when death is still less than 1.5% per day (Fig. 48).

When applied to the 4m epilimnion, the maximum sinking loss of approximately

22% per day yields a sinking speed of 88 cm per day.

In <u>Asterionella</u> the correlation between death and sinking is also

significant but no maximum could be established (Fig. 49). The slope of the

relationship is much lower than that for <u>Tabellaria</u> (note scales) indicating

that sinking is less affected by the presence of dead cells. Yet, as much

higher death rates of up to 14% per day were observed, the net effect is

even higher rates of sinking up to 35% per day, corresponding to a sinking

speed of 140 cm day^{-1}. One possible explanation for the difference in

sensitivity to death between the two species is that <u>Asterionella</u> was

heavily colonized by the colorless flagellate <u>Salpingoeca frequintissima</u>

which, under the microscope, was observed to propel the entire colony through

Figure 46. Correlation between observed population growth

rate (k) and sinking rate (s) in Asterionella

formosa (k = 1.286 s + 0.170, r = 0.92, n = 7, p < 0.01).
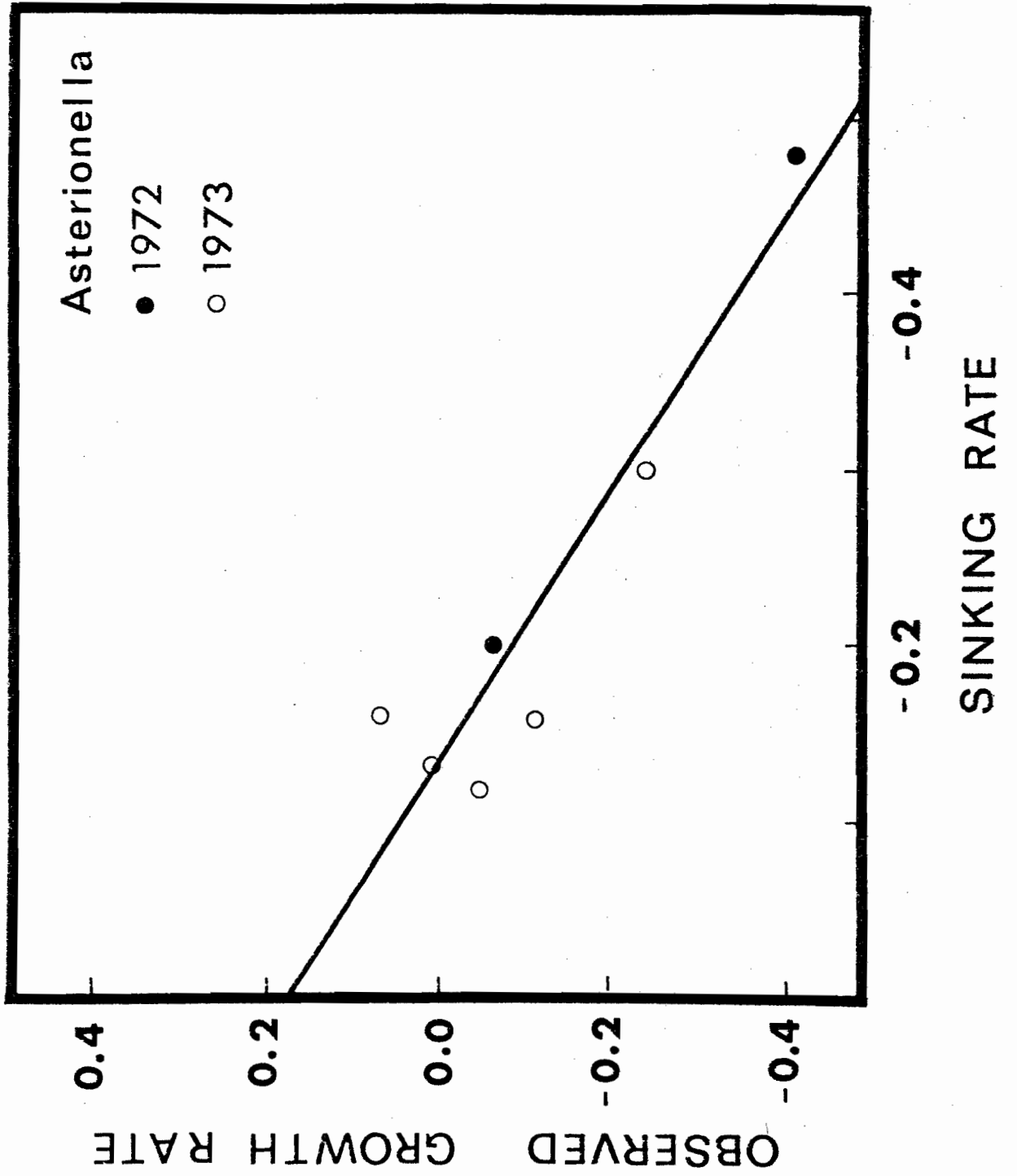
Figure 47. Correlation between observed population growth

rate (k) and sinking rate (s) in Tabellaria

fenestrata (k = 1.225 s + 0.177 r = 0.95 n = 15,

$p < .001$).
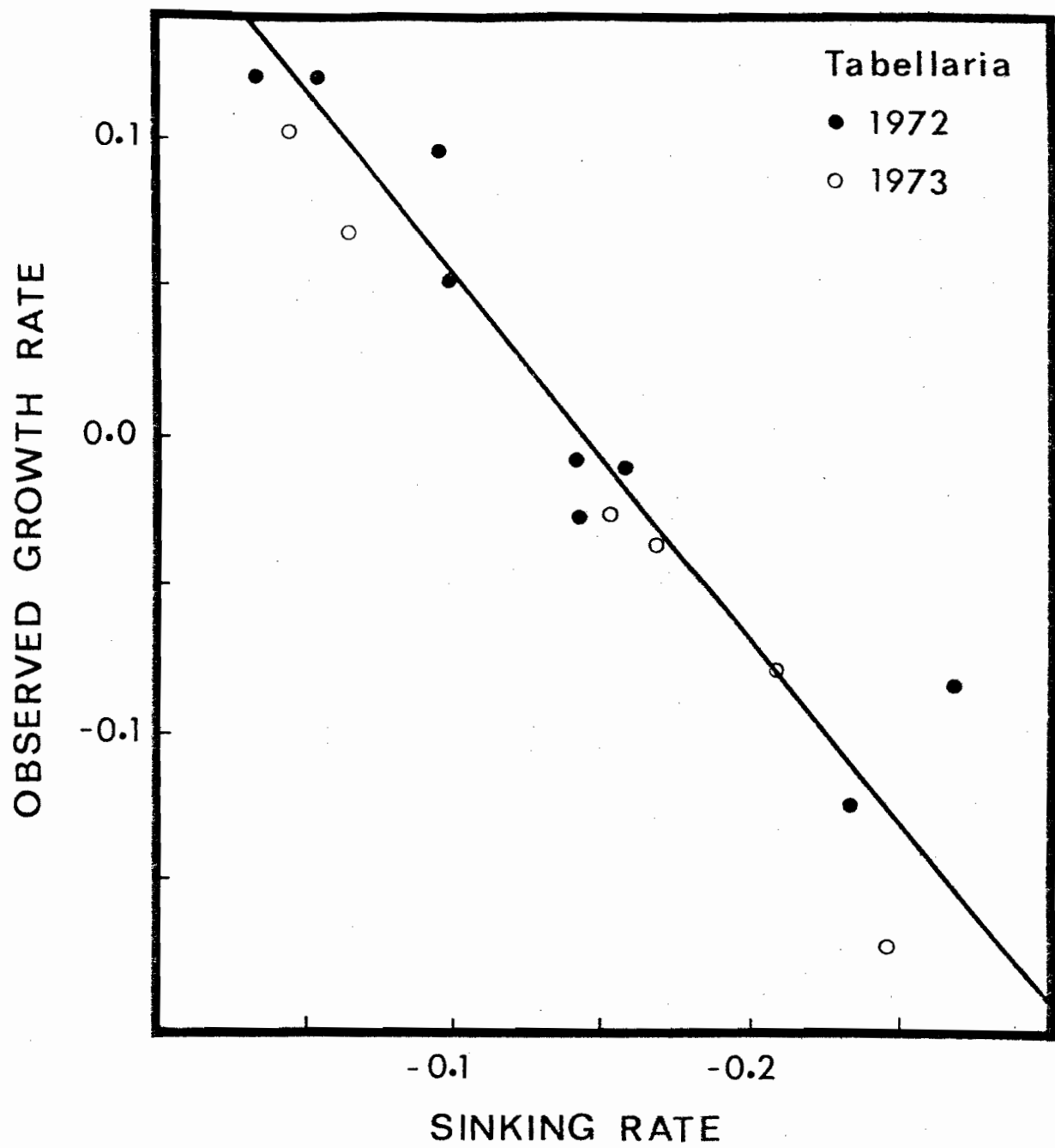
Figure 48. Correlation between sinking rate (s) and death

rate (d) in _Tabellaria_. Principal axis was

determined with the point at far right omitted

($S = 12.864$ d - 0.021, $r = 0.70$, $n = 15$, $p < 0.01$).

The data suggest a hyperbolic relationship with

maximal sinking realized at death rates of only

0.015.

Figure 49. Correlation between sinking rate (s) and death rate
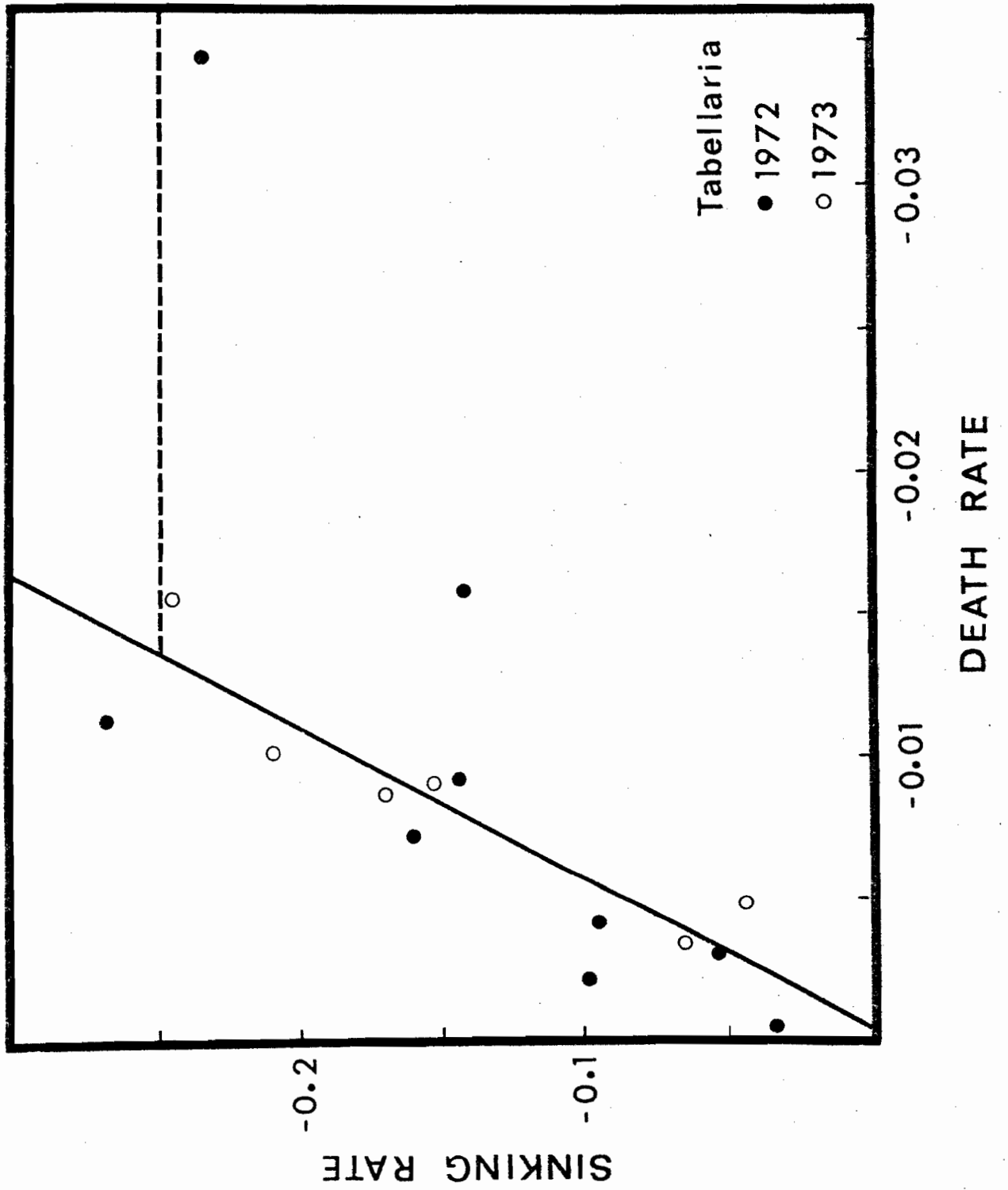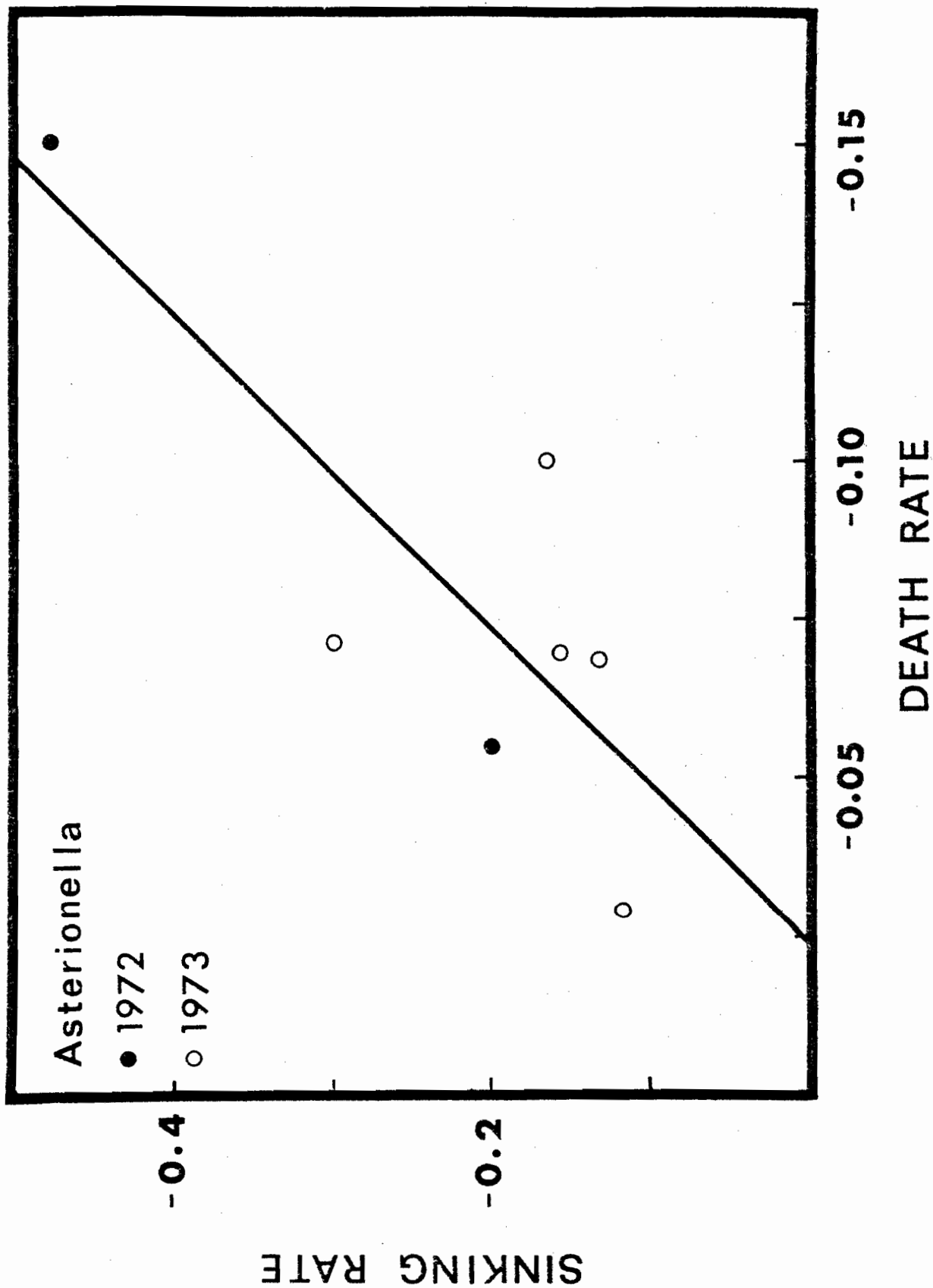
(d) in Asterionella (s = 4.136 d + 0.103, r = 0.81,

n = 7, p < 0.05).

the water. If the epiphytes are at all positively phototactic their presence will reduce diatom sinking, enabling the colony to maintain position in the water column, as suggested by Huber-Pestalozzi (1941). _Fragilaria_ was lightly colonized by a second flagellate, _Bicoeca_ _lacustris_ while _Tabellaria_ was rarely colonized at all.

The hypothesis that colonies with dead cells sink faster due to their increased density was postulated by Lund (Lund et al. 1963) as a possible cause for the _Asterionella_ decline in Lake Windermere. Earlier, when comparing growth of _Anabaena_ _planctonica_ and _Tabellaria_ _fenestrata_ for 1973 (Part 3, this thesis)   , we expressed doubt that this was the case as we found no strong correlation between the proportion of dead cells and the predicted sinking rate. Upon re-examination of the data we find that the discrepancy results from the way in which observed growth was calculated. In the earlier study observed growth was computed for the entire water column and thus the estimates at times included cells that had been lost from the epilimnion, but not from the water column as a whole. This introduced enough variance into the estimates to obscure the relationship between sinking and death. The present study shows that approximately 65% of the variance in sinking speed of both species can be explained through the correlation between sinking and death. Attempts to correlate sinking with wind records, an indirect measure of turbulence, were unsuccessful.

The presence of a good relationship between sinking and death in the epilimnion, as well as between sinking and growth, suggests a very simple means of estimating diatom growth rates through correlation with the percentage of dead cells. Using the proportions of dead cells at the end of a time interval as a correlate accounts for 78% of the variance in observed growth of _Tabellaria_ (Fig. 50) while using the initial proportion dead yields an explained variance of only 29%. For _Asterionella_, explained

Figure 50. Correlation between observed population growth

rate (k) and the proportion dead cells present

at the end of the sampling interval for

Tabellaria fenestrata (k = 0.101 - 0.885 x, r = -0.88,
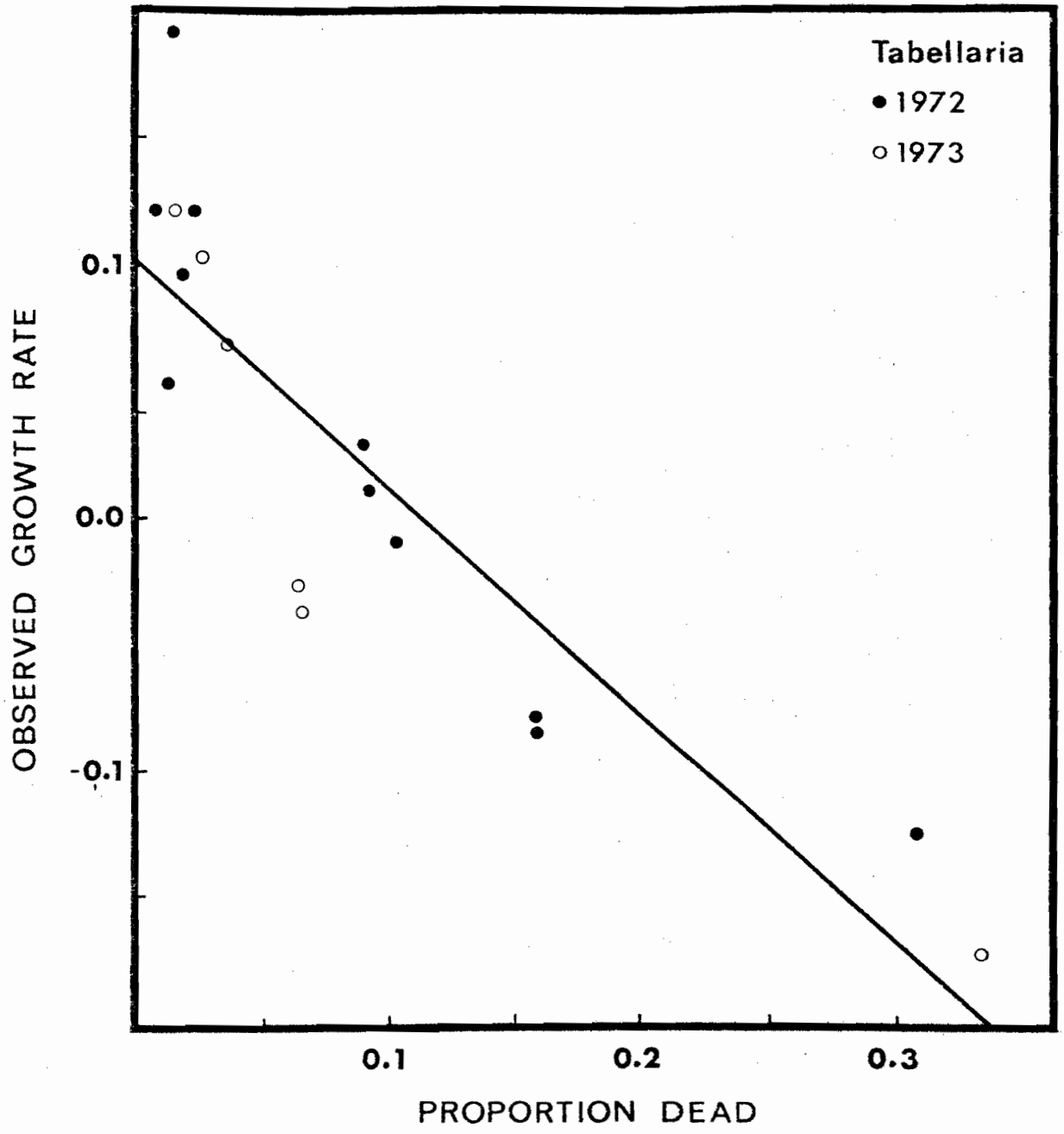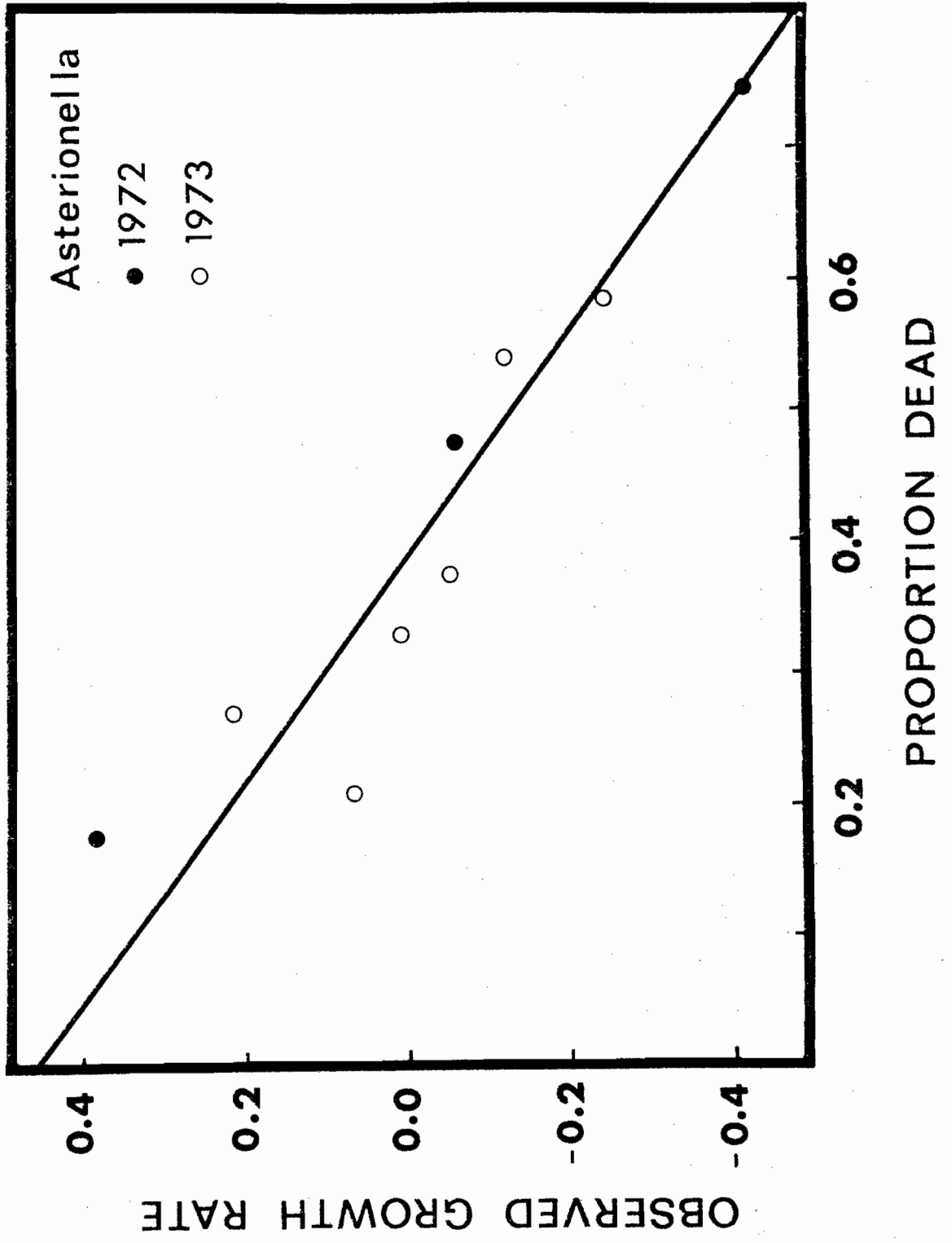
n = 17, p < .001).

Figure 51. Correlation between observed population growth

rate (k) and the proportion dead cells present at

the end of the sampling interval for <u>Asterionella</u>

<u>formosa</u> (k = 0.454 - 1.159 x , r = -0.93, n = 9,

p <.001).

variance in the predictive mode is zero, while retrospectively 87% of the variance is accounted for (Fig. 51). Thus a simple dead cell estimate at the end of an interval explains nearly as much variance in observed growth as does sinking (Table 9) and is in fact a better measure than the actual death rate. While these findings provide encouraging insight into the mechanisms of population dynamics they allow only minimal prediction of future events. Improved means of predicting death rates must be found as well as ways of accounting for more of the variance in sinking rate.

Although it would appear logical for death to be associated with slow growth, we find no evidence for this in Tabellaria or Asterionella (Table 9). Diatom declines have been related to silica depletion (e.g. Lund 1950, 1963), however in Lac Hertel the Asterionella and Fragilaria populations decline while the silica supply is still sufficient, as indicated by the continued increase of Tabellaria (Fig. 32). The decline of Asterionella does not appear attributable to chytrids either as infection rates observed were insufficient (<10%) to halt population growth (Canter and Lund 1948, 1951, Lund 1965 p. 268). Thus the precise causes of death in these diatom populations remain obscure.

CONCLUSION

The present study has shown that cell growth rate is determined primarily by the P_{max}. In nature the P_{max} is usually controlled by nutrient supply rather than temperature or photoreceptor capacity, as is often the case in culture. Photoinhibitory effects are also much stronger in nature and thus the I_k plays an important role in response optimization. Cell growth determines only the maximum possible population growth rate while losses, primarily through sinking, determine the actual population size.

Sinking, in turn, is largely a function of the death rate. Thus knowledge of both growth and loss rates is prerequisite to an understanding of diatom population dynamics in nature.

References

Antia, N.J., C.D.McAllister, T.R.Parson, K.Stephans, and J.D.H.Strickland. 1963. Further measurements of primary production using a large volume plastic sphere. Limnol. Oceanogr. 8:166-183.

Brown, A.H. and D. Weis. 1959. Relation between respiration and photo-synthesis in the green alga, <u>Ankistrodesmus</u> <u>barunii.</u> Plant Physiol. 34:224-234.

Canter, H.M. and J.W.G. Lund. 1948. Studies in plankton parasites. I. Fluctuations in the numbers of <u>Asterionella</u> <u>formosa</u> Hass in relation to fungal epidemics. New Phytol.47:238-261.

Canter, H.M. and J.W.G. Lund. 1951. Studies on plankton parasites. III. Examples of interaction between parasitism and other factors determining the growth of diatoms. Ann. Bot. 59:359-371.

Crow, E.L. and R.S. Gardner. 1959. Confidence intervals for the expect-ation of a Poisson variable. Biometrika 46: 441-453.

Elliott, J.M. 1971. Some methods for the statistical analysis of samples of benthic invertebrates. Freshwat. Biol. Assoc. Publ.25.144 pp.

Hiller, R.G.,and C.P. Whittingham1959. Further studies on the carbon dioxide burst in algae. Plant Physiol. 34:219-222.

Huber-Pestalozzi,G. 1941. Das Phytoplankton des Susswassers. Die Binnengewasser 16(2): 294.

Hutchinson,G.E. 1941. Limnological studies in Connecticut. IV. The mechanisms of intermediary metabolism in stratified lakes. Ecol. Monogr. 11:21-60.

Jorgensen, E.G. 1969. The adaptation of plankton algae IV· Light adaptation in different algal species. Physiol. Plant. 22:1307-1315.

Knoechel, R. and J.Kalff. 1975. Algal sedimentation: the cause of a diatom blue-green succession. Verh. Internat. Verein. Limnol. 19: in press (Part 3, this thesis).

Knoechel, R. and J.Kalff. 1976a. Track autoradiography, a method for
    the determination of phytoplankton species productivity.
    Limnol.Oceanogr.: in press (Part 2, this thesis).

Knoechel, R. and J.Kalff. 1976b. The applicability of grain density
    autoradiography to the quantitative determination of algal species
    production: a critique. Limnol. Oceanogr. in press (Part 1, this thesis)

Lehman, J.T., D.B.Botkin, and G.E. Likens. 1975. The assumptions and
    rationales of a computer model of phytoplankton population
    dynamics. Limnol. Oceanogr. 20:343-364.

Levi, H. and A.W. 1969. On the quantitative evaluation of autoradiograms.
    Mat. Fys. Medd. Dan. Vid. Selsk. 33(11); 51 p.

Lund, J.W.G. 1950. Studies on Asterionella formosa Hass. II. Nutrient depletion
    and the spring maximum. J.Ecol. 38:15-35.

Lund, J.W.G. 1965. The ecology of the freshwater phytoplankton. Biol. Rev.
    40:231-293.

Lund,J.W.G., C.Kipling and E.D.LeCren. 1958. The inverted microscope method
    of estimating algal numbers and the statistical basis of
    estimations by counting. Hydrobiologia 11:143-170.

Lund, J.W.G., F.J.H. Mackereth and C.H. Mortimer. 1963. Changes in depth
    and time of certain chemical and physical conditions of the
    standing crop of Asterionella formosa Hass. in the north basin
    of Windermere in 1947. Phil.Trans. B. 246:255-290.

McAllister, C.D., N.Shah, and J.D.H.Strickland. 1964. Marine phytoplankton
    photosynthesis as a function of light intensity: a comparison
    of methods. J.Fish. Res.Bd. Canada 21:158-181.

Nauwerck, A. 1963. Die Beziehungen zwischen Zooplankton und Phytoplankton im See Erken. Symb. Bot. Ups. 17(5); 163. p.

O'Brien, W.J. 1974. The dynamics of nutrient limitation of phytoplankton algae: a model reconsidered. Ecology 55; 135-141.

Rich, P.H., and R.G. Wetzel. 1969. A simple, sensitive underwater photometer. Limnol. Oceanogr. 14; 611-613.

Sanford, G.R., A.Sands and C.R.Goldman. 1969. A settle-freeze method for concentrating phytoplankton in quantitative studies. Limnol. Oceanogr. 14; 790-794.

Saunders, G.W., F.B.Trama, and R.W. Bachmann. 1962. Evaluation of a modified C-14 technique for shipboard estimation of photosynthesis in large lakes. Mich. Univ. Great Lakes Res. Div. Publ. 8: 61 p.

Sokal, R.R. and F.J. Rohlf. 1969. Biometry. W.H.Freeman and Co., San Francisco. 776. p.

Stauffer, R.E. and G.F. Lee. 1973. The role of thermocline migration in regulating algal blooms. in "Modelling the eutrophication process", E.J. Middlebrooks, D.H. Falkenborg and T.E. Maloney (eds.) Ann Arbor Science 228 p.

Steemann Nielsen, E. 1962. Inactivation of the photochemical mechanism in photosynthesis as a means to protect the cells against too high light intensities. Physiol. Plant 15:161-171.

Steemann Nielsen, E. and E.G. Jorgensen. 1968. The adaptation of plankton algae. I. General part. Physiol. Plant 21:401-413.

Strathmann, R.R. 1967. Estimating the organic carbon content of phytoplankton from cell volume or plasma volume. Limnol. Oceanogr. 12;411-418.

Strickland, J.D.H. 1958. Solar radiation penetrating the ocean. A
review of requirements, data and methods of measurement,
with particular reference to photosynthetic productivity.
J. Fish. Res. Bd. Canada. 15: 453-493.

Talling, J.F. 1955. The relative growth rates of three plankton diatoms in relation
to underwater radiation and temperature. Ann. Bot. 19:329-341.

Talling, J.F. 1965. Photosynthetic behaviour in stratified and unstratified
lake populations of a planktonic diatom. J. Ecol. 54:99-127.

Tregunna, E.B., G. Krotkov and C.D. Nelson. 1966. Effect of oxygen on the
rate of photorespiration in detached tobacco leaves.
Physiol. Plant. 19:723-733.

Vollenweider, R.A. (ed.). 1974. A manual on methods for measuring primary
production in aquatic environments. I.B.P. handbook No.23
(2nd ed.). Blackwell Scientific Publications, Oxford. 225 p.

Weis, D. and A.H. Brown. 1959. Kinetic relationships between photosynthesis
and respiration in the algal flagellate, Ochromonas mal-
hamemsis. Plant Physiol. 34:235-239.

Zelitch, I. and P.R. Day. 1968. Glycolate oxidase activity in algae. Plant
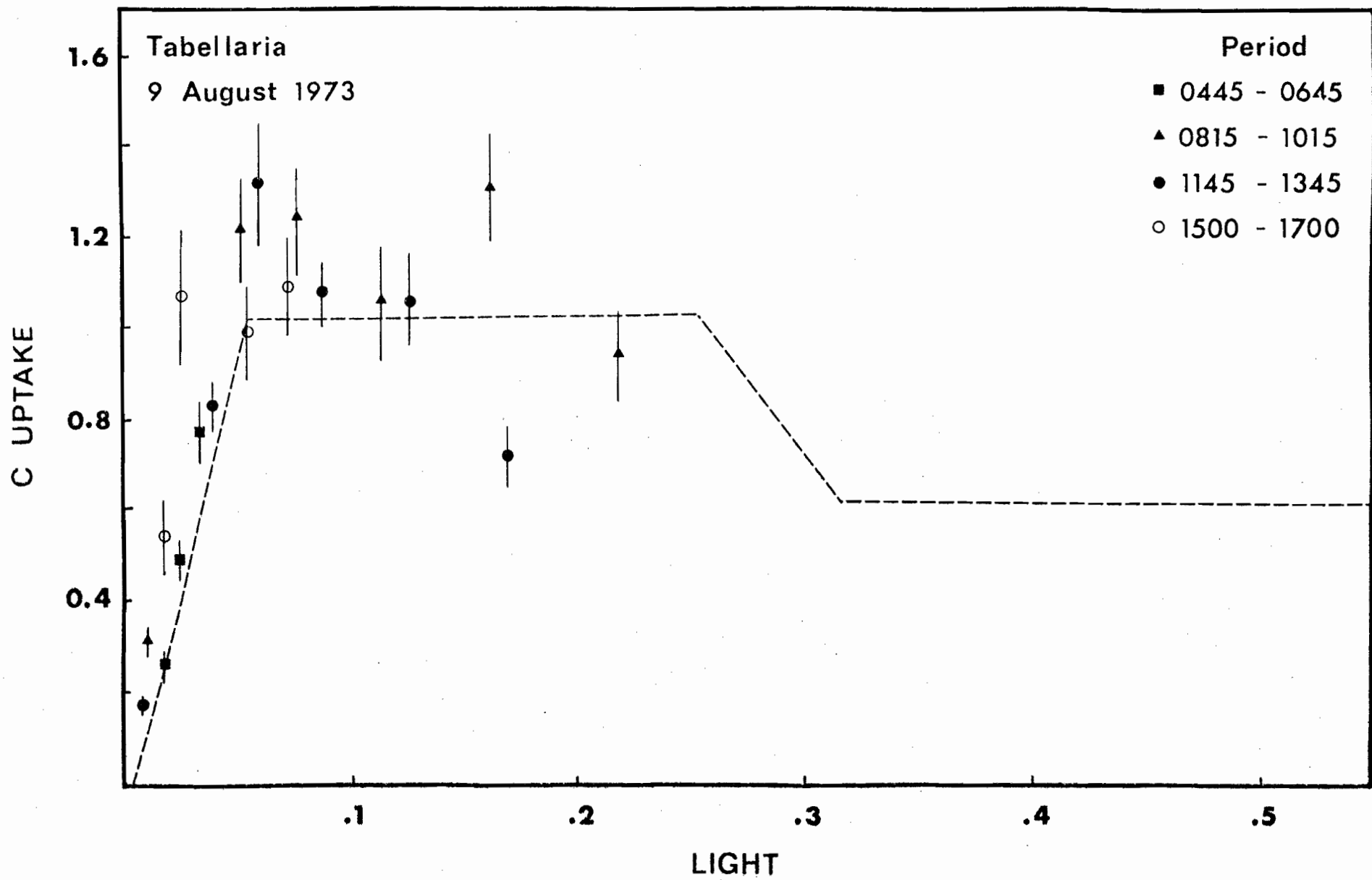Physiol. 43:288-291.

APPENDIX 1

Diurnal rates of photosynthesis

There are a number of factors which might cause diurnal variation

in photosynthetic rate. Morning depletion of a critical nutrient pool

(e.g. Schindler and Fee 1973), or photooxidative damage to the photo-

receptor system (Steemann Nielsen 1962) would lead to afternoon

depression of the P_{max}. Nutrient limitation would not be expected to

alter the light limited response slope while photooxidation would

result in a decrease. In the absence of nutrient limitation and photo-

oxidation, periodicity in pigment production could produce an increase

in the light limitation slope (Steemann Nielsen and Jorgensen 1968) and

therefore cause a decrease in the I_k.

A diurnal series of incubations was carried out on 9 August 1973

to test for the presence of diurnal changes in either P_{max} or light limited

response slope in Tabellaria. There was moderate depression in the Om

sample during both the 0815 a.m. and 1145 a.m. incubation periods

(Fig. 52), however, the rate was normal again at 1500 p.m. and thus

photooxidation is doubtful. If nutrient depletion is the cause it was

restricted to the surface and of short duration even though this experiment

was performed during an Anabaena bloom (cf. Fig. 14) when maximal depletion

would be expected. The absence of an afternoon decrease in the light

limitation slope argues against photooxidation. If anything, there is an

increase in slope but more data are necessary before this can be established

for certain. The short term inhibition with a rapid return to higher

P_{max} during the 1500 p.m. incubation is most readily explained through

photorespiration (see Part 4).

Figure 52. Photosynthetic carbon uptake ($gC \times 10^{-15} \mu m^{-3} h^{-1}$) of _Tabellaria_ _fenestrata_ as a function of light ($ly\ min^{-1}$ PAR) on 9 August 1973 during a diurnal incubation series. There is no 2m value for the 1500 p.m. incubation. Results are not presented for 3,4 and 6 m 0445 a.m. and for 6 m 1500 p.m. as there was insufficient light to permit measurable uptake.

Tabellaria
9 August 1973

Period
■ 0445 – 0645
▲ 0815 – 1015
● 1145 – 1345
○ 1500 – 1700

C UPTAKE

1.6
1.2
0.8
0.4

LIGHT

.1   .2   .3   .4   .5

The P_{max} based only on the midday incubation is 1.084. If the
calculation is based on all of the diurnal data in addition the value
becomes 1.109, an increase of only 6%. Thus, on the basis of these
data, there is no substantial diel cycle in photosynthetic response
requiring attention in our model.

REFERENCES

Schindler, D.W. and E.J. Fee. 1973. Diurnal variation of dissolved
inorganic carbon and its use in estimating primary production and
CO_2 invasion in lake 227. J. Fish. Res. Board Can. 30: 1501-1510.

Steemann Nielsen, E. 1962. Inactivation of the photochemical mechanism
in photosynthesis as a means to protect the cells against too high
light intensities. Physiol. Plant. 15: 161-171.

Steemann Nielsen, E. and E.G. Jorgensen. 1968. The adaptation of plankton
algae. III. With special consideration of the importance in nature.
Physiol. Plant. 21: 647-654.

APPENDIX 2

Estimation of hourly incident radiation from sunshine records

INTRODUCTION

There is a need for an inexpensive, simple and reliable means of
estimating incident radiation for field research on photosynthesis.
Instrumentation capable of providing short term integrative measurements
is usually expensive or requires time consuming data reduction. The
Campbell-Stokes sunshine meter has the advantages of relatively low cost,
no moving parts, rapid record analysis, and widespread use at meteorological
stations around the world. Its primary drawbacks are the need for daily
chart changes and, until now, a lack of precision and inability to
produce short term estimates.

Past attempts to predict incident shortwave radiation from sunshine
records have concentrated on predicting total daily radiation as a function
of the percentage of possible sunshine received (Becker and Boyd 1957,
Fritz and MacDonald in List 1966). While this relationship is highly
significant, the explained variance is relatively low ($r^2 = 0.67$, $r^2 = 0.77$).
Much variance results from the failure to consider the time of day when
the sunshine was received even though this information is usually available
because standard record analysis involves recording hourly sunshine values
and summing these to yield the daily total (for technique see Robinson 1966).
This paper presents a method of predicting with high precision both daily
and hourly radiation flux from sunshine records.

METHODS

A computer program estimated hourly radiation flux based on three variables: time of day, date, and percent sunshine. The first two factors are used to calculate the total possible radiation from first principles as:

$$Q_t = \frac{2.0}{r^2} \quad (\sin\theta \, \sin\delta + \cos\theta \, \cos\delta \, \cos h)$$

Q_t = total possible radiation

θ = latitude of observer

δ = declination of the sun

r = radius vector

h = hour angle of the sun

Tables (List, 1966) are consulted for values of δ and r, which vary seasonally, while h is computed as 15° times the number of hours from solar noon. The mean of two successive estimates at hourly intervals is used as the estimate for the intervening hour. This value is inserted into an equation for percent of possible radiation using the coefficients suggested by Angstrom (in List, 1966).

$$Q_r = Q_t \, (0.235 + 0.765 \, S_r)$$

Q_r = radiation received

S_r = proportion possible sunshine received

This equation was originally designed to predict total daily radiation but functions equally well on an hourly basis. The equation is modified by the addition of an atmospheric turbidity factor. For this study a factor, $T = 0.70$, was empirically determined by comparing predicted and measured radiation on cloudless days. Incident radiation (I_o) is thus

computed as:

$$I_o = Q_r \ (T)$$

The resulting hourly estimates, when summed, provide a value for daily

shortwave incident radiation.

Computed values were compared with radiation estimates obtained with

a Kipp & Zonen pyranometer with recorded output. I thank Dr. B. Garnier

of the Geography Department, McGill University for supplying the radiation

and sunshine records.

RESULTS

There is a strong correlation between daily incident radiation

predicted from sunshine records and values measured with the Kipp & Zonen

pyranometer (Fig. 53, r = 0.97, n = 216, 1 April - 30 November). The

explained variance (r^2) is 94% and the standard errors are comparable

(13.4 vs. 13.5 ly day^{-1}). This is a marked improvement over previous

techniques (see Introduction). In comparison the correlation between

the Kipp & Zonen records and those from an actinograph over the same

period was only slightly, but significantly, higher (r = 0.98, r^2 = 0.96,

n = 209, 95% confidence limits of correlation coefficients non-overlapping).

Thus the sunshine meter is nearly equivalent to the actinograph. The

correlation between predicted hourly radiation and Kipp & Zonen measure-

ments was also high (r = 0.932, n = 2355, 1 April - 30 September) yielding

an explained variance of 87% with a standard error of .008 ly min^{-1}

for both methods.

Figure 53. Correlation between daily incident radiation
(ly day^{-1}) predicted on the basis of Campbell
-Stokes sunshine meter records and that actually
measured by a Kipp and Zonen pyranometer
($y = 0.99 \ x + 13.37$, $r = 0.97$, $n = 216$, $p < .001$).

(
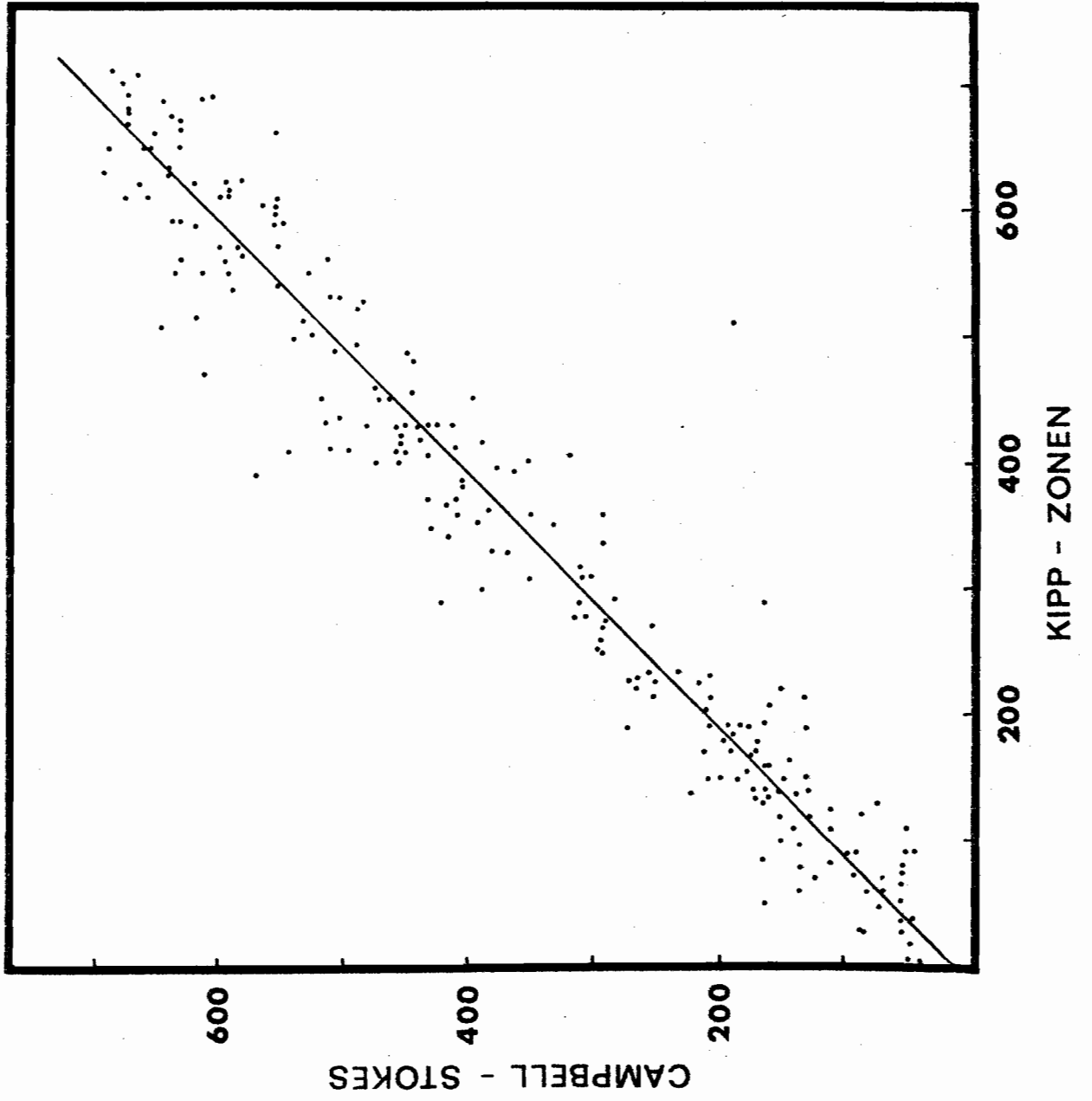
DISCUSSION

The results show that the Campbell-Stokes sunshine meter can be used, with high precision, to measure both hourly and daily incident shortwave radiation. The standard error of daily and hourly radiation estimates using the method described here is essentially identical to that using a Kipp & Zonen pyranometer with recorded output.

There is a potential for further increasing accuracy by considering cloud type (cf. data of Haurwitz in List 1966) as a variable affecting transmission or by utilizing visibility records as estimates of variation in atmospheric turbidity. However, this increase in accuracy would be at the expense of simplicity and seems unwarranted for most ecological purposes.

In remote locations instrument reliability is often of paramount importance. During the course of this study, the Kipp and Zonen was inoperative for a total of 23 days (9.4%) and the actinograph for 7 days (2.9%) while the sunshine recorder was operational 100% of the time.

In summary, the Campbell Stokes sunshine meter can provide hourly and daily incident radiation estimates with sufficient accuracy for most ecological studies and with both a minimum of expense and a maximum of reliability.

REFERENCES

Becker, C.F. and J.S. Boyd. 1957. Solar radiation availability on surfaces in the United States as affected by season, orientation, latitude, altitude, and cloudiness. J. Solar Ener. Sci. Engr. 1:13-21.

List, R.J. (ed.) 1966. Smithsonian Meterological Tables 6th edition. Smithsonian. Robinson N. (ed.) 1966. Solar Radiation. Elsevier.

GENERAL CONCLUSIONS

An investigation of grain density autoradiography as a possible method for measuring in situ species carbon fixation indicated that, although the method can provide quantitative results, its application is difficult because of complex procedures necessary to control for latent image fading, chemography, and specimen geometry. Instead, track autoradiography was adapted to phytoplankton studies and it was demonstrated that the technique yields quantitative results.

Analysis of in situ diatom photosynthesis indicated that photo-inhibition is much stronger in nature than is usually noted in culture and that it has the general characteristics of photorespiration. Unlike cultured algae, photosynthesis was essentially unaffected by temperature, over the range encountered. The I_k permits optimization of the light response but the general magnitude of growth is determined by the P_{max}. The dependency of Tabellaria's P_{max} on meteorologic and geologic nutrient inputs was demonstrated.

While cell growth determines the maximum rate of population increase, the population size actually realized in the lake is largely a function of losses, primarily from sinking. Sinking in turn is principally a function of the death rate. As the result of a very low death rate, Tabellaria succeeded Asterionella and Fragilaria even though it had a lower cell growth rate. In contrast, a blue-green alga, Anabaena planctonica, was not subject to the relatively high sinking losses characteristic of these diatoms and was thus able to replace Tabellaria during late summer when cell growth rates of both were low. Succession in the six species studied was therefor largely the result of differential loss rates rather than differential growth rates.